Non-invasive measurement of quality attributes of processed pomegranate products

by

Emmanuel Ekene Okere

Thesis presented in partial fulfilment of the requirements for the degree of Master of Engineering (Electronic) in the Faculty of Engineering at Stellenbosch University

Supervisor: Prof Willem Jacobus Perold
Prof Umezuruike Linus Opara
Dr Ebrahiema Arendse

March 2020

Declaration

By submitting this thesis electronically, I declare that the entirety of the work contained therein is my own, original work, that I am the sole author thereof (save to the extent explicitly otherwise stated), that reproduction and publication thereof by Stellenbosch University will not infringe any third party rights and that I have not previously in its entirety or in part submitted it for obtaining any qualification.

Date: .....

Abstract

Pomegranate fruit has witnessed tremendous growth over the past decade in production, consumption, processing and research within South Africa. Currently, in order to provide value-addition and effective utilisation of pomegranate fruit parts, the edible portion has been processed by the food industry into various co-products such as juices, dried arils, seed oil and powders. The food processing industry is frequently confronted by new technological challenges to meet the increasing demand for quality assured processed products. This, however, has led to a shift in agribusiness reliance from subjective assessment of quality and authenticity to increasing adoption of objective, quantitative and non-invasive measurement.

For pomegranates, non-invasive techniques such as X-ray computed tomography and infrared spectroscopy have successfully been used to evaluate postharvest rind disorders, quality attributes of whole fruit, and several of its co-products such as fresh arils and pomegranate juice. For processed agricultural and horticultural products, non-invasive techniques have been successfully used to evaluate and predict quality attributes related to juice, powders oils and minimally processed products. However, limited information on non-invasive techniques exist for evaluating different processed pomegranate co-products such as dried arils, powders and seed oil. Therefore, the aim of this research study was to develop non-invasive methods using infrared spectroscopy to predict the quality attributes of pomegranate co-products (dried arils and seed oil). Section I (Chapter 1) provides background information and the problem statement, including the aims and objectives of the research study. Chapter 2 provides a review of literature on non-invasive methods used to predict the quality attributes for different processed horticultural products with emphasis on juices, oils and powdered products and highlights potential research scientific gaps.

Section II covers the application of infrared (FT-NIR and FT-MIR) spectroscopy in evaluating pomegranate co-products (dried arils and seed oil). In Chapter 3, Fourier-transform near infrared (FT-NIR) spectroscopy and associated chemometric analysis was used to evaluate quality attributes of dried pomegranate arils. This study compared two different regression techniques, namely partial least squares (PLS) and support vector machine (SVM), to develop calibration models over a spectral region of 800 – 2500 nm. Model development was based on pre-processing methods that yielded higher values of coefficient of determination (R^2) and residual predictive deviation (RPD), and root mean square

error of prediction (RMSEP). It was found that SVM could predict acidity (R^2= 0.85, RMSEP = 0.04%, RPD = 2.50), redness (a^*) colour attributes (R^2 = 0.72, RMSEP = 1.82%, RPD = 1.71) and intensity (Chroma) (R^2 = 0.70, RMSEP = 1.99%, RPD = 1.77). PLS regression also accurately predicted sensory attributes (pH, (R^2 = 0.86, RMSEP = 0.13%, RPD = 2.38 and TSS:TA ratio, R^2= 0.74, RMSEP = 1.68%, RPD = 1.68). These results suggest that SVM was better suited to evaluate the quality attributes of dried pomegranate arils. Chapter 4 (Section III) evaluated the quality of pomegranate seed oil by comparing two different spectrophotometers, namely; the Multipurpose Analyzer (MPA) in the FT-NIR spectral region of (12500 – 4000 cm^{-1}) and the Alpha ATR-FT-MIR in the spectral region of 4000 – 400 cm^{-1}. The MPA (FT-NIR) showed good prediction in the FT-NIR spectral region for total carotenoid content (R^2 = 80.45, RMSEP = 0.0185 β-carotene/ mL oil, RPD = 2.28) and yellowness index (R^2 = 53.19, RMSEP = 14.30%, RPD = 1.49). The Alpha (FT-IR) instrument in the FT-MIR spectral region provided good prediction for refractive index (R^2 = 80.92, RMSEP = 0.0003%, RPD = 2.32) and prediction for peroxide value (R^2 = 62.00, RMSEP = 3.88 meq O_2/mL oil, RPD =1.62). In this study, FT-MIR spectroscopy provided better prediction statistics compared to than FT-NIR spectroscopy for evaluating the quality attributes of pomegranate oil. This research study has demonstrated that infrared spectroscopy and associated chemometric analysis has the ability to predict the quality attributes of pomegranate dried arils and seed oil.

List of submitted manuscripts from this thesis

Submitted article

1. Emmanuel Ekene Okere, Ebrahiema Arendse, Fredrick Isingizwe Nturambirwe, Helene Nieuwoudt, Olaniyi Amos Fawole, Willem J. Perold & Umezuruike Obia Opara, 'Application of Fourier-transformed near infrared spectroscopy (FT-NIRS) combined with chemometrics for evaluation of quality attributes of dried pomegranate arils', *African Journal of Science, Technology, Innovation & Development.*

Prepared to be submitted articles

1. Emmanuel Ekene Okere, Ebrahiema Arendse, Helene Nieuwoudt, Olaniyi Amos Fawole, Willem J. Perold & Umezuruike Obia Opara, 'Non-invasive methods for predicting the quality of processed horticultural products – A review', *Scientia Horticulturae.*

2. Emmanuel Ekene Okere, Ebrahiema Arendse, Helene Nieuwoudt, Olaniyi Amos Fawole, Willem J. Perold & Umezuruike Obia Opara, 'Application of Fourier transform (FT) near-infrared (NIR) and attenuated total reflection (ATR) FT mid-infrared (MIR) spectroscopy for the evaluation of pomegranate seed oil quality', *Biosystems Engineering.*

Acknowledgements

My sincere and profound gratitude and appreciation goes to my supervisor, Prof Willem J Perold for all his fatherly advice and encouragement throughout the project. His guidance and support are acknowledged and greatly appreciated. Also, on this list is my co-supervisor, Prof Umezuruike Linus Opara, his patience and inputs had been immense, especially during the Postharvest Discussion Forum (PDF). It indeed has been greatly helpful in assisting me put this thesis together. Thank you very much for all your support and feedback on my work. Your inputs were highly valuable and are acknowledged.

I would like to thank Dr Helene Nieuwoudt from the Institute for Wine Biotechnology for her help with the experimental work and for providing and introducing me to OPUS software. Not forgetting Dr Frederic Nturambirwe. Your assistance is truly treasured and valued.

To Dr Arendse Ebrahiema, written words cannot thank you enough for your tireless effort on making sure I finish this research work. I appreciate every input, correction, meeting, advice and push geared towards my success. I must admit, you are the best mentor anyone could ever wish for.

Special thanks to Prof Olaniyi Amos Fawole for all the encouragement, inputs and suggestions throughout this work. I greatly acknowledge and appreciate you.

I would also like to thank Nazneen Ebrahim for her administrative duties and technical support throughout the course of this research work. Not forgetting Page Pierre for the company and assistance in the Postharvest Laboratory.

Special thanks to my friends and postgraduate colleagues at SARChI Postharvest Technology Research Laboratory for their friendliness, encouragement and input all along this project. Lastly, I would like to send a special thanks to my family, my parent, siblings and friends especially Ms Vuyiswa Dlamini for your support and prayers.

This work is based on the research supported wholly/in part by the *National Research Foundation* of South Africa (Grant Number: 64813). The opinions, findings and conclusions or recommendations expressed are those of the author(s) alone, and the NRF accepts no liability whatsoever in this regard.

Contents

Abbreviations

1^{st}: First Derivative

2^{nd}: Second Derivative

cm^{-1}: Per centimetre

meq O_2/mL: Milligram equivalent-Oxygen per mil

mg GAE/mL: milligram- Gallic Acid Equivalent per mil

nm: Nanometre

a^*: Redness

C^*: Chroma

ATR-FT-MIR: Attenuated Total Reflectance-Fourier Transform-Mid-Infrared Spectroscopy

Corr: Correlation Coefficient

CV: Coefficient of Variation

FT-MIR: Fourier Transform- Mid-infrared

FT-NIR: Fourier Transform- Near-infrared

GAE: Gallic Acid Equivalent

h°: Hue Angle

IR: Infrared

L^*: Lightness

LDA: Linear Discriminant Analysis

LOD: Limit of Detection

LV: Latent variables

Max: Maximum

Min: Minimum

MIR: Mid-Infrared

MPA: Multi-Purpose Analyser

MSC: Multiplicative Scattering Correction

MUFA: Monounsaturated Fatty Acid

n: Number of samples

NIR: Near-Infrared

NMR: Nuclear Magnetic Resonance

PCA: Principal Component Analysis

PLS: Partial Least Squares

PLS-DA: Partial Least Squares-Discriminant Analysis

PSO: Pomegranate Seed Oil

PUFA: Polyunsaturated Fatty Acid

PV: Peroxide Value

R^2: Coefficient of Determination

RI: Refractive Index

RMSEC: Root Mean Square Error of Calibration

RMSECV: Root Mean Square Error of Cross-Validation

RMSEP: Root Mean Square Error of Prediction

RPD: Ratio of Prediction to Deviation

RSD: Relative Standard Deviation

SD: Standard Deviation

SFA: Saturated Fatty Acid

SLS: Straight Line Subtraction

SNV: Standard Normal Variate

SPA: Successive Projections Algorithm

SR: Selectivity Ratios

SVM: Support Vector Machine

TA: Titratable Acidity

TAC: Total Anthocyanin Content

TCC: Total Carotenoid Content

TPC: Total Phenolic Content

TSS: Total Soluble Solid

TSS/TA: Total Soluble Solid/ Total Acid

VIP: Variable Importance in Projection

YI: Yellowness Index

List of Figures

List of Tables

Chapter 1

General Introduction

1.1 Background

Pomegranate, scientifically known as *Punica granatum* L., is a fruit-bearing deciduous shrub or small tree in the family of Lythraceae. The fruit is spherically shaped, has a thick leathery exocarp and an interior that is separated by membrane walls and packed into compartments. The compartments consist of edible portions called arils, and each aril contains a seed which is surrounded by a translucent sac containing juice. The edible portion (arils) consist of 50 to 70% of the total fruit weight, While the juice volume consists of 60-80% the aril weight or 30-40% of the fruit weight and the seeds constitute 3-5% of the total fruit weight [1, 2, 3]. The fruit (and its co-products) has captured increasing consumer interest due to its multi-functionality human diet as 'superfruit'. The fruit has been reported to possess high nutritional content, potent pharmacological and antioxidant properties which have been related to improved human health [4, 5]. Scientific studies have linked pharmacological activities of pomegranate to several groups of phytochemicals found within the fruit. These phytochemicals include polyphenolic compounds, which have been reported to possess anti-microbial, anti-diabetic, anti-mutagenic, antioxidant, anti-hypertension, anti-inflammatory and atherosclerotic properties [4, 6]. The fruit is frequently consumed fresh; however, despite the nutritional and health benefits, consumption is still limited due to the difficulty of extracting the arils. Currently, in order to increase fruit consumption, the edible portion (containing sacs of arils) has been processed into ready-to-eat fresh arils. However, fresh arils have a relatively short shelf-life of 5-8 days. To overcome this limitation, the pomegranate industry has promoted research and development of value-added pomegranate co-products such as dried pomegranate arils, pomegranate seed oil, dehydrated powder and juices (Fig. 1.1).

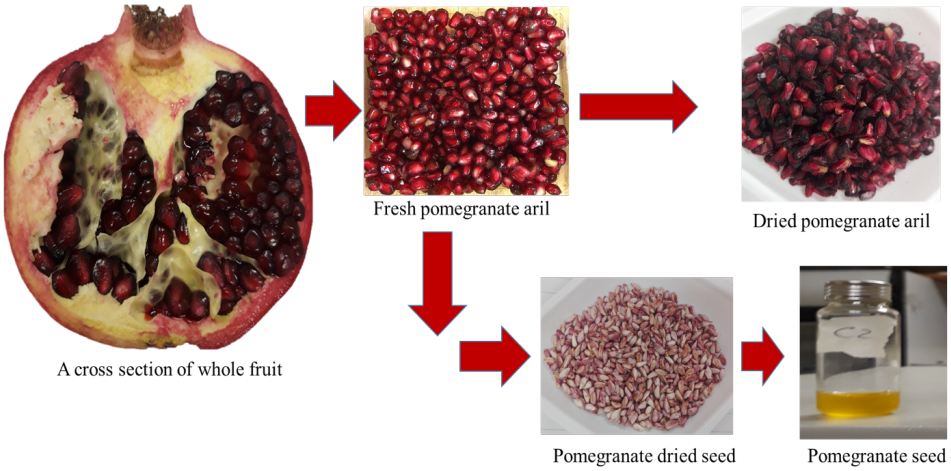

Figure 1.1: Basic structure of a pomegranate fruit with its co-products

Processed pomegranate products such as dried arils are rich sources of vitamins, polysaccharides, mineral elements, fatty acids and antioxidant compounds [7]. Processing of fresh pomegranate arils into dried arils has several advantages these include extended shelf-life and preservation of several nutritional compounds [8]. The seeds are a by-product of the food processing industry, but recent reports have highlighted their potential use as a source of seed oil with health beneficial attributes [1, 6, 9]. Pomegranate seed oil (PSO) contains high levels of punicic acid (>60%) and several other fatty acids such as palmitic, stearic, oleic and linoleic acid. Several studies have shown that PSO are good sources of phytochemical and antioxidant compounds [2, 9].

Pomegranate fruit has witnessed a tremendous growth since 2009 in production, marketing, consumption, processing and research globally and within South Africa. Over the last decade, pomegranates have been grown for commercial export, with over 8000 tons currently being produced and South Africa exports more of its pomegranate than is consumed locally. Approximately 80% of pomegranate produced locally is consumed in the international markets, 9% consumed locally and 11% is used in the processing industry [10]. The Wonderful cultivar constituted about 6% of total production and exports in 2017, this cultivar rank 18th in terms of fruits consumed annually in the world [11]. The 11% of pomegranates used for processing constitute approximately 900 tonnes that has an estimated value of 42-79 million Rands (based on R46 617 - R87 923 per tonne) depending on season and demand for the fruit [12]. Therefore, the production of pomegranate by-products such as the seed oil and powder from fruit waste can contribute to value addition, thereby reducing waste and increasing profits for growers and processors. The South African pomegranate industry aims at increasing pomegranate yield and quality to meeting meet rising export and local demands [10, 12].

Quality testing is very vital in the agricultural industry as it guarantees confidence to consumers and food processors alike. Several standard analytical tech-

niques are currently been employed for authenticity, quality control, and contamination assessment in agro-food products. These standard techniques include high performance liquid chromatography (HPLC), gas chromatography-mass spectrometry (GC-MS), spectrometric and colorimetric methods. Although, reliable, these methods are time consuming, expensive and requires specialized sample preparation. Additionally, these methods only evaluate a single sample batch and do not reflect the quality of the entire consignment, considering that samples may exhibit significant variation in both external and internal quality due to variability amongst cultivars, fruit maturity status, and even processing conditions. The high market value associated with processed pomegranate products have spurred the agribusiness industry to invest in research and application for fast, accurate and objective assessment for authenticity, food quality and contamination [13, 14].

Several objective and non-invasive methods include infrared spectroscopy (IRS), hyperspectral imaging (HSI), Raman spectroscopy, nuclear magnetic resonance and X-ray computed tomography [15, 16]. From the above-mentioned non-invasive methods, IRS coupled with chemometric analysis have shown to be the most highly effective in the measurement and prediction of various quality parameters in fresh and processed horticultural produce. IRS is fast, accurate, does not require sample preparation and can simultaneously analyse several constituents within a sample. IRS in the near infrared (NIR) (12,000–4000 cm^{-1}, 833–2500 nm) and the mid infrared (MIR) (4000–400 cm^{-1}, 2500–25,000 nm) spectral regions has been extensively applied as alternative analytical tools in the food industry [17]. For pomegranates, IRS have been successfully applied to evaluate whole fruit quality [18], fresh pomegranate arils [19] and even fresh juice [20]. However, a review of literature suggest that limited information exist on the suitability of non-invasive measurement such as infrared spectroscopy for the assessment of pomegranate co-products such as dried arils, powders and seed oil. Non-invasive assessment of processed pomegranate co-products can contribute to the implementation of suitable management strategies to predict and control desired quality attributes. The implementation of non-invasive techniques such as infrared spectroscopy will ensure that the agricultural industry and consumers are provided with high quality processed pomegranate products free from contamination and that is safe to consume.

1.2 Research Aim and Objectives

The overall aim of this research study is to develop non-invasive methods to measure and predict the quality attributes of different processed pomegranate products. To achieve this aim, the study included the following specific objectives:

1. Determine optimum conditions for near infrared spectroscopic measurement by evaluating the accuracy of various analytical techniques to quantify physicochemical and phytochemical properties of dried pomegranate arils.

2. Compare the application of different infrared spectroscopic measurement ranges (NIR & MIR), to measure and predict the chemical and phytochemical attributes of pomegranate seed oil.

1.3 Thesis structure

This thesis is structured as follows:

- Chapter 1 and Chapter 2 provide background information, discussing the general aim and objectives (General introduction) of the thesis study and also provides a review of literature on previous work done on different non-invasive techniques for evaluating different processed horticultural products over the last ten years.
- Chapter 3 and Chapter 4 evaluate different infrared spectroscopic techniques for the measuring of physicochemical and phytochemical quality attributes of different pomegranate co-products these include dried arils and seed oil.
- Chapter 5 presents a general discussion which integrates the results from previous chapters. It highlights the important practical contribution of this thesis towards successful non-invasive evaluation of pomegranate co-products.

Chapter 2

Non-invasive methods for predicting the quality of processed horticultural food products, with emphasis on dried powders, juices and oils: A review

This review covers recent developments in the field of non-invasive techniques for quality assessment of processed horticultural products over the past decade. A section on the concept of quality and various quality characteristics related to evaluate processed horticultural products are discussed. A brief overview of each non-invasive methods is presented, including spectroscopic, nuclear magnetic resonance and hyperspectral imaging techniques, followed by discussion on the applications to predict quality attributes of different processed horticultural products (powders, juices and oils). A concise summary of their potential commercial applications in quality assessment, control and monitoring of processed agricultural products is explored. Finally, we discuss their limitations, and highlight other emerging non-invasive techniques applicable for monitoring and evaluating the quality attributes of processed horticultural products.

2.1 Introduction

Horticultural crops play an essential role in human nutrition and health as they are known to be a major source of beneficial phytonutrients, dietary fiber and other micro-nutrients [16]. The majority of fruits and vegetables are consumed fresh, and hence remain perishable along the value chain. In order to reduce waste and extend the shelf-life of horticultural crops, fruits and vegetables are processed into various products for direct consumption and as food ingredients. During processing, the main objective is to preserve the colour, flavour, texture, and nutrition while prolonging the shelf-life of perishable fruits and vegetables [21]. Consequently, during postharvest processing, storage, and transportation,

the physiological quality of harvested foods continue to change. Food safety issues especially processed food must be effectively monitored by the food industry [22]. Food processing chains undergo many steps which pre-expose them to pathogenic infestation, adulteration, contamination with unwanted chemical compounds or defect deliberately or accidentally. This safety concerns with pre-exposure of the processing chain can not only reduce their functional properties and nutritive values, or even pose a serious health risk to humans and consumers. Accordingly, it is highly important and necessary that processed horticultural products such as oils, powders and juices are often subjected to stringent inspection for quality and authenticity.

The global food processing industry is frequently confronted by new technological challenges to meet the increasing demand for quality-assured processed products. Consequently, this has led to a shift in agribusiness reliance on subjective assessment of quality and authenticity to increasing adoption of objective, quantitative and non-invasive measurement.

During the last decade, several novel systems have been developed to measure quality attributes non-destructively. Several of them are now commercially available as desktop units or mounted on a grading line so that quality control of individual products becomes feasible. Several studies have highlighted the potential of different non-invasive approaches and methods applied to processed horticultural products and promoting its use as a rapid and non-invasive analytical method for quantitative or qualitative analysis [23, 24, 25, 26]. These include infrared spectroscopy [15], hyperspectral and multispectral imaging [27, 28], Raman spectroscopy [29], nuclear magnetic resonance (NMR) [30] and X-ray computed tomography [31]. Several of these techniques have been successfully employed in classification, authenticity and quantification in commercial juices, oils, powders and dried products.

Currently, scientific literature and reviews on non-destructive quality assessment of fresh fruit and vegetables are abundant. However, there is a dearth of literature reviews on non-invasive measurement of processed horticultural products. A refined Scopus search over the last decade revealed that there are currently 59 reviews for non-destructive assessment of fresh fruit and vegetable quality, only 3 reviews included information on aspects of some processed horticultural products [16, 32, 33]. Additionally, the fore-mentioned reviews with information on some processed horticultural products mainly focus on assessing either a specific product or non-destructive technique and do not integrate assessing different products or reviewing other possible non-destructive techniques. The limited information on non-invasive quality evaluation for different processed horticultural products could provide readers with insight towards current usage of non-invasive methods, highlighting a potential research scientific gap. The objective of this review is to provide an overview of recent developments in non-invasive quality measurements applied for different processed horticultural products with emphasis on juices, oils

and powdered products.

2.1.1 The concept of quality

The word "quality" is derived from the Latin "qualitas", which means attribute, property or basic nature of an object [34]. Several experts within the field have proposed brief definitions of quality: "fitness for use" [35], "conformance to requirements" [36], "loss avoidance" (Taguchi, cited in [37], "degree of excellence or superiority" [38], understanding and optimizing the whole system of value exchange [39, 40]. Regardless of the time period or context in which quality is examined, the concept has had multiple and often confusing definitions and has been used to describe a wide variety of phenomena.

For the agricultural industry, the quality of fresh and processed horticultural produce is assessed based on the combination of values from several attributes or characteristics specific to the commodity. Quality of fresh and processed produce encompasses sensory properties (appearance, texture, taste and aroma), nutritive values, chemical constituents, mechanical properties, functional properties and defects [41]. Therefore, it is difficult to decide on a single universal definition of quality with regards to horticultural products considering the different views on quality held by major stakeholders in the field of horticulture [42, 43].

2.1.2 Quality measurement and evaluation

The measurement of quality attributes of horticultural produce plays an important role in quality management during postharvest handling. These measurements allow for comparison against industrial standards by ensuring that the product meets the limits of acceptability by the consumer [44]. Product quality attributes may be evaluated using a sensory panel or instrumental analysis. The quality of agricultural commodities is characterized based on individual or a combination of various properties such as physical, chemical, and microbial characteristics [33]. These quality attributes includes appearance (size, shape, gloss and colour, freedom of defect and decay), texture (firmness, crispness, juiciness, mealiness), flavour (sweetness, acidity, astringency, aroma and off-flavours) and nutritive value (dietary fiber, vitamins, minerals, phytonutrients) [25, 45, 46]. Other measurable quality attributes like fat content, moisture and protein content are also analysed [47]. A block diagram of different food quality aspects and related parameters are presented in Figure 2.1.

The block diagram shows different food quality aspect and related parameters. The upper line indicates the different food quality aspects, while the bottom line is the different attributes on the different quality aspects.

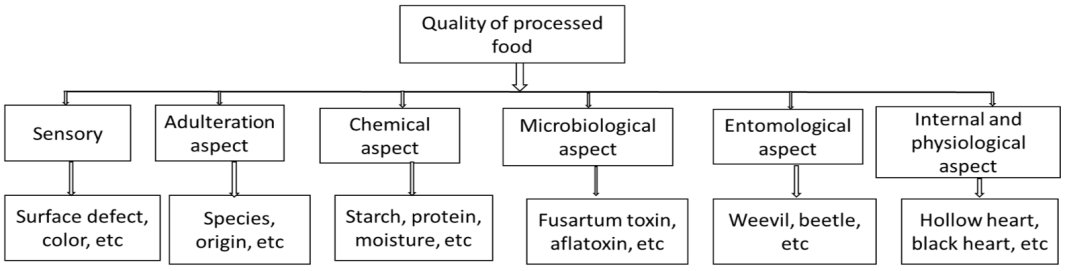

Figure 2.1: A block diagram of different food quality aspect and related parameters

2.1.3 Parameters used for evaluating models performance

For non-invasive quality analysis, the performances of multivariate models have been assessed based on different factors of merit. One of the mostly used is the coefficient of determination (R^2), for prediction (R^2_p), for calibration (R^2_c) and for cross-validation (R^2_{cv}).

Other statistical parameters explaining a good model includes root mean square error (RMSE) for calibration (RMSEC), prediction (RMSEP) and cross-validation (RMSECV), residual predictive deviation (RPD) and bias. Further information on different parameters used for evaluating the models performance have been extensively reviewed by [16, 48, 49].

2.2 Infrared spectroscopy (IRS)

2.2.1 Overview of infrared spectroscopy

Infrared (IR) spectroscopy includes visible to near infrared (Vis/NIR) and mid infrared (MIR) region of the electromagnetic spectrum. IRS technology employs the principle of interactions between matter that contains molecular bonds with the electromagnetic radiation in the near and mid infrared range. Vis/NIR and MIR spectroscopy cover an electromagnetic range of 12500 – 4000 cm^{-1} or 800 – 2500 nm (NIR), and 4000 – 400 cm^{-1} or 2500 – 25000 nm (MIR), respectively. The NIR spectrum of a biological product consists of broad bands arising from overlapping absorptions, corresponding mainly to overtones and combinations of vibrational modes. Chemical bonds between light atoms, such as C–H, O–H, and N–H, generally have high vibrational frequencies, which result in overtones. NIR spectroscopy has several advantages. It has the added versatility of penetrating food samples at finite distances and provides spectral information of surfaces and internal characteristics [15]. IR spectroscopy, on the other hand, captures more spectral information due to the higher resolution of the fundamental vibrational absorption bands compared to the broad overtone and combination absorption bands in the NIR region [20, 50]. A block diagram illustrating the basic steps for NIR spectral acquisition and model development is presented in Figure 2.2.

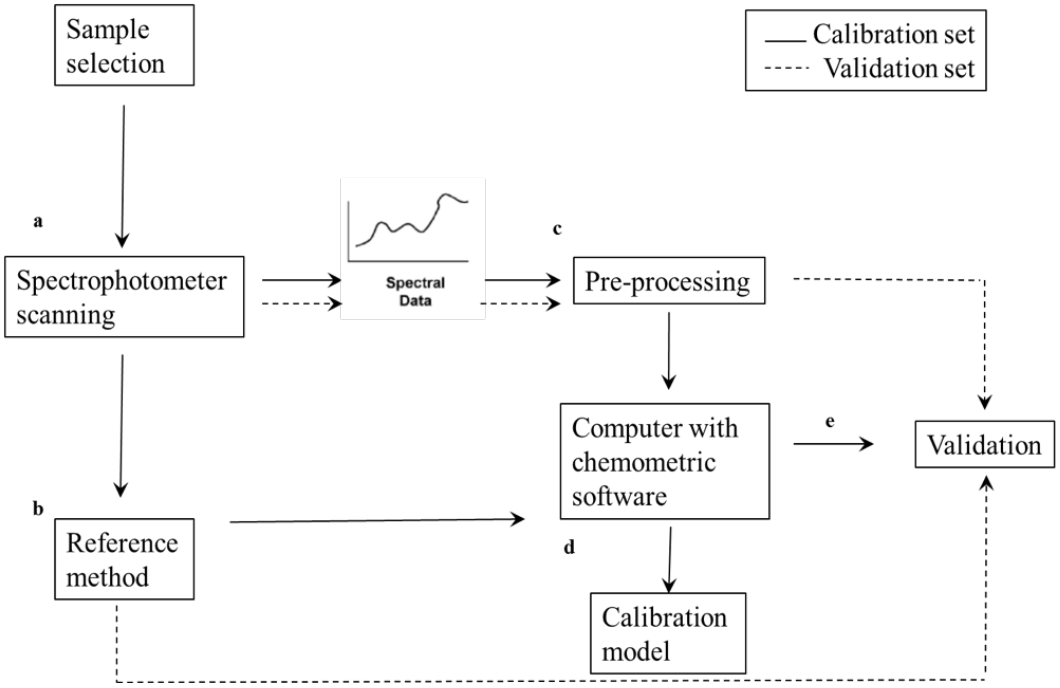

Figure 2.2: Block diagram with basic steps for developing NIR calibration model a) the sample is irradiated with NIR radiation, b) a fundamental analytical method also known as reference method is used to obtain the dependant variable to be calibrated, c) the acquired spectral data is subjected to pre-processing methods using chemometrics, d) the combination of reference and spectral data are used to develop calibration model, e) calibration model are validated to test the model performance.

2.2.2 Application of infrared spectroscopy for assessment of processed horticultural products

NIR and MIR spectroscopy in combination with multivariate data analysis has extensively been used for the characterization of food attributes, providing accurate, fast and cost-effective non-destructive quantification of major components in different food and processed agricultural materials.

2.2.2.1 Dried horticultural products

Food powders are dried solid materials and should meet specific quality standards, including moisture content, particle size, and particle morphology. Attention needs to be given to quality evaluation of powdery food particles, with emphases on parameters such as chemical composition (regarding starch, protein), adulteration and mycotoxin content. Recent progress and applications of IR spectroscopic technologies for non-invasive quality determination of powdery horticultural products are reviewed (Table 2.1). For the evaluation of tea powder, FT-NIR spectroscopy provided a satisfactory performance for the prediction of catechin, with prediction statistics of R^2 as high as 0.980, and RMSEP as low as 0.017% [51]. MIR spectroscopy was applied in a study by Li et al. [52] for the detection of polyphe-

nols in tea powder. In this study, the authors combined the wavelength selection algorithms of backward interval partial least squares (biPLSR). The partial least square (PLS) model provided comparable results (R^2=0.708) to the full spectral model (R^2=0.713), which demonstrated the effectiveness of the PLS regression model and the biPLSR-RF algorithm. In a different study, Li et al. [53] investigated FT-MIR spectroscopy to quantify talcum powder contamination in tea powder. Based on a hybrid of biPLSR, competitive adaptive reweighted sampling (CARS) and selection of 18 characteristic variables. The authors obtained better detection results of talcum concentration (R^2=0.927, RMSEP=0.137). Other physicochemical properties that were evaluated in using IR spectroscopy include starch [54], protein [55], metanil yellow [56] and total phenolic content [57].

Table 2.1: Summary of infrared spectroscopy applied for quality evaluation of different horticultural dried products

Products	Non-invasive analysis used	Parameters	Wavelength range	Predictors accuracy	References
Black tea	NIRs	Caffeine Free amino acid Total phenolics Water extract	12500 – 4000 cm^{-1}	R^2 = 0.955, RMSEP = 0.16% R^2 = 0.927, RMSEP = 0.273% R^2 = 0.954, RMSEP = 0.594% R^2 = 0.962, RMSEP = 0.685%	[57]
Chilli powder	NIRs	Aflatoxin B1	12000 – 4000 cm^{-1}	R^2 = 0.967, RMSECV = 0.654%	[23]
Chilli powder	NIRs	Sudan I dye adulterant	9000 – 4000 cm^{-1}	R^2 = 0.991, RMSEP = 0.141%	[58]
Corn flour	NIRs	Protein	10000 – 4000 cm^{-1}	R^2 = 0.882, RMSEP = 0.413%	[144]
Garlic powder	MIRs	Starch	4000 – 650 cm^{-1}	R^2 = 0.950 for VIP, R^2 = 0.890 for SR	[54]
Lotus root flour	MIRs	Starch	4000 – 500 cm^{-1}	R^2 = 0.981, SDR = 5.47%	[145]
Tea powder	MIRs	Catechin	1000 – 4000 cm^{-1}	R^2 = 0.921-0.971, RMSEP = 0.017%-0.384%	[51]
Tea powder	MIRs	Polyphenol	4000 – 400 cm^{-1}	R^2 = 0.708 - 0.713	[52]
Tea powder	MIRs	Talcum concentration	4000 – 400 cm^{-1}	R^2 = 0.927, RMSEP = 0.137%	[53]
Turmeric powder	MIRs	Metanil yellow	4000 – 650 cm^{-1} 3700 – 100 cm^{-1}	Detection of 5% (w/w) 1% (w/w)	[56]

RMSEP: root mean square error of prediction, NIRs: Near-infrared spectroscopy, MIRs: Mid-infrared spectroscopy, RMSECV: Root mean square error of cross validation, R^2:Coefficient of determine for validation, VIP: Variable importance in projection, SR: Selectivity ratios.

IR spectroscopy has been successfully used in detection and classification of mycotoxins and adulteration of powdered foods. For instance, Tripathi and Mishra, [23] used FT-NIR spectroscopy to detect Aflatoxin B1 in chilli powder. The developed PLSR model provided satisfactory prediction statistics with R^2 of 0.967 and RMSECV of 0.654%. For adulteration Haughey et al. [58], applied NIR spectroscopy to detect fraudulent adulteration of chili powder using Sudan dye (0.1 – 5%). The developed quantitative models determined that the limit of detection was 0.25%, and coefficients of determination (R^2) were found to be between 0.991 and 0.994. Hu et al. [59] also investigated the use of Fourier transform mid infrared spectroscopy to both identify adulteration of Sichuan pepper, and examine the authenticity of black pepper samples using both GA-SVM and PLS-DA calibration and prediction set models achieved 100% accurate classification rate. These studies have reported successful applications of both FT-NIRs and

FT-MIRs in the different horticultural dried or powdered products, suggesting that the techniques can be further explored for quality assessment of other dried fruit samples like dried pomegranate aril, banana slices, and others.

2.2.2.2 Juice products

Over the last decade, several research publications on the usage of IR spectroscopy for quality control and authenticity of commercial juices were published (Table 2.2). Xie et al. [60], investigated the usage of NIR spectroscopy to determine individual sugars (glucose, fructose, sucrose) in bayberry juice in the NIRS region of 800 – 2400 nm. According to Włodarska et al. [61], the NIRS region of 6896, 5587, and 4413 cm^{-1} as optimal for the assessment of sucrose, fructose, and glucose in apple juice. Masithoh et al. [62] reported Vis/NIR measurements for soluble solid content (SSC) and titratable acidity (TA) of Satsuma mandarin juice in the region of 600 – 1100 nm, with calibration model to predict SSC yielding $R^2 = 0.92$, standard error of prediction (SEP) = 0.42 °Brix and $R^2 = 0.56$ °Brix, SEP = 0.14% for acidity.

Table 2.2: Summary of infrared spectroscopy applied for quality evaluation of different horticultural juice products

Product	Non-invasive method	Parameters	Wavelength range	Predictors accuracy	References
Apple juice	NIRs	SSC TA SSC/TA	12500 – 4000 cm^{-1}	R^2 = 0.881, RMSECV = 0.277% R^2 = 0.761, RMSECV = 0.239% R^2 = 0.843, RMSECV = 0.113%	[61]
Bayberry juice	NIRs	Glucose Fructose Sucrose	800 – 2400 nm	R^2 = 0.74669 – 0.85492 R^2 = 0.69893 – 0.96364 R^2 = 0.89083 – 0.99321	[60]
Black currant juice	MIRs	SSC TA	7000 – 600 cm^{-1}	R^2 = 0.97, RMSECV = 1.14% R^2 = 0.96, RMSECV = 2.61%	[67]
Grape juice	Vis/ NIRS	SSC pH	325 – 1075 nm	R^2 = 0.979, RPD = 6.971 R^2 = 0.951, RPD = 5.432	[65]
Grape juice	MIR/NIR	TAC TPC	10000 – 829.11 cm^{-1} 10000 – 823.52 cm^{-1}	R^2 = 0.81, RMSEP = 4.22% R^2 = 0.90, RMSEP = 0.21%	[69]
Mango juice	MIRs	ASC TSS RJC	4000 – 650 cm^{-1}	R^2 = 0.996 R^2 = 0.997 R^2 = 0.986	[68]
Pomegranate juice	NIRs/MIRs	TSS TA TSS/TA	12500 – 4000 cm^{-1}	R^2 = 0.9234, RMSEP = 0.31%, RPD = 3.63 R^2 = 0.8623, RMSEP = 0.11, RPD = 2.7 R^2 = 0.8176, RMSEP = 1.04%, RPD = 2.35.	[20]
Strawberry juice	MIRs	Glucose, Sucrose, Fructose	1200 – 900 cm^{-1}	$R^2 \geq 0.97$	[63]
Satsuma mandarin	Vis/NIRs	SSC TA	600 – 1100 nm	R^2 = 0.92, SEP = 0.42 ºBrix R^2 = 0.56, SEP = 0.14%	[62]
Tomato juice	NIRs	SSC pH	800 – 2400 nm	100% accuracy	[66]
Tomato juice	MIRs	Glucose, Fructose, TSS, Viscosity	1460 – 950 cm^{-1}	$R^2 \geq 0.82$	[64]

R^2: coefficient of regression, RMSECV: root mean square error of cross validation, RMSEP: root mean square error of prediction, RPD: residual predictive deviation NIRs: Near-infrared spectroscopy, MIRs: Mid-infrared spectroscopy

In a recent study, Cassani et al. [63] investigated the usage of FT-MIR spectroscopy to simultaneously quantify simple sugars and exogenously added fructo-oligosaccharides (FOS) in 4 types of strawberry juices during storage. The authors performed principle component analysis which explained (76–97%) of the variation and observed high correlation coefficient R^2 >97% for the developed PLS models. Ayvaz et al. [64] applied FT-MIR spectroscopy in the spectral region of 1460–950 cm^{-1} for predicting glucose, fructose, total reducing sugars, soluble solids (°Brix) and serum viscosity in tomato juice. Using PLS regression analysis the authors predicted glucose (R^2=0.95%, SEP=1.4 g/L), fructose (R^2=0.95%, SEP=1.46 g/L), total reducing sugars (R^2=0.97%, SEP=2.06 g/L), soluble solids (°Brix) (R^2=0.99%, SEP=0.12 g/L) and serum viscosity (R^2=0.85%, SEP=1.32) with good accuracy. MIR spectroscopy has successfully been applied to evaluate the quality of several juices including grape [65], tomato [66], blackcurrant [67], mango [68] and pomegranates [20].

From the published literature, MIR spectroscopy seems better suited to evaluate the quality attributes of juices due to the higher resolution of the fundamental vibrational absorption bands compared to the broad overtone and combination absorption bands in the NIR region. For comparison between NIR and MIR spectroscopy, Caramês et al. [69] conducted a study to develop calibration models to predict total phenolic content (TPC) and total anthocyanin content (TAC) in grapefruit. In their study, 65 samples of grapefruit juice were used to develop calibration models employing partial least squares regression (PLSR) to predict TPC and TAC in grape juice. Results showed that MIR and NIR had a similar satisfactory performance to predict TAC presenting low RMSEP (4.22 mg/100 mL and 4.44 mg/100 mL). In TPC prediction, MIR provided an RMSEP (0.21 mg GAE/mL) slightly better compared to that of NIR (0.37 mg GAE/mL), indicating that MIR spectra are more accessible to interpret than the NIR spectra. In another study, Arendse et al. [20] statistically compared the usage of several NIR and MIR instruments for quality evaluation of pomegranate juices. The authors observed that MIR spectroscopy performed better in the prediction of quality parameters such as TSS, TA. However, their statistical approach based on Bland and Altman, and Passing-Bablok suggested that there were no significant differences between the results obtained with NIR or MIR spectroscopic measurements. This means that both spectra ranges of the infrared spectroscopy can be applied for quality analysis of juice samples.

IR spectroscopy have been used classification and authentication of adulterated juices. Xie et al. [70] reported that NIR spectroscopy has the ability in discriminating adulteration of bayberry juice with water using radial basis function neural network classifiers, acquiring a classification accuracy of 97.62%. Snurkovic et al. [71] demonstrated that NIR spectroscopy could detect a mixture of various substance such as water, sugar and other juice to fruit juices as evidenced by discriminant analysis applied to spectral data. Other reports on applications of infrared spectroscopy for authentication and detecting adulteration of fruit juices

have proven the relevance and effectiveness of this technique, based on studies predominantly in the 'mid-infrared' spectral range [68, 72].

2.2.2.3 Oil products

One of the quality control aspects of edible fats and oils is the determination of oxidation products. Oxidation of fats and oils produces either primary (peroxides) or secondary oxidation products. Recently, FT-IR spectroscopy, in combination with chemometrics, has been developed to monitor certain absorption bands that changed during oxidation. Table 2.3 compiles the usage of IR spectroscopy for quality assessment of different oil sample and oil blends samples that appear in several publications from 2009–2019. Marina et al. [73] applied 30 Fourier transform infrared (FT-IR) spectroscopy on 30 samples of virgin olive oil for the quantitative analysis of peroxide value (PV) using. In their study, calibration models were obtained that yielded satisfactory results with RMSEP value of 0.4978% and R^2=0.9826. In a similar study, Marina et al. [74] investigated the free fatty acid profile of virgin coconut oil using FT-MIR spectroscopy in the spectral region of 1730–1690 cm^{-1}. The authors obtained satisfactory results with (R^2=0.9281 and RMSEP=0.1264. Results show great potential of the application of FTIR in the rapid, accurately quantify VCO. In another study. Three essential quality of binary blend of palm and canola oil assessment was investigated by Mba et al. [75]. The authors achieved accurate results for iodine value (IV), free fatty acid (FFA) and peroixde value (PV) with (R^2 values $\geq$ 0.99 and RPD ranging from 6.11–11.60. Other quality parameters of different edible oils have been evaluated using IR spectroscopy. These include acid value [76], peroxide value [24, 77], total phenolic content [76], Squalene [14], and total sterol content [78].

Table 2.3: Summary of infrared spectroscopy applied for quality evaluation of different horticultural oil products

Products	Non-invasive method	Regression Analysis	Parameters	Wavelength range	Predictors accuracy	References
Extra Virgin Olive oil	NIRs	PLS	TSC SFA MUFA PUFA	9403 – 749 cm^{-1} 6800 – 6098, 5450 – 4597 cm^{-1} 5450 – 4597 cm^{-1} 9403 – 7498, 5025 – 4597 cm^{-1}	R^2 = 0.839, RPD = 2.64 R^2 = 0.998, RPD = 21.8 R^2 = 0.997, RPD = 18.7 R^2 = 0.998, RPD = 25.1	[78]
Olive oil	NIRs	PLS	MUFA PUFA SFA PV	3033 – 700 cm^{-1} 3033 – 700 cm^{-1} 3033 – 700 cm^{-1} 4000 – 700 cm^{-1}	R^2 = 0.89, REP = 1 % R^2 = 0.98, REP = 4 % R^2 = 0.71, REP = 6 % R^2 = 0.99, REP = 20 %	[77]
Olive oil	NIRs Vis/NIRs	PLS	Squalene Squalene	350 – 2500 nm 1100 – 2300 nm	R^2 = 0.83, RPD = 2.31 R^2 = 0.74, RPD = 1.94	[14]
Virgin olive oil	NIRs	PLS	SFA PV TPC	12,500 – 4000 cm^{-1}	R^2 = 0.42, RPD = 1.13 R^2 = 0.79, RPD = 1.64 R^2 = 0.79, RPD = 1.71	[24]
Virgin coconut oil	ATR-FT-MIRs		PV	4000 – 650 cm^{-1}	R^2 = 0.9826, RMSEP = 0.4978	[73]
Virgin coconut oil	ATR-FT-MIRs		FFA	1730 – 1690 cm^{-1}	R^2 = 0.9281, RMSEP = 0.1264	[74]
Rapeseed and canola oil blend	NIRs	PLS	AV TPC	1800 – 2200 nm 1100 – 1800 nm	R^2 = 0.99, RPD = 12.8 R^2 = 0.98, RPD = 7.8	[76]
Palm and canola oil blend	FT-NIRs	PLS	IV FFA PV	9404 – 7498 cm^{-1} 7502 – 6098 cm^{-1} 6102 – 5446 cm^{-1}	R^2 = 0.98, RPD = 6.11 R^2 = 0.99, RPD = 11.60 R^2 = 0.97, RPD = 6.40	[75]

FFA: Free fatty acid, PLS: partial least square, R^2: coefficient of determination for validation, REP: relative error of prediction, PV: Peroxide value, TSC: Total sterol content, SFA: saturated fatty acid, MUFA: Monounsaturated fatty acid, PUFA: Polyunsaturated fatty acid, NIRs: Near infrared spectroscopy, vis/NIRS; Visible infrared spectroscopy.

Researchers have also compared the performance of MIR and NIR in classification, authentication and adulteration detection for different horticultural oil products [79, 80, 81, 82]. Their findings showed the ability of this technique to successfully replace the existing traditional wet chemistry analytical methods of quality analysis.

2.3 Hyperspectral imaging (HSI) and multispectral imaging (MSI)

2.3.1 Overview of hyperspectral imaging (HSI) and multispectral imaging (MSI)

Hyperspectral imaging (HSI) also known as chemical and spectroscopic imaging integrates the main features of spectroscopic and imaging or computer vision [49]. It is often used to collect images with high spatial and spectral resolutions and has been widely used for the studied for food technique. It acquires monochromatic images with numerous (hundreds) continuous wavebands, and a full spectrum which are extracted for each pixel in an image. The data obtained from HSI systems are 3-dimensional (3-D) structures that consist of two spatial and one spectral dimension [16]. The process usually involves a significant amount of time for image acquisition under laboratory conditions and relatively complicated

procedures for offline image analysis. Multispectral imaging (MSI) on the other hand, is considered a reformation of the hyperspectral imaging [83]. It involves creating images using more than one spectral component of the electromagnetic wavelength from the same region of an object and at the same scale [48, 84]. MSI aims to acquire spatial and spectral information which is useful for real time applications (packinghouses and food processing plants). MSI accomplish this by capturing two or more waveband monochromatic images with a few (generally less than 10) discrete wavebands in the spectrum [85]. This process involves fast image acquisition and simple algorithms for image processing and decision making.

HSI and MSI make use of one of three methods to generate 3-D hyperspectral cubes [hypercubes (x, y, k)] namely, point (whiskbroom) scanning, line (pushbroom) scanning, and area scanning (tunable filter or staredown). A block diagram illustrating the basic steps HSI and MSI spectral acquisition and model development is presented in Figure 2.3.

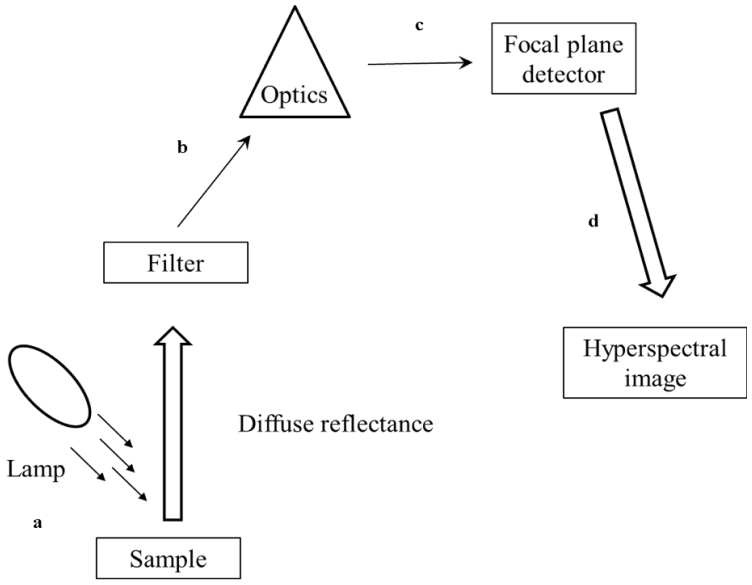

Figure 2.3: Block diagram of basic steps for hyperspectral imaging. a) The sample is radiated with NIR radiation, b) the reflected radiation is captured by a filter and optics which is responsible for wavelength selection, separation and measurement, c) the spectrum of each pixel is captured and is recorded by a detector, d) the image of the sample at each wavelength is recorded resulting in image slices

MSI for real-time application is not feasible as the point-scan method may not be suitable for fast image acquisition due to scanning along two spatial dimensions as it makes it time-consuming. Moreover, the previously mentioned methods (i.e. line-scan and area-scan) can be adjusted to meet the requirements for rapid image acquisition. Hyperspectral imaging when compared to traditional analytical methods is highly sensitive to minor constituents but has a poor limit of detection [86]. Further information on the principles of these technologies can be found in a review by Qin et al. [87].

2.3.2 Application of hyperspectral imaging (HSI) and multispectral (MSI) for assessment of processed horticultural products

As can be inferred from the research of Wu & Sun, [49] most of the applications of hyperspectral imaging concern the analysis of solid food products. MSI and HSI techniques have successfully been applied for the quality and safety assessment of intact fruits and vegetables mainly through reflectance mode in the ranges 400–1100 and 900–1700 nm. Their applications to fresh fruits and vegetables have been applied to determine contamination, bruises, surface defects, insect damage, microbial diseases, starch index, firmness, soluble solid content, sugar content, bitter pit, and chilling injury. However, on processed horticultural products, limited investigation has been conducted. For the evaluation of powdery foods, research and application of HSI have mainly been applied to the evaluation of agronomy powders such as soybean flour, wheat flour, spent flour and oat flour. The ranges usually considered were: 400–1000, 700–1000, 960–1750, and 1100–2400 nm [83]. These powders have been successfully analysed for colour classification, authenticity, contamination, and mycotoxins.

2.3.2.1 Dried horticultural products

The application of HSI to horticultural products have been on dried seed where it was used to discriminate different varieties of tomato. Wang et al. [88] applied the PLS-DA to distinguish different varieties of tomato. The authors applied on a spectral range of 375–970 nm and reported an accuracy of above 82%. In another study, Shrestha et al. [89] also discriminated tomato seed using PLS-DA and spectral range. The authors reported better accuracy of 99.6%. The polyphenols in tea was assessed using the HSI [90]. The authors reported regression of determination, R^2=0.915. Other applications of HSI has been reported on spinach seed [91] and watermelon seed [92].

2.3.2.2 Juice products

From literature search, it can be observed that limited information is available on the application of HSI and MSI on quality evaluation of horticultural processed juices. Reason for this may be due to the homogeneous nature of juice samples. Future research focus must be on this aspect of processed juice.

2.3.2.3 Oil products

The HSI has also successfully been applied for classification, authenticity detection and quality evaluation of edible oils. In a study on near-infrared hyperspectral imaging (NIR-HSI), Gou et al. [93] used HSI to classify edible oil and waste vegetable oil based on their spectral characteristics with the spectral region of 350–2500 nm. By applying unweighted distance method and interior square sum distance, the authors successfully classified 22 corresponding types based on clustering their hyperspectral digital numbers. Martinez-Gila et al. [94] applied HSI

for the evaluation of three chemical indexes: acidity, peroxide index and humidity content in virgin olive oil. The authors evaluated using 2 component algorithms, namely partial least squares regression (PLS) and genetic algorithm (GA-PLS). The authors reported comparable results for the two algorithms for acidity, peroxide index and humidity content, with R^2 of 0.95, 0.98, and 0.91, respectively for PLS and R^2 of 0.93, 0.92 and 0.92 for GA-PLS. Their results suggest that HSI can quickly and simultaneously predict various oil quality parameters. A summary of the different applications of HSI and MSI for quality evaluation of processed horticultural products is summarized in Table 2.4.

Table 2.4: Application of hyperspectral imaging in the evaluation of different processed horticultural products

Product	Non-invasive method	Regression Analysis	Parameters	Wavelength range	Predictors accuracy	Reference
Tea	HSI	PLS	Polyphenols	405 – 970 nm	$R^2 = 0.915$	[90]
Tomato seed	HSI	PLS-DA	Variety discrimination	375 – 970 nm	99.60 %	[89]
Tomato seed	HSI	PLS-DA	Variety discrimination	375 – 970 nm	≥ 82 %	[146]
Spinach seed	HSI	PLS-DA	Germination ability	395 – 970 nm	68 %	[91]
Virgin olive oil	HSI	PLS	Acidity	900 – 1700 nm	$R^2 = 0.95$	[94]
			Peroxide index humidity content		$R^2 = 0.98$ $R^2 = 0.91$	
		GA-PLS	Acidity	900 – 1700 nm	$R^2 = 0.93$	
			Peroxide index humidity content		$R^2 = 0.92$ $R^2 = 0.92$	
Watermelon	HSI	PLA-DA	Virus infection	1411 – 1867 nm	83.3 %	[92]
Edible cooking oils blend	HSI	PLS	Classification	350 – 2500 nm	100 %	[93]

GA-PLS: Genetic algorithm-Partial least squares, PLS: partial least squares, PLS-DA: Partial least squares-discriminant algorithm, R^2: coefficient of determination for validation

2.4 X-ray micro-computed tomography

2.4.1 Overview of X-ray micro-computed tomography

Microfocus X-ray computed tomography (μCT) is a visualization technique that reconstructs and render three-dimensional images which is used for characterization and defect detection [95, 96]. X-ray CT is a proven method for evaluating a cross-section of an object using a movable X-ray source and detector assembly to accumulate data from thousands of projected slices of a sample. The basic principle behind the CT is that the internal structure of an object can be reconstructed from multiple projections of the object [97].

X-ray computed tomography is based on X-ray radiograph. An X-ray beam is focused towards the sample, and the transmitted radiation is recorded by a multichannel detector. The transmission of the radiation depends on the mass density and mass absorption coefficient of the scanned material. A series of 2-dimensional

(2D) images are captured while rotating the sample between 0° and 180°, using filtered back-projection algorithm the volume of the object can be reconstructed into a 3-dimensional (3D) image which is superimposed information (projection) of the stack of (2D) images [95]. A block diagram illustrating the basic steps X-ray CT and image development are presented in Figure 2.4. X-ray CT allows for the

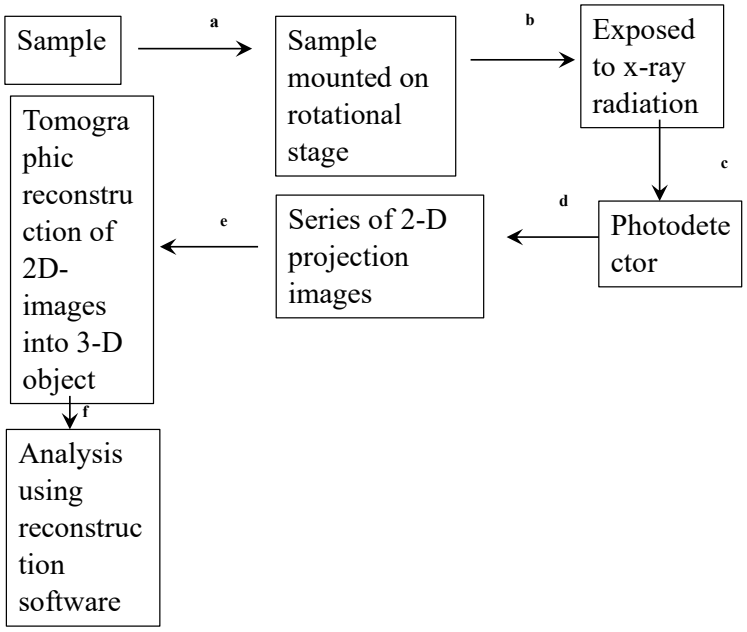

Figure 2.4: Block diagram of X-ray-CT acquisition and reconstruction process a) selected sample mounted on a rotational stage, b) A collimated X-ray radiation is focused on the sample c) the remainder radiation is captured by a multi-channel detector, d) which transmits a response signal to a computer and produces a series of 2-D projection images, e) 2-D images are then reconstructed into a 3-D object, f) the 3-D object is analysed using reconstruction software

visualization, characterisation and analysis of physical and physiological structures of biological materials with a resolution as low as few micrometres. Considering that fruits and vegetables have a high moisture content, water dominates X-ray absorption and defects that affect the density and the water content can, therefore, be visualized [95]. X-ray CT is one of the most powerful non-destructive techniques for the evaluation of internal and external characteristics including the detection of defects in agricultural products [84]. Further information on the principles of these technologies have been explained and extensively reviewed by Kotwaliwale et al. [96].

2.4.2 Application of X-ray computed tomography for assessment of processed horticultural products

The use of X-rays in the inspection of agricultural commodity is still in primary stage. Use of X-ray imagery for agricultural product inspection offers considerable

advantages and complements present inspection techniques [98]. Research studies with regards to X-ray μCT have mainly been focused on non-destructive characterisation of food microstructure for fresh horticultural fruits (Table 2.5). However, limited information has been published on any horticultural products processed into powders (dried) and seed oil. The application of X-ray has been shown to be an effective technique for estimation and characterization of internal structures. For instance, Arendse et al. [31] estimated the juice content of pomegranate fruit *cv*. 'Wonderful' grown in South Africa. The authors predicted the juice volume (142.7±16.4 mL) constituting 89.8% of the total aril volume (162.5±16.2 mL). In a similar study on the same fruit, Arendse et al. [99] quantified volumes of key parts of pomegranate fruit (*cv*. Wonderful) relevant to the food and beverage industry. These authors were able to estimate the total amount of arils per fruit and quantify volumes of arils, kernels, albedo and juice content. Magwaza & Opara [100] estimated the volume of minimally processed pomegranate arils. The limited knowledge of X-ray μCT applied on dried fruit samples and seed oil provides novel research opportunities that may evaluate the quality of these processed horticultural products.

Table 2.5: Summary of the information concerning the application of X-ray micro computed tomography in the evaluation of different processed products

Products	**Tube voltage and current**	**Spatial resolution**	**Application**	**Reference**
Banana slices	60 kV, 167mA	15 µm	Effect of far-infrared radiation on the microstructure	[101
Coffee beans	29 kV, 175 µm	2.8 µm	Microstructural changes induced by roasting	[103]
Coffee beans	19 and 20 keV	9 µm	Evaluation of microstructural properties	[102]
Minimally processed pomegranate arils	200 kV, 100 µA	71.4 µm.	Characterization and estimation of pomegranate arils	[100]
Pomegranate juice	245 kV, 300 µA	71.4 µm	Characterization and estimation of pomegranate juice, aril and peel	[31]
Pomegranate fruit parts	100 kV, 200 µA	71.4 µm	Estimation of pomegranate whole fruit and different parts	[147]

Although scientific literature is replete with studies exploring the research as-

pect of X-ray μCT for non-destructive defect detection and characterisation of internal and external structures of biological materials [101, 102, 103], on-line and real-time applications are limited. Some of the drawbacks of X-ray μCT systems is that they are expensive, bulky and more complicated to use than some other non-invasive technologies. Additionally, the vast amounts of data acquired during acquisition involve significant amount of time and relatively complicated procedures for offline image analysis. Another potential aspect includes the health and safety concerns that may arise from equipment usage. However, these drawbacks provide novel research opportunities in reducing large data size and time required for image analysis to provide rapid real time non-destructive characterisation and detection of internal defects.

2.5 Raman Spectroscopy

2.5.1 Overview of Raman spectroscopy

Raman spectroscopy is another analytical vibrational spectroscopy which has been employed for food quality analysis and authenticity. Theoretically, Raman spectroscopy is based on the principle that when light incident on a molecule interacts with the electron cloud of the bonds within a molecule, and the incident photon excites an electron into a virtual state. When a molecule is excited from the ground state to a virtual energy state and then relaxes into an excited vibrational state [104]. This scatter is referred to as Raman scattering. In this process, an elastic collision between the incident photon and the molecule of the sample occurs [105]. The scattered light is collected, then dispersed in a monochromator and then detected by a sensor [106]. As a result, the vibrational or rotational energy of the molecule is changed, and the scattered radiation is shifted to a different wavelength. The frequency difference between scattered radiation and incident radiation is called a Raman shift. If the molecule gains energy, scattered photons are shifted to longer wavelengths, giving rise to stokes lines in the Raman spectrum; otherwise, they are shifted to shorter wavelengths, giving rise to anti-stokes lines in the Raman spectrum [105]. The spectra that are generated from this relaxation and excitation of molecules of samples by radiation of light can provide a fingerprint of a specific substance, indicating the analysis of this compound, which offers the basis for structural analysis and qualitative analysis. A block diagram illustrating the basic steps of Raman spectroscopy is presented in Figure 2.5.

Raman spectroscopy has also been used to perform quantitative analysis because the intensity of an analyte band is linearly proportional to the analyte concentration, which can be represented by

$$I_v = I_o K_v C \tag{2.5.1}$$

where I_v is the measured Raman intensity, I_o is the excitation intensity, K_v is the constant and C is the analyte concentration. The vibrational spectrum as in the case of Raman spectroscopy provides similar information as the infrared (IR)

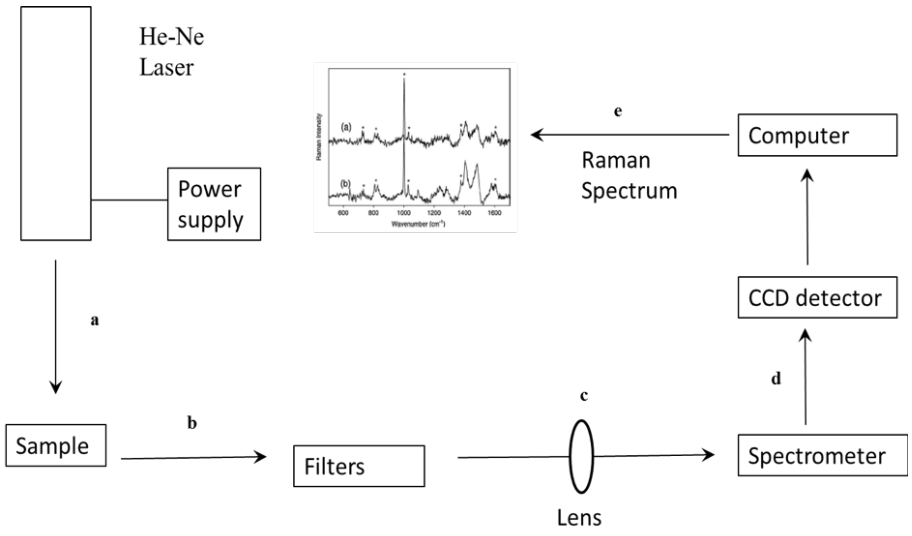

Figure 2.5: Block diagram illustrating basic steps using FT-Raman scattering a) high powered He-Ne laser provide an excitation signal to excite the sample of interest, b) the Raman signal scatters on the sample and passed though filters which eliminate the scattered Rayleigh light and transmit the desired wavelength only, d) the lens then focus and transfers the scattering signals to the Raman spectrometer which is detected by the CCD detector, e) a computer analyses the signals to form a set of spatially offset Raman spectra.

vibrational spectrum, but they have few important distinctions. For instance, Raman spectroscopy has high specificity, Raman bands have a good signal-to-noise ratio (SNR) and are non-overlapping, which allows Raman spectroscopy to be used for fingerprinting of samples to conduct analysis. Additionally, Raman spectroscopy provides good compatibility for the analysis of aqueous systems, since Raman spectra of water are weak and unobtrusive, making it an ideal tool for the application in aqueous solutions.

2.5.2 Application of Raman spectroscopy for assessment of processed horticultural products

Advances in instrumentation coupled with chemometric analysis have led to Raman spectroscopy being used as the tool of choice for an increasing number of applications in the food and beverage industry. Raman spectroscopy has several advantages. It is a rapid analysis, requires minimal sample preparation and compatibility with aqueous solutions. Such features make it a versatile tool for in-line or on-line analysis in different fields, including agricultural, pharmaceutical, biomedical, material science, geological and environmental science.

2.5.2.1 Dried horticultural products

Several studies on dried powder products have been done on processed horticultural products (Table 2.6). Reis et al. [107] applied Raman spectroscopy for the

detection of the adulteration of Sudan I dye in chilli powder. The authors observed high accuracy in their prediction model with R^2=0.994. Similarly, Pei et al. [108] discriminated between Sudan dye I and II in chilli powder and was able to detect to a limit of 0.6 mg/kg for Sudan I and 0.4 mg/kg for Sudan II respectively. This was also reported by [109], for paprika powder with good prediction model. The presence of melanin yellow was successfully detected in turmeric powder within the frequency range of 1800–200 cm^{-1} [56]. The authors obtained a classification model with a prediction coefficient of determination of 0.916 and a limit of detection (LOD) of 1%. Li et al. [110] applied the Raman spectroscopy to detect the presence of lead chrome green in tea powder at different concentrations. The models were developed using SPA and PLSR (Partial least square regression) multivariate analysis. Successive projection algorithm was used for wavenumber selection and of the selected 8, the corresponding characteristic wavenumbers were 2775, 2176, 1666, 1541, 1297, 988, 547 and 262 cm^{-1}. Based on these 8 characteristic wavenumbers, the detection model was built using PLSR. The authors reported the PLS model to give the best performance with R^2_p=0.936 and RMSEP=0803 with a LOD of lead chrome green was 0.651 mg/g.

Table 2.6: Summary of Raman spectroscopy applied for quality evaluation of powdered products

Products	Parameters	Wavelength range	Multivariate Analysis	Predictors accuracy	References
Chili powder	Sudan I dye adulterant	2000 – 200 cm^{-1}	SG, SNV, PCA, PCR, PLSDA	R^2 = 0.891 – 0.994	[107]
Chili powder	Sudan I, Sudan II adulterants	1700 – 400 cm^{-1}	PCA	Detection of 0.6 mg/kg and 0.4 mg/kg for sudan I and II respectively	[108]
Turmeric powder	Melanil yellow	3700 – 100 cm^{-1}	SG, MSC, BR	LOD = 1%	[56]
Tea powder	Lead chrome green	2804 – 230 cm^{-1}	PLSR, SPA	R^2 = 0.858	[110]
Chilli powderr	Sudan dye adulterant	2000 – 200 cm^{-1}	PLS, PLS-DA, PCA, PCR	R^2 = 0.971, LOD = 0.88%	[58]
Paprika powder	Sudan I adulterant	2200 – 200 cm^{-1}	PCA, PLSR	R^2 = 0.788 – 0.983	[109]

PLS-DA: partial least square discriminant analysis, LOD: Limit of detection, PCA: principal component analysis, SPA, successive projections algorithm, SNV: standard normal variate, SG: Savitzky-Golay, MSC: multiplicative scatter correction, BR: band ratio, PCR: principal components regression.

In another study, Ma et al. [111] applied Surface-enhanced Raman scattering (SERS) for authentication and detection purposes. The authors compared SERS and high-performance liquid chromatography (HPLC) for the detection of Carbendazim (CBZ) presence in tea. Their result detected CBZ to a limit of 0.1 mg kg^{-1} with an accuracy of R^2=0.9546 and RSD=12.4%.

2.5.2.2 Juice products

For the evaluation of juice quality, several researchers have applied Raman spectroscopy. A summary of Raman spectroscopy applied for quality evaluation of

horticultural juice products is presented in Table 2.7. For instance, Shende et al. [112] applied Surface-enhanced Raman spectroscopy (SERS) coupled with solid-phase extraction on orange juice to detect the presence of chlorpyrifos-methyl (CPM). The artificial addition of CPM to orange juice was detected in 12 minutes and at a concentration level of 50 ppb. This concentration was well below the EPA tolerance levels of 0.1 ppm for CP in citrus fruit. Malekfar et al. [113] reported the detection of carbohydrate and protein in tomato juice using the SERS Raman spectroscopy. The authors applied a spectral range of 100 and 4000 cm^{-1} and carbohydrates and protein were detected and assigned wavelengths of 738 cm^{-1}, 1333 cm^{-1} and 2930 cm^{-1}. The authors also observed that SERS proved to be an advantageous method to evaluate major parameters of tomato fruit in comparison with the normal spontaneous Raman spectroscopy and was suitable for application in quality control lines and fruit processing industries.

Table 2.7: Summary of Raman spectroscopy applied for quality evaluation of horticultural juice products

Products	Parameters	Wavelength range	Predictors accuracy	References
Apple juice	Detection of phosmet concentration in standard apply	200 – 2000 cm^{-1}	R^2 = 0.905 – 0.984	[148]
Citrus juice	Degree of freshness	100 – 1800 cm^{-1}	C_{fresh} range from 2.8 to 3.5	[114]
Pear juice	Detection of *A. alternate*	400 – 1800 cm^{-1}	LOD = 1.0 * 10^3 cfu/mL	[149]
Tomato juice	Carbohydrate, protein	700 – 1600 cm^{-1}	738 cm^{-1}, 1333 cm^{-1} and 2930 cm^{-1} assigned to Carbohydrate	[113]
Orange juice	Chlorpyrifos-methyl (CPM)	600 – 785 cm^{-1}	LOD = 50 ppb	[112]
Carrot juice	Polyacetylenes, carotenoids	400 – 550 nm	LOD = 1400 µg/g	[150]

Cfu: colony forming unit, C_{fresh}: coefficient of freshness, LOD: Limit of detection, PLSR: partial least square regression, PPB: parts per billion, SGS: Savitzky-Golay smoothing.

Nekvapil et al. [114] assessed the freshness of citrus juice using the Raman spectroscopy technique. Raman spectroscopy within the spectral range (100–1800 cm^{-1}) using two highly sensitive, high-resolution portable Raman systems with fiber optic probes. The authors reported that the coefficients of freshness (CFresh) value for the three varieties of citrus juice (the values associated to freshness) ranged from 2.8 to 3.5 for clementine (Day 1), 1.5 for both mandarins and tangerines, respectively. Meanwhile, the lowest values ranging between 0.5 and 0.8 were observed at a different time course for different species.

2.5.2.3 Oil products

The application of Raman spectroscopy for authentication, detection of adulteration and evaluation of quality attributes of oil have been reported by various

authors (Table 2.8). El-Abassy et al. [115] applied Raman spectroscopy to develop a calibration model using partial least squares regression. In this study, the degradation of carotenoid content in extra virgin oil was monitored when heated by microwave and conventional process in the spectral range of 945–1600 cm^{-1}. Their model result showed a high correlation coefficient R^2=0.99 and low RMSE of 0.027 and 0.079 for calibration and prediction respectively. El-Abassy et al. [116] in another study, detected adulteration of extra virgin olive oil with sunflower oil using the SERS technique. The authors obtained a very accurate model for their study. Ahmad et al. [117] used the Raman spectroscopy to define the cooking range of extra virgin olive oil at 140–150 °C at a wavenumber range of 540–1800 cm^{-1}. Sesame seed oil was assessed for authenticity and adulteration with other processed seed oils (vegetable oils from almond, castor, coconut, argan, avocado, macadamia, peanut, pumpkin, soybean, sunflower, olive carrot, jojoba, wheat seed, wild rose, marigold and pomegranate). The authors reported that the develop models were able to discriminate to an accuracy of 99.83% for all the oil samples due to a specific spectral band at 1651 cm^{-1} associated with the C=C stretching mode [118]. The linear discriminant analysis (LDA) was used for discriminant analysis, and sesame oil was successfully discriminated from other oil samples with accuracy of 100%.

Table 2.8: Summary of Raman spectroscopy applied for quality evaluation of horticultural oil products

Products	Parameters	Wavelength range	Multivariate Analysis	Predictors accuracy	References
EVOO	Carotenoid content	700–3100 cm^{-1}	PLSR	R^2 = 0.99	[115]
EVOO and Sunflower	Adulteration detection	700–3100 cm^{-1}	PCA and PLSR	$R^2 \geq 0.971$, LOD ≥ 1%	[116]
EVOO	Cooking temperature range	540 – 1800 cm^{-1}	SGS	Cooking range was established at 140 – 150 ºC	[117]
Different blends of edible oil	Discrimination of fatty acids.	800 – 3100 cm^{-1}	PLS	99.83%	[118]

LOD: Limit of detection, PCA: Principal component analysis, PLSR: partial least square regression, SGS: Savitzky-Golay smoothing, EVOO: Extra virgin olive oil, PLS: partial least square, R^2: coefficient of regression.

Raman spectroscopy is an emerging non-invasive technique and has enormous potential for biochemical and chemical structural analysis, which can be used in situation without the need of sample pre- treatment. One major advantage of this technique is its ability to provide information about concentration, structure, and interaction of biochemical molecules within intact cells and tissues [119]. Its applications in oil quality evaluation, however, is mainly focus on fat content, lipid oxidation and protein structures. As a single point spectroscopic technique, it is more efficient for adulteration detection and quality assessment for homogeneous samples. In most heterogeneous food samples, like in powdered products, the

Raman HSI is preferably applied for analysis purposes. The Raman HSI is a combination of Raman and hyperspectral imaging technique.

2.6 Nuclear magnetic resonance (NMR)

2.6.1 Overview of nuclear magnetic resonance

Nuclear magnetic resonance (NMR) is a quantum mechanical phenomenon that was discovered by scientists in the late 1930s. Historically, its discovery is credited to Isidor Rabi, who in 1938 successfully designed an experiment to detect and measure the magnetic spin of atomic nuclei in gases [120]. NMR is widely used to investigate the structure of various materials in different fields of science and medicine. Some of these materials include organic molecules, fresh and processed produce in the food industry and living tissue [120]. A block diagram illustrating the basic steps of the NMR technology is presented in Figure 2.6.

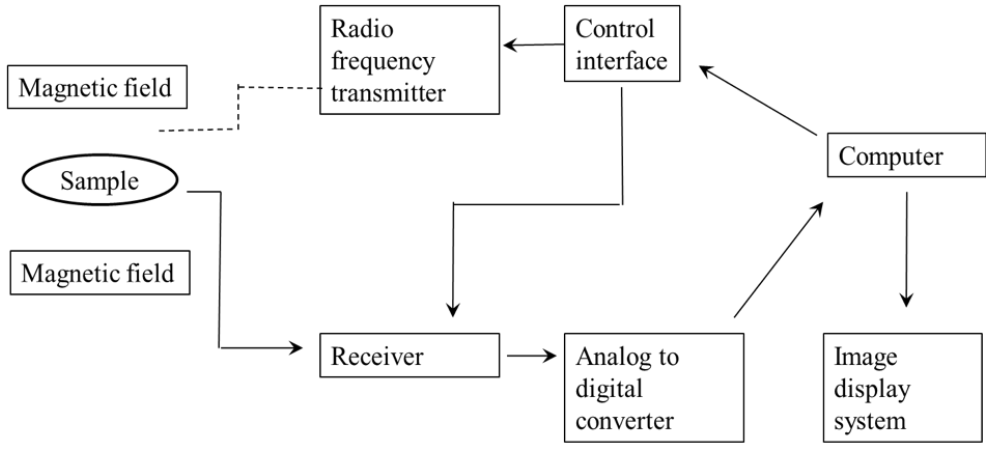

Figure 2.6: Block diagram of NMR imaging process. (a) Very strong magnetic fields is generated using superconducting electromagnets (b), the Radio frequency input signal receiver collects input from the response of the sample (c-g) signal produced by interaction of the sample and magnetic field is not ready for interpretation. It needs to be detected and processed to provide useful information which is then transmitted to (d) a computer and (e) produces an NMR spectrum.

The applications of various NMR methods can be divided into three main groups based on the type of equipment being used, which can provide versatile information about the chemical composition and structure of various biological systems. These include magnetic resonance spectroscopy (NMR), magnetic resonance imaging (MRI) and low-field (LF) NMR [121]. NMR is based on the principle that nuclei manifest when exposed to a magnetic field and electromagnetic (EM) pulse(s), which consists in the EM absorption of the pulse energy by the nuclei, followed by the back radiation of the absorbed energy at a specific resonance frequency [84]. One of the most important applications of NMR technique is to

measure water content and water distribution due to certain elements, especially hydrogen nuclei, which show high response to magnetic fields. NMR has unique advantages of detecting the variations in concentration or state of water and fats in fruits and vegetables. This derived information can be useful for the assessment of ripeness, defects, or decay in fruits and vegetables. NMR instruments require high magnetic fields and sophisticated electronics, so they are generally large and may be very expensive [122].

2.6.2 Application of nuclear magnetic resonance on assessment of processed horticultural products

A summary of the application of nuclear magnetic resonance in quality assessment on horticultural products is presented in Table 2.9. Review of literature has shown that NMR is mainly affected by the presence of water in food matrixes. Recent literature search indicates that much application of NMR on processed products has been deployed in measuring quality of whole fruits and liquid samples like in fruit juice and oil samples.

Table 2.9: Summary of nuclear magnetic resonance spectroscopy applied for quality evaluation of horticultural juice products

Products	Parameters	Frequency range	Multivariate Analysis	Predictor's Accuracy	References
Mango juice	Discrimination of different cultivars	0.8 MHz	PCA	LOD = 3.0 – 5.5 ppm	[126]
Orange juice	TSS pH	8.5 MHz	PLSR, S-GA	SEP = 0.88 SEP = 0.17	[123]
Orange juice	Discrimination of pure and adulterated orange juice	400 MHz	PLSR, PCR, GA-PLS	R^2 = 0.79	[125]
Pomegranate juice	TA TSS pH	1.7 MHz	PLS	R^2 = 0.54 R^2 = 0.60 R^2 = 0.63	[151]

PCA: principal component analysis, PLSR: Partial least square regression, PCR: Principal component regression, GA-PLS: Genetic algorithm-Partial least square, PLS: Partial least square, PPM: parts per million, LOD: limits of detection, SEP: standard error of prediction, R^2: coefficient of regression.

2.6.2.1 Juice products

Applications of NMR on fruit juices have been reported by several authors. Flores et al. [123] applied time domain nuclear magnetic resonance (TD-NMR), coupled with chemometrics for the prediction of different quality attributes in orange juice. The authors reported the standard error of prediction (SEP) of 0.88 and 0.71 for TSS and pH, respectively. The sensitivity and selectivity values of classification in the prediction set (n=90) were 0.81 and 0.90, respectively. These values are very close to 1, thus indicating the suitability of the method to classify oranges in terms of low and high TSS using the TD-NMR and PLSR.

Caroline et al. [124] applied the ^{1}H NMR at a frequency range of 400.13 MHz in grape juice. Their model was able to detect the addition of other juices successfully. Principal component analysis (PCA) was performed and a classification accuracy of 0.93 was achieved.

Vigneau et al. [125] applied the ^{1}H NMR at 400 MHz for the qualitative evaluation of orange juice. The authors discriminated between authentic and adulterated (clementine juice) samples of orange juices. A total of 150 samples, including both authentic and adulterated orange juices ranging in different concentrations (10–60%). The authors applied PLSR, PCR and GA-PLS on the obtained NMR spectral data and reported the GA-PLS algorithm should be used as it provided the best performing model for GA-PLS for R^2=0.79. In a study to discriminate between five different mango cultivars, Koda et al. [126] applied ^{1}H NMR on mango juice samples. The authors successfully applied a combination of unsupervised principal component analysis (PCA) with low-field region on the spectrum obtained. ^{1}H NMR spectra obtained by band-selective excitation provided a good discriminant model for the five mango cultivars. The authors identified several minor components in mango juice and assigned a signal of the minor components this includes arginine, histidine, phenylalanine, glutamine, shikimic acid, and trigonelline. Their study showed that these components were important for the classification of the five mango cultivars.

2.6.2.2 Oil products

NMR has been successfully applied for quality measurement and quality control of oil products derived from horticultural produce. Skiera et al. [127] applied the ^{1}H NMR on 120 samples of blends of different edible oils to determine the acid value (AV) and peroxide value (PV). The authors used a frequency of 400.17 MHz and reported a relative sensitivity ($RS_{NMR/AV}$ of 0.90). Their result from the model indicated that both methods (Classical and ^{1}H NMR) of analysis, exhibited a similar analytical performance. Andrade et al. [128] assessed the presence of fatty acids methanol esters (FAME) in different vegetable oil blends (soybean, corn, sunflower, canola, linseed, cottonseed and jatropha) within a spectral wavelength of 200 MHz. The authors reported a chemical shift that is characteristic of the methoxyl groups in methyl esters. Their findings showed the limitation of ^{1}H-NMR in the characterization of FAME products and its success as it obtained a good resolution for all the ^{1}H- NMR spectra of the transesterification products.

Sega et al. [129] observed the ozonation of sesame oil using the NMR. In their study, they established relationship between the integral values of the signals corresponding to protons which resonate at either both 5.29 and 1.97 ppm, or 5.11–5.08 ppm in the ^{1}H NMR and the iodine values (IV) and peroxide value (PV) respectively. Table 2.10. provides a summary of NMR applied for the quality evaluation on processed horticultural oil products.

Table 2.10: Summary of nuclear magnetic resonance applied for quality evaluation of horticultural oil products

Products	Parameters	Wavelength range	Predictor's Accuracy	References
EVOO	Stability of oil	300 MHz	Order of stability are MO > EVOO > AKO > SO.	[152]
Different blend of edible oil	Free fatty acid	400.17 MHz	$R^2 = 0.9$.	[127]
Different blends of vegetable oils	SFA, linoleic acid	200 MHz	methoxyl ($\delta = 3.70$) and glyceryl methylene ($\delta = 4.10 – 4.40$) protons, respectively.	[128]

EVOO: extra virgin olive oil, R^2: coefficient of determination, SFA: saturated fatty acids, δ: chemical shift, MO: moringa oil, AKO: apricot kernel oil, SO: sunflower oil

2.7 Other spectroscopy technologies

2.7.1 Dielectric spectroscopy

2.7.1.1 Overview of dielectric spectroscopy on assessment of processed horticultural products

Dielectric spectroscopy is another non-invasive technological tool useful for examining the interaction between the electric field and tested material. It springs from the effect of dielectric mechanisms and polarization effect, which comprise the dielectric permittivity of the object. The dielectric properties of binary mixture of solids and liquids have been researched extensively by various researchers [130]. Dielectric spectroscopy provides information about the dielectric response of materials to electromagnetic fields. It is a convenient method for evaluating food quality, especially for detecting moisture content in foods [131]. The dielectric properties of interest in most applications are the dielectric constant ϵ' and loss factor ϵ''. The dielectric constant indicates the ability of a material to store electric energy in the material, and the loss factor, which is associated with energy dissipation or conversion from electric energy to heat energy.

Different factors influence the dielectric properties of materials such as frequency of the applied alternating electric field, moisture content, bulk density, temperature, ionic nature, concentration (density), structure and constituents of materials [132]. Dielectric properties usually correlate to temperature, frequencies, and these findings have been reported for different agricultural commodities.

2.7.1.2 Application of dielectric spectroscopy for the assessment of processed horticultural products

Research had shown that the dielectric properties of processed agricultural products are linked to their internal features or composition [132]. For instance, quantitative determination of the levels of adulterant in extra-virgin olive oil was researched by [130]. Their results showed good prediction capability for the concentration of the vegetable oil adulterant on the olive oil. PCA was used to classify the adulterant while the PLS model showed good prediction with RMS = 0.053

and $R^2 = 0.967$ with LOD below 5%.

Sosa-Morales et al. [133] measured dielectric properties and sweetness (TSS) of freshly harvested melons with an open-ended coaxial-line probe using an impedance analyser over the frequency range from 10 MHz to 1.8 GHz at 25 °C and reported that correlations were low for both the dielectric constant and the loss factor at most frequencies

2.7.2 Fluorescence spectroscopy

2.7.2.1 Overview of fluorescence spectroscopy on assessment of processed horticultural products

Fluorescence spectroscopy is an analytical technique whose theory and methodology have been extensively applied for studies of molecular structure and function in the discipline of chemistry and biochemistry. The introduction of new commercially available instruments for fluorescence analysis, particularly, front-face fluorescence spectroscopy (FFFS), has caused a recent rise in the use of the fluorescence technique for food analysis [134]. Fluorescence is the emission of light subsequent to absorption of ultraviolet or visible light of a fluorescent molecule or substructure, called a fluorophore [135]. Thus, the fluorophore absorbs energy in the form of light at a specific wavelength and liberate energy in the form of emission of light at a higher wavelength. In theory, when electrons are excited by fluorescent light, this light is absorbed by the molecule, and it is transferred to an electronically excited state, meaning that an electron goes from the ground singlet states, S^0, to an excited singlet state, S'^1. This is followed by a vibrational relaxation where the molecule undergoes a transition from an upper electronically excited state to a lower one, S^1, without any radiation. Finally, the emission occurs typically 10^{-8} s after the excitation. In molecules, each electronical state has several associated vibrational states. In the ground state, almost all molecules occupy the lowest vibrational level. By excitation with ultraviolet or visible light, it is possible to promote the molecule of interest to one of several vibrational levels for the given electronically excited level. Therefore, excitation and emission spectra are obtained to describe the detailed fluorescence characteristics of molecules. In fact, fluorescence is characterized by two wavelength parameters that significantly improve the specificity of the method, compared to spectroscopic techniques based only on absorption: the quantum yield and the excitation and emission spectra.

The spectrofluorimeter, which is the instrument for measuring steady state fluorescence consists of the following components; a light source. This is usually xenon or mercury lamp. Then two monochromator(s) and/or filter(s), one for selecting the excitation wavelengths and the other for selecting the emission wavelengths. The other components include a sample compartment; a detector, which converts the emitted light to an electric signal; and a unit for data acquisition and analysis. The FFFS and SFS (synchronous fluorescence spectroscopy) are two fluorescence spectroscopy methods that have been utilized to determine

the quality of processed food substances with thick surfaces. In the coming years, FFFS and SFS combined with chemometric tools could be a reliable tool for understanding the bases of molecular food structure and, consequently, their quality characteristics.

2.7.2.2 Application of fluorescence spectroscopy for assessment of processed horticultural products

Recently, fluorescence spectroscopy in combination with multi-dimensional multivariate techniques have been applied for the evaluation of food, dairy and vegetable products. For instance, Boubellouta & Dufour [136] reported using synchronous fluorescence spectroscopy for the determination of fat melting and cheese melting of two cheese varieties (Comté and Raclette). Saito [137] showed that Napa cabbage (*Brassica rapa* L.) laser-induced fluorescence (LIF) spectra of a normal core and a rotten core show greater intensities in the green wavelength range of the LIF spectrum of the rotten core in comparison to that of the normal core. The integrated peak area between 450 and 600 nm for the rotten core was more than twice that for the normal core. In a study on oil sample, Jiang et al. [138] applied the synchronous front-face fluorescence spectroscopy for the discrimination of used frying oil (UFO) from edible vegetable oil. Partial least squares regression (PLSR) was used on 50 adulterant samples prepared in the range of 1–50%. From their results, model exhibited high linearity (R^2>0.96), with both root mean square error of cross-validation (RMSECV) and root mean square error of prediction (RMSEP) values lower than 3%. The high accuracy and sensitivity of the model indicates that the synchronous front-face fluorescence spectroscopy can be an effectively and accurately used to measure quantitatively and qualitatively the quality of horticultural and agricultural oil sample. Other applications of fluorescence spectroscopy on different food materials includes measuring PV and acidity of olive oil [139], detection of adulteration of orange juice with grape fruit [140], and to monitor thermal degradation of different oil samples [141].

Though this review focuses on examples from processed horticultural products, the principles are broader, and fluorescence could be applied to whole fruits or other fields (pharmaceutical, biotechnology). Fluorescence spectroscopy being a very sensitive tool, is always limited to samples or materials that have fluorescence effect [135]. Traditional right-angle fluorescence spectroscopic technique cannot be applied to thick substances due to large absorbance and scattering of light.

2.8 Future Prospects

The application of infrared spectroscopy has shown that it is suitable for an array of applications in the food and beverage industry. IS spectroscopy combined with advanced chemometric software packages has been applied successfully for online and inline analysis including the development of portable hand-held devices mak-

ing it the preferred method for non-invasive measurement.

Hyperspectral imaging, however, differs from the other techniques for non-invasive analysis of horticultural processed food products. It is a point-based scanning technique and only examine a relatively small area of a specimen; thus, these techniques are unable to provide spatial information that is important for many food inspection applications, especially involving heterogeneous food samples [142].

Considering that limited information exists on the application of HSI and MSI on quality evaluation of horticultural powders and liquids, future research with HSI and MSI should focus on developing models to predict various quality parameters including, detection of adulteration. Furthermore, in order to develop systems for commercial application additional research needs to focus on reducing the total volume of the data, which is the key for building effective HSI and MSI systems. In practice, this means acquiring images with relatively low spatial resolutions at a few important wavelengths, thereby improving speed required for analysis. Currently, with the large accumulation of vast amounts of data due to multi-dimensional datasets from HSI, this application is currently used for academic research.

NMR on the other hand, is best suited for measurement and evaluation of food and processed agricultural products with high water content and water distribution. It is due to certain elements being present, especially hydrogen nuclei from water molecules which shows high response to magnetic fields. Although, the disadvantage of NMR systems that prevent it from being used outside the research field is that they require high magnetic fields, sophisticated electronics and therefore are generally quite large and expensive. Further research into fabrication of small, easy and cost-effective hand-held NMR devices is encouraged [143].

Compared to other non-invasive techniques, the Raman spectroscopy can be used on solids, liquids and gasses food substances and requires no prior sample preparation and can be applied regardless of sample thickness, shape or size. It provides information about concentration, structure and interaction of biochemical molecules within intact cells. However, when comparing Raman spectroscopy to IR spectroscopy, Raman spectroscopy has a low sensitivity for detection of concentration for substance. Also, Raman spectroscopy involves heating of samples using a laser. This means that samples placed on metals and alloys cannot be analysed. The FT-IR and Raman spectroscopies can only acquire spectral data from a single point of a sample to determine food quality attributes of heterogeneity. It indicates that these single point spectroscopies (such as FT-IR and Raman) are more effective for inspection of adulteration and chemical properties. Imaging techniques such as the X-ray CT is not effective for checking the composition of homogeneous samples but are more valuable for detecting particulate impurities that tend to random probability distribution [16].

2.9 Concluding remarks

As discussed in this review, diverse processed products contain fingerprint and valuable information regarding the composition and nutritional properties. The vast potential for the application of the various spectroscopy techniques combined with multivariate statistical analyses for the evaluation of processed products has been demonstrated. Differences between food substances have been related to the dissimilarities in the molecular structure of the samples when they are irradiated under different wavelengths ranges. Several of these methods are suited as an effective research tool and can be a part of the evaluation procedure for processed food quality.

The diverse chemometric analysis methods are combined with various non-invasive technique to enable the extraction of relevant information from different processed food samples. The different spectroscopic technological tools reviewed offer potential for non-destructive measurement and prediction of various quality attributes. However, these applications face many challenges. For instance, challenges such as online application is still a problem. This is due to factors such as practicality, high cost of equipment, data acquisition and processing times, potential health hazard when utilizing equipment such as X-ray CT and NMR is still an issue with regards to analysis [84].

Considering the prospects of non-destructive and non-invasive approaches in quality assessment for processed food products in recent research studies, further work is required to utilize more refined and effective chemometric algorithms to increase the evaluation accuracy of processed horticultural products. Primary emphasis should be aimed at the selection of a practicable models for quality parameter calibration and prediction, as it is a critical step to achieving reliable results. Another focus is on acquiring spectroscopic data, with their valuable imaging information, that can provide more details on the quality attributes of food powders [16]. Therefore, to fully exploit the full potential of the above-described technologies for successful application, future research needs to focus on reliability and robustness of objective measurements as well as reduction of data acquisition and processing times.

Chapter 3

Application of Fourier-transformed near infrared spectroscopy (FT-NIRS) combined with chemometrics for evaluation of quality attributes of dried pomegranate arils

Pomegranate fruit contains high nutritional and potent pharmacological properties and is currently ranked 18^{th} as the most consumed fruit in the world. Like in many horticultural crops, fresh pomegranate arils have a relatively short shelf-life of 5 to 8 days and hence high postharvest losses. In order to overcome this limitation, the pomegranate industry has promoted research and development of value-added pomegranate co-products such as dried pomegranate arils, pomegranate seed oil, dehydrated powder and juices. However, the quality and safety of processed products are a major concern for processors and consumers. Standard techniques used for quality and microbial evaluation are labour intensive, not consistent and often require specialized sample preparation. Therefore, in this study we investigated the usage of Fourier-transformed near infrared (FT-NIR) reflectance spectroscopy as a fast and non-destructive method. FT-NIR spectroscopy was used over a spectral range of 800–2500 nm to develop multivariate prediction models for physical, chemical and phytochemical parameters of dried pomegranate arils (*cv.* Wonderful). Results from two different regression techniques, namely partial least squares (PLS) and support vector machine (SVM) were compared. Model development results showed varied success with statistics from PLS regression showing reliable prediction for pH (R^2=0.86, RMSEP=0.13, RPD=2.38) and TSS/TA (R^2= 0.74, RMSEP=1.68, RPD=1.68). SVM performed better for the prediction of titratable acidity ((R^2=0.85, RMSEP=0.04, RPD=2.50) and colour attributes for redness (a^*) (R^2=0.72, RMSEP=1.82, RPD=1.71) and Chroma (C^*) (R^2=0.70, RMSEP=1.99 RPD=1.77). In summary, SVM performed better than PLS re-

gression in the prediction of quality attributes for died pomegranate arils. This study demonstrated that FT-NIRs with SVM regression algorithm can be used as a non-invasive technique to evaluate key visual and sensory attributes of dried pomegranate arils.

3.1 Introduction

Pomegranate (*Punica granatum* L.) is a fruit bearing deciduous shrub or small tree belonging to family punicaceae. The fruit originates from Persia (Iran) and has widely been cultivated in the Mediterranean region [153]. The fruit is spherically shaped, has a thick leathery exocarp and an interior that is separated by membrane walls and packed into compartments. The compartments consist of edible portions called arils, which are surrounded by a translucent sac containing juice and each aril has a seed. The combined aril weight ranges from 40 to 60% of the total fruit weight, whereas the juice volume comprises about 70 to 80% of the total aril weight [19, 154]. The consumption of pomegranate fruit has remarkably increased in recent years, the fruit is currently ranked 18th as the most consumed fruit within the world [10]. This is primarily due to the extensive knowledge acquired on the health benefits linked to its consumption and increased public awareness as a functional food [13, 14]. Scientific evidence have linked the consumption of pomegranate fruit and its co-products such as arils, juice and oils to improved human health as result of the unique and high phytochemical composition, which have been reported in literature to provide potent pharmalogical properties [1, 5]. Despite the nutritional and health benefits, consumption is still limited due to the difficulty of extracting the arils. Currently, in order to increase consumption of pomegranate fruit by consumers, the edible portion has been processed by the food industry into ready to eat fresh arils. However, fresh arils have a relatively short shelf-life of 5 to 8 days [155] Therefore, to overcome this limitation of short shelf-life the pomegranate industry has promoted research and development of value-added pomegranate co-products such as dried pomegranate arils, pomegranate seed oil, dehydrated powder and juices.

One of the many opportunities identified for extending the shelf-life of pomegranate arils was to add value through dehydration. Products in this category are characterized with low moisture content and thus the rate of quality deterioration is minimised. Dried pomegranate arils are consumed in large quantities and are commercially available in West and East Asian counties. Within South Africa, dried pomegranate arils are an emerging and rapidly growing product. Dried pomegranate arils are reported to have a high source of vitamins, mineral elements, fatty acids and antioxidant compounds [7, 8]. Through value addition, the pomegranate industry can reduce waste and provide products with higher resale value and longer shelf life.

The quality and safety of fresh and processed food are usually defined by its physical, chemical and microbial characteristics. Traditionally, assessment of

quality and safety involves human visual inspection, in addition to chemical or biological determination experiments which are tedious, time-consuming, destructive, and sometimes environmentally unfriendly. Some of these existing standard destructive methods used for quality control include high performance liquid chromatography (HPLC), gas chromatography-mass spectrometry (GC-MS), spectrometric, colorimetric and microbiological methods [15, 156, 157]. This has led the agribusiness industry to invest in objective, fast, real-time and non-chemical detection technology, for quality assessment on colour [46], on sweetness [33] and on textural [25, 158] characteristics.

Near infrared spectroscopy (NIRS) is a vibrational spectroscopic technique that has been proven to overcome the limitations from standard destructive methods for quality evaluation for a variety of fruits and vegetables [15, 95, 159]. NIRS is based on the absorption of electro-magnetic radiation at wavelength in the range 780–2500 nm [160] The NIR spectra of food comprise of broad bands arising from overlapping absorptions corresponding mainly to overtones and combinations of vibrational modes involving C–H, O–H, and N–H chemical bonds. Due to the broad and overlapping bands associated with NIR spectra, multivariate statistical approaches are required to extract useful information from the NIR spectra [161]. Several factors may affect the spectral quality such as wavelength-dependent scattering effects, instrumental noise, ambient effects and several other sources of variability [162]. Therefore, in order to correlate spectral data (independent variables) to a specific quality attribute (dependent variables) regression techniques are required [26]. As a result, studies have focused on developing calibration models, testing and comparing different pre-processing methods and optimizing only a specific regression method [18, 163, 164, 165].

In the present study, two different regression algorithms are compared: partial least squares (PLS) and support vector machine (SVM). PLS is today probably the most widely linear applied method in chemometrics and was first developed by Herman Wold and introduced in the 1975 to deal with problems concerning econometric path-modelling [166]. In PLS regression an orthogonal basis of latent variables (LV) is constructed. In quantitative spectroscopy, PLS analysis is commonly used to compare spectroscopic data (X) with associated physico-chemical data (Y) [167]. In this way it is ensured that the latent variables are ordered according to their relevance for predicting the Y-variable [15]. Furthermore, PLS analysis always gives the lowest number of LV and excludes LVs that are not important in describing the variance of the quality parameter [167]. Whereas, SVM has gained widespread acceptance in data-driven applications and the ability for non-linear modelling applications. SVM was introduced by Vapnik and others in the early 1990s as machine learning systems that utilize a hypothesis space of linear functions in a high dimensional feature space, trained with optimization algorithms that implements a learning bias derived from statistical learning theory. The basic principle behind SVM regression is to map the original data set from the input space to a high dimensional, or even infinite-dimensional feature space

so that classification problem becomes simpler in the feature space. SVMs have the potential to pro-create an unknown relationship present between a set of input variables and the output of the system. The main advantage of SVM is that, it uses kernel trick to build expert knowledge about a problem so that both model complexity and prediction error are simultaneously minimized [168].

For pomegranates, Fourier-transformed near infrared spectroscopy (FT-NIR) combined with multivariate analysis have successfully been used to evaluate postharvest rind disorders [169], quality attributes of whole fruit [18], and several of its co-products such as fresh arils [170] and pomegranate juice [20]. However, this research study is the first application of FT-NIRs in the evaluation of quality attributes of dried pomegranate arils. Therefore, this research study was undertaken to explore the usage of these two different regression algorithms specifically PLS and SVM for evaluating the organoleptic and phytochemical attributes of dried pomegranate arils.

3.2 Materials and methods

3.2.1 Fruit procurement and sample preparation

This research was performed during the 2018 season with pomegranate fruit (*cv.* Wonderful). A total of 210 fruit, 70 from each of three different commercial orchards were procured from Sonlia pack-house and transported to Postharvest Technology and Research Laboratory, Stellenbosch University. Upon arrival, fruit without any physical defect and with good appearance were sorted and placed under cold storage at 10 °C before being processed into arils. Arils from each fruit were manually extracted at ambient conditions (21 °C ± 65% RH). Fresh pomegranate arils were placed onto an aluminium dish and subjected to hot air dryer (OTE 160, PROLAB South Africa). Samples were dried at 60 °C for 16-18 h in order to obtain a moisture content of 10-12%. After drying, a total of 25 samples for each orchard containing approximately 45 g of dried arils was used for spectral acquisition and reference methods. The dried arils were then placed and marked inside metallized bags and stored at ambient conditions (21 °C ± 65% RH) until further use.

3.2.2 FT-NIR spectral acquisition

NIR spectral acquisition was performed on 70 samples each containing 45 grams of dried arils in diffuse reflectance mode within the spectral range of 800–2500 nm using a Multi-Purpose Analyzer (MPA) FT-NIR spectrophotometer (Bruker Optics, Ettlingen, Germany). The MPA was equipped with an integrating sphere (IS) for direct contact with the sample and fitted with a permanently aligned and highly stable RockSolid^{TM} interferometer which comprised of gold coated mirrors. The NIR beam is directed into the sphere and travels directly through the centre of the sphere and the optical window into the aril sample. Due to the gold coating, all

light beams are collected and directed towards the detector [163]. The integrating sphere makes use of a high sensitivity PbS detector with nonlinearity correction [163]. An internal gold reference spectrum was obtained by mechanically closing the optical window with a gold reference plate. The MPA scanning settings used a resolution of 8 cm^{-1} and scanner velocity of 10 kHz. A total of thirty grams of dried pomegranate arils was placed in a 50 mm width accessory sample holder. For each sample a single scan was taken and for each spectrum a total of sixty-four scans were acquired with a scanning time of about 60 s per sample and the spectra was averaged to obtain a single spectrum. Instrument control, processing and data acquisition were performed using OPUS software (v.6.5 Bruker Optics, Ettlingen, Germany).

3.2.3 Reference measurements

Aril colour was measured in CIELAB coordinates (L^*, a^*, b^*) with a Minolta Chroma Meter CR-400 (Minolta Corp, Osaka, Japan). Measurements were performed on dried arils in a glass petri dish. From the L^*, a^*, b^* values, the colour components' Chroma and Hue (h°) values were calculated according to Pathare et al. [171].

Total soluble solids (TSS) was measured using digital hand-held refractometer (Palette, PR-32α, Atago, Tokyo, Japan) and results were expressed as percentage. The pH values were determined at room temperature using a calibrated pH meter (Crison, Model 00924, Barcelona, Spain). Titratable acidity (TA) was measured by diluting 2 mL of supernatant in 70 mL of distilled water and titrating with 0.1M NaOH using a Metrohm 862 compact titrosampler (Herisua, Switzerland) results were expressed in percentage of citric acid. TSS/TA was also calculated [18]. These measurements were performed in triplicate and average was calculated expressed as mean ±SD.

Total phenolic content was quantified using Folin-Ciocalteu method [172] with modification according to Fawole et al. [173]. Briefly, in triplicate 50 μL of juice supernatant was diluted with 450 μL of 50% methanol (v/v) before the addition of 1N Folin C (500 μL) and 2% sodium carbonate (2.5 mL). The mixture was stored in a dark environment for 40 min before the absorbance and measured at 725 nm against blank of 50% aqueous methanol. The final results were expressed as grams gallic acid equivalents per gram of dried arils.

The quantification of total anthocyanin concentration was performed using the pH differential method [174] with modification according to Arendse et al. [175]. The extract (1 mL) was diluted with 9 mL of pH 1.0 (potassium chloride, 0.025 M) and pH 4.5 (sodium acetate, 0.4 M) buffers, respectively. Samples were stored in dark for 10 min before reading the absorbance at 510 and 700 nm respectively against 50% blank aqueous methanol using a UV–visible spectrophotometer. Results was expressed as grams of cyanidin-3-glucoside equivalents per gram of dried arils.Aril firmness was measured by compression test using a texture profile an-

alyzer XT Plus (Stable MicroSystem Ltd., Godalming, UK). Optimal operating settings: pre-test speed 1.5 mm s^{-1}, probe test speed 1 mm s^{-1}, post-test speed 10.0 mm s^{-1}, compression force 10 N and compression distance of 10 mm. The data attained from the texture profile analyser were interpreted using software Exponent v.4 (Stable MicroSystem Ltd., Godalming, UK). Aril compression was performed on 5 individual arils per fruit and the results presented as mean ± standard error.

3.2.4 Precision and accuracy of destructive reference measurements

Precision and accuracy of destructive measurements were performed as described by Arendse et al. [18]. Reference measurements were evaluated for intra-day and inter-day variability testing. This was performed as in order to test their repeatability. For intra-day variability five replicates was performed within 1 day; while, inter-day was done for 3 consecutive days. The relative standard derivation (RSD) was calculated in order to determine their repeatability, using

$$\mathrm{RSD} = \mathrm{SD.X} \times 100 \tag{3.2.1}$$

where RSD is relative standard deviation, SD and X are standard deviation and the average obtained from replicate measurements respectively. RSD values for quality parameters ranged from 0.30 to 0.90% indicating acceptable accuracy. The coefficient of variation (CV), is also determined (Table 3.1). This is defined as the ratio of the standard deviation to the mean of the reference values was calculated and multiplied by 100 and reported as a percentage [167].

3.2.5 Chemometric analysis

Two different regression algorithms were used for model development, namely; PLS and SVM. Model development was performed using Solo software package, a standalone version of PLS-Toolbox (Eigenvector Research, Inc., USA). First, the spectra were pre-processed by applying the SNV (standard normal variate) algorithm. In order to construct calibration models with robustness, the data for all three orchards were combined and randomly split into 2:1 subset these included calibration (70%) and prediction (30%). The data were divided in two sets by way of the Kennard and Stone duplex algorithm [26]. PLS regression was calculated using the SIMPLS algorithm with venetian blinds (with 10 splits and blind thickness=1) used for cross validation. SVM algorithm was applied, by choosing the E-SVR (epsilon- support vector regression) algorithm [26] with the following parameters: SVM kernel type: radial basis function, cost=100, epsilon=0.01, gamma=10.

The spectral data were also subjected to various pre-processing methods in order to correct light scattering, reduce the changes of light path length and reduce noise. Pre-processing methods were tested individually and in combination with others. These include Savitzky–Golay transformation (first derivative),

Table 3.1: Mean, standard deviation (SD) range and coefficient of variation (CV) for calibration and validation subsets for dried pomegranate arils

Quality parameter	Calibration set				Validation set				
	Mean	SD	Min	Max	Mean	SD	Min	Max	Overall CV (%)
L*	25.15	3.00	20.54	33.62	24.46	2.20	21.39	28.46	10.46
a*	18.51	3.16	12.26	24.44	19.38	3.24	15.11	26.97	16.89
C*	19.72	3.61	12.84	29.83	19.69	3.65	13.51	26.36	18.42
h°	17.23	3.68	12.00	27.10	16.55	2.82	12.43	21.41	19.20
TSS	3.96	0.88	2.65	6.05	3.83	0.63	3.05	5.65	19.33
TA	0.30	0.06	0.20	0.48	0.30	0.10	0.23	0.43	26.66
pH	3.70	0.28	3.25	4.30	3.65	0.31	3.26	4.26	8.030
TSS/TA	10.78	2.15	7.50	16.88	11.18	3.05	6.86	17.60	23.61
Brim A	3.07	0.67	2.15	5.14	3.18	0.68	1.70	4.50	21.60
Firmness (N)	82.17	16.78	43.39	125.26	89.28	10.27	63.81	105.47	15.96
TPC (g/L)	19.91	6.93	10.31	42.62	19.73	10.87	10.47	41.38	44.95
TAC (g/L)	12.00	3.88	6.79	19.59	11.97	2.80	6.68	15.70	27.86

L^*: lightness, a^*: redness, C^*: Chroma, h^*: hue angle, TSS: total soluble solid, TA: titratable acidity, TSS/TA: total soluble solid/ total acid, TPC: total phenolic content, TAC: total anthocyanin content, SD: standard deviation, CV: coefficient of variation, Min: minimum, Max: maximum

multiplicative scattering correction (MSC) and vector normalisation (SNV) [161]. The developed models were selected based on statistical parameters that provided higher coefficient of determination (R^2), lowest root mean square error of calibration (RMSEC) and root mean square error of prediction (RMSEP) and lower number of latent variables (LV) [176, 177, 178, 179]. Other additional statistical parameters that were considered were the bias (systematic difference between the predicted and reference data) and residual predictive deviation (RPD). Literature suggested that RPD values is an important statistical parameter used to confirm the reliability of the developed model even if significant relationship is observed between the NIR predicted and actual laboratory values [180]. Several studies suggested that if an RPD value <1.5 it means that the model is unreliable and cannot be used, while those between 1.5 and 2.0 are appropriate for rough predictions, those between 2.0 and 2.5 are fit for quantitative predictions, those between 2.5 and 3.0 are considered good models while those >3.0 are regarded as satisfactory models [18, 20, 163, 165].

3.3 Results and discussion

3.3.1 Spectra characteristics

The spectral absorbance profile for dried pomegranate arils for pomegranate arils (cv. Wonderful) are presented in Figure 3.1. The spectral range was trimmed from the region of 800 to 2400 nm to remove noise. The assignment of peaks

for the acquired spectra was implemented according to a review of literature [15, 167]. The acquired spectra showed contours bands having noticeable peaks in the region of 1100, 1350, 1488, 1606, 1775, 1915, 2029 and 2221 nm. The spectral peaks observed between 1100 nm (O–H bond stretching and second water overtone) and 1488 nm (O–H bond stretching and first water overtone) have been reported to be closely associated with the O–H stretching modes of water absorption. Prominent peaks observed in the region of 1100, 1775 and 1915 nm correspond to the second and first overtones of C–H stretching as well as the third overtone of OH, CH and CH_2. These peaks have been associated with the absorption profile of various compounds. For instance, Manley et al. [181] reported that peaks in the region of 1488 to 2221 nm corresponds to moisture (1440–1500 nm), proteins (2100–2200 nm) and fats (1725–2310 nm) for different biological materials. Sugars and organic acids have been reported to display bands in the wavelength regions of 1100–1600 and 1700–2300 nm [167, 182, 183]. The spectral profile for dried pomegranate arils is similar to profiles for other commodities such as fresh pomegranate arils [19], avocado fruit [165] and oranges [163].

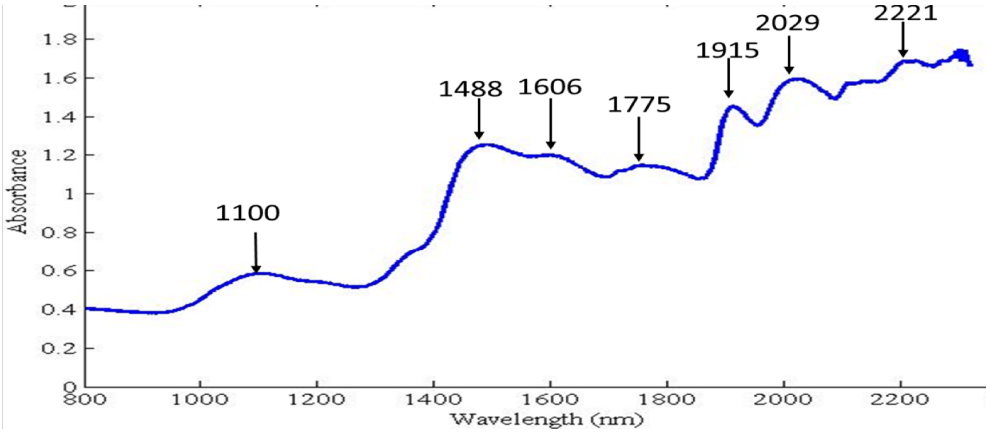

Figure 3.1: Representative absorbance unprocessed spectrum for averaged sample of dried pomegranate aril

3.3.2 Distribution statistics for calibration and validation reference data

Table 3.1 shows the distribution statistics (mean, standard deviation and coefficient of variation (CV%) for calibration and validation data sets for all the studied attributes of the dried pomegranate arils. In this study, it was observed that the investigated parameters were normally distributed around the mean values for each parameter. Lu et al. [184] stated that the validation and accuracy of calibration models would depend on enough variation being present within a sample set. NIRs have been reported to show better prediction capability when a sample has a large variation within their calibration and validation data set [163, 185]. For this study, the standard deviation (SD), minimum-to-maximum range and CV% statistics has clearly shown that most parameters had high an overall CV% values

of up to 44.95% with both calibration and validation data sets covering a wide range of values.

3.3.3 Model development for two regression algorithms (PLS vs SVM)

The development of models using PLS and SVM regression algorithms was done for each quality parameter while evaluating different pre-processing methods; whereby, the latter were selected based on high R^2 and RPD values, and low RMSEP values (Appendix A, Supplementary information, Tables 1–4). The best selected FT-NIR models for quality parameters are presented in Table 3.2. The scatter plots representing the relationships between selected measured quality parameters and model predictions are presented in Figure 3.2. Physical parameters such as fruit firmness can be determined indirectly through the light scattering properties associated with the tissue [15]. The prediction statistics for fruit firmness for both algorithms are comparable with one another with PLS (R^2=0.53, RMSEP=10.75, RPD=0.92) and SVM (R2=0.49, RMSEP=7.82, RPD=1.27) respectively. For colour parameters, model development using SVM regression provided better prediction statistics for redness a^* (R^2=0.72, RMSEP=1.82, RPD=1.71) and C^* (R^2=0.70, RMSEP=1.99, RPD=1.77). The intensity of the colour hue (h°) and lightness (L^*) for both regression techniques performed relatively poor as characterized by the low R^2 and low RPD values. The wavelength range used for the development of models for colour (a^*, C^*) were found to be in the region of 1445–1640 and 1881–2319 nm. This wavelength region is comparable to those reported by for colour model development of fresh pomegranate arils [170].

Table 3.2: Summary of best performing models for two different regression algorithms for dried pomegranate arils cv. (Wonderful)

Quality parameter	Regression analysis	Pre-processing	Calibration model			Validation model			
			R^2	RMSEC	Bias	R^2	RMSEP	RPD	Bias
a*	SVM	Smoothing	0.77	1.84	0.17	0.72	1.82	1.71	-0.56
C*	SVM	None	0.75	2.15	0.25	0.70	1.99	1.77	-0.49
TA	SVM	None	0.79	0.04	-0.00	0.85	0.04	2.50	-0.01
pH	PLS	MSC	0.81	0.12	-0.00	0.86	0.13	2.38	-0.03
TSS/TA	PLS	MSC+SNV	0.53	1.47	-0.00	0.74	1.68	1.68	-0.35

L^*: lightness, a^*: redness, C^*: Chroma, TA: Total acid, pH: Potential hydrogen, TSS/TA: Total soluble solid/ total acid, R^2: Coefficient of determination: PLS: Partial least squares, SVM: Support vector machine, MSC: multiplicative scatter correction, SNV: Standard normal variate, RMSEC: Root mean square error of calibration, RMSEP: Root mean square error of prediction, RPD: Residual prediction deviation.

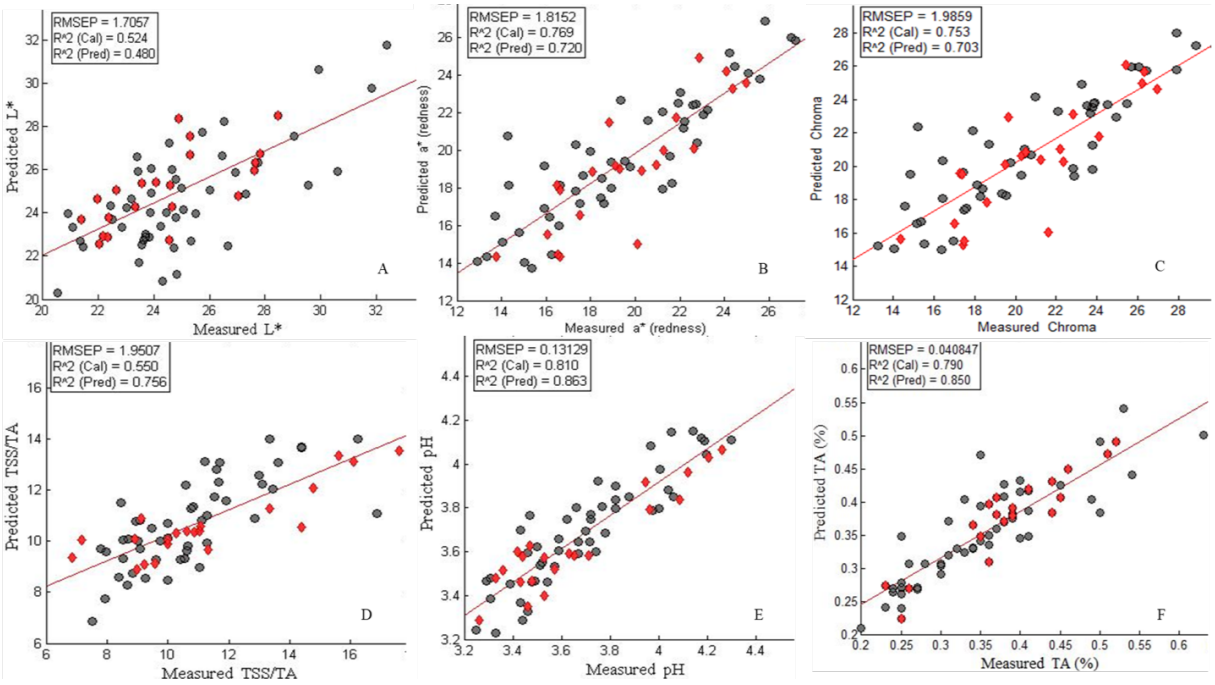

Figure 3.2: Score plots of FT-NIR predicted dried aril quality against reference (measured) constituent values for L^* (A), a^* (B), Chroma (C), TSS/TA (D), pH (E) and TA (F).

The prediction statistics for model development using PLS and SVM provided reasonably accurate calibration models for several of the chemical parameters. For instance, model development using PLS regression gave better prediction statistics for TSS/TA ratio (R^2=0.74, RMSEP=1.68, RPD=1.68) compared to SVM (R^2=0.58, RMSEP=1.31, RPD=1.52). For colour parameters, model development using SVM regression provided better prediction statistics for redness a^* (R^2=0.72, RMSEP=1.82, RPD=1.71) and C^* (R^2=0.70, RMSEP=1.99, RPD=1.77). Similarly, pH was best predicted with PLS regression with an R^2 of 0.86 and RPD of 2.38. Titratable acidity was best predicted with SVM regression (R^2=0.85, RMSEP=0.04, RPD=2.50). The R^2 values for prediction for TA was similar to model developed by Arendse et al. [170]. The RPD values for TA and pH indicated that the models were fit for quantitative prediction of the parameters in dried pomegranate arils. The RPD value for TSS and BrimA suggested that the developed models were unreliable. The developed models for physical (a^*, C^*) and chemical parameters (TA, TSS/TA ratio, pH) had low bias values (0.02–0.08) indicating robust fitting and stability and therefore not sensitive to the external factors such as growing location.

For the prediction of phytochemical compounds such as total phenolics and total anthocyanin, both PLS and SVM calibration models performed poorly (Table 3.3). The poor predictions of the developed models (TSS, TPC, TAC) could possibly be related to the significantly wide variation in the reference values obtained from the samples. The heterogeneity of the phytochemical composition could be

the reason for the inconsistency of TPC and TAC values. Therefore, in order to get better prediction of TSS, BrimA, TAC and TPC future research on dried pomegranate arils should consider the application of other regression techniques and include more spectral acquisition scans due to the heterogeneity of the sample set as indicated by its min-max and CV%. This is to guarantee a wider variation to avoid the low predictability of the models.

Table 3.3: Summary of best model calibration and prediction performance for both PLS and SVM analysis

Quality parameter	Regression analysis	Pre-processing	Calibration model			Validation model			
			R^2	RMSEC	Bias	R^2	RMSEP	RPD	Bias
L*	PLS	None	0.52	1.92	-0.03	0.48	1.71	1.29	0.67
	SVM	MSC+SNV	0.75	1.41	0.01	0.27	2.33	1.06	1.04
a*	PLS	MSC	0.86	1.41	0.00	0.26	2.83	1.10	0.95
	SVM	Smoothing	0.77	1.84	0.17	0.72	1.82	1.71	-0.56
C*	PLS	MSC	0.79	2.00	0.00	0.36	2.53	1.40	0.12
	SVM	None	0.75	2.15	0.25	0.70	1.99	1.77	-0.49
h°	PLS	MSC	0.30	2.27	0.00	0.19	2.23	1.29	0.14
	SVM	1st derivative	0.12	3.18	-0.18	0.11	2.74	1.05	-0.38
TSS	PLS	None	0.05	0.77	-0.01	0.22	0.78	0.83	-0.31
	SVM	1st derivative	0.24	0.77	-0.07	0.01	0.65	0.97	0.01
TA	PLS	1st derivative	0.69	0.05	0.00	0.58	0.07	1.43	0.03
	SVM	None	0.79	0.04	-0.00	0.85	0.04	2.50	-0.01
pH	PLS	MSC	0.81	0.12	-0.00	0.86	0.13	2.38	-0.03
	SVM	1st derivative	0.82	0.13	-0.01	0.83	0.13	1.92	0.09
TSS/TA	PLS	MSC+SNV	0.53	1.47	-0.00	0.74	1.68	1.68	-0.35
	SVM	None	0.86	1.09	-0.21	0.58	1.31	1.52	0.34
Brim A	PLS	1st derivative	0.74	0.39	-0.00	0.17	0.77	0.71	0.27
	SVM	MSC+SNV	0.27	0.70	0.10	0.27	0.65	0.85	0.22
Firmness (N)	PLS	1st derivative	0.60	10.52	-0.05	0.30	8.69	1.22	0.99
	SVM	MSC	0.65	10.78	-1.09	0.49	7.81	1.27	-2.20
TPC	PLS	MSC	0.02	14.80	0.00	0.06	10.44	0.82	3.33
	SVM	Smoothing	0.95	4.35	-0.58	0.03	10.34	0.82	6.28
TAC	PLS	1st derivative	0.69	3.36	0.00	0.05	5.84	0.62	-0.66
	SVM	1st derivative	0.17	15.92	0.50	0.22	3.82	0.95	1.42

SVM: Support vector machine, MSC: Multiplicative scatter correction, SNV: Standard normal variate, PLS: Partial least square, 1st derivative: first-order derivative, R^2, Coefficient of determination, SVM: Support vector machine, MSC: multiplicative scatter correction, SNV: Standard normal variate, RMSEC: Root mean square error of calibration, RMSEP: Root mean square error of prediction, RPD: Residual prediction deviation.

3.4 Conclusion

In this study, FT-NIR diffuse reflectance spectroscopy combined with chemometrics allows us to determine the best modelling conditions for optimal prediction of a given attribute for dried pomegranate arils. The usage of two different regression techniques allowed us to determine which attributes were best predicted by a given or specific regression method. For instance, PLS regression showed good prediction of sensory quality (TSS:TA ratio), while SVM regression were best used in the prediction of visual properties (colour parameters) of dried pomegranate arils. Limitations of the study were related to the standardization of the spectra collection since only one scan was taken per sample and low accuracies of the calibration models. This study suggested the importance of proper scheduling and multiple

scanning or positioning of the sample for spectra collection. Therefore, it may be possible to improve the model performance, through implementation of different regression techniques, include more spectral acquisitions scans of the sample, including larger datasets, different cultivars, which encompasses several orchards, fruit maturity status and seasons towards improving model predictability and robustness. Additional, efforts should be made towards exploring other vibrational spectroscopic techniques which have not been sufficiently explored such as Raman spectroscopy which will reduce the effects of water on the absorption profile of the spectra and reduce scattering effects. This may lead to novel and better calibration models especially for textural related attributes. These findings can be employed by the pomegranate processing industry to develop a grading/sorting system to rapidly evaluate several organoleptic and physicochemical attributes of dried pomegranate arils.

Chapter 4

Application of Fourier transform near-infrared (NIR) and attenuated total reflection FT mid-infrared (MIR) spectroscopy for quality evaluation of pomegranate seed oil

Pomegranate seed oil (PSO) has gained global attention as a result of the health benefits linked with its consumption. Agribusiness as are moving away from subjective, expensive and time-consuming methods of analysis to alternative ways that provide objective, rapid and cost-effective ways of non-invasive measurement. This chapter evaluated Fourier transform (FT) near-infrared (NIR) and attenuated total reflection (ATR) FT-mid-infrared (MIR) spectroscopy as a non-invasive method to predict the quality attributes of pomegranate seed oil. Partial least squares (PLS) regression calibration models were constructed to predict total phenolic content (TPC), total carotenoid content (TCC), peroxide value (PV), yellowness index (YI) and refractive index (RI) using the spectral regions of NIR (500–4000 cm^{-1}) and MIR (4000–400 cm^{-1}), respectively. Generally, the models generated with MIR spectra showed better prediction performance compared to than that developed with NIR spectra. FT-NIRS showed superior prediction statistics for TCC (R^2=80.45, RMSEP=0.0185, RPD=2.28) and YI (R^2=53.19, RMSEP=14.30, RPD=1.49), while FT ATR-MIRS gave the best prediction statistics for RI (R^2=80.92, RMSEP=0.0003, RPD=2.32), and PV (R^2=62.00, RMSEP=3.88, RPD =1.62). These results have established that infrared spectroscopy combined with chemometric analysis is a very useful technique that allows rapid screening of PSO to estimate their quality parameters.

4.1 Introduction

Standard analytical and wet chemistry methods are mainly used to evaluate various chemical constituents and detect fraud within oil products. These methods

are used for their ability to provide precise and accurate measurement of quality attributes. However, these approaches are time-consuming, expensive and not always practical for large-scale commercial application as it involves the use of trained sensory panellists or individual. These drawbacks have promoted the researchers and to consider interest in the development of objective and non-invasive techniques for faster and less expensive the assessment of oil quality attributes.

Infrared spectroscopy (IRS) combined with chemometrics is one of the most widely used non-invasive tools used by food and beverage industry as an alternative to the analytical methods in quality assessment for food and processed agricultural produce. This is due to its rapid, accurate, simple and cost-effective way to evaluate chemical constituents [80, 186]. IR spectroscopy is appropriate for the prediction of compounds containing polar functional groups such as –OH, C–O, and N–H. In the agricultural industry, IR spectroscopy in the near-infrared (NIR, 12500–4000 cm^{-1}) and the mid infrared (MIR, 4000–400 cm^{-1}) spectral region have been applied as a non-invasive analytical tool. In combination with chemometric tools, NIR spectroscopy (NIRS) is attractive and has more versatility compared to MIR spectroscopy (MIRS). For instance, NIRS has cheaper instrumentation cost and more robust components than MIRS. NIRS is attractive due to the fact that it is rapid and non-invasive, and it has the additional benefit of penetrating finite distances in fruit and can be utilized for the acquisition of surface and internal characteristics of foods [15]. While, MIRS contains more spectral information due to the higher resolution of the fundamental vibrational absorption bands and can identify very complex or similar structures compared to the broad overtone and combination absorption bands in the NIR region [181, 186, 187].

Oils are an essential component of diet because of their nutrition and biological properties. Different types of oils are commercially available. The oils that are mainly derived from plants such as palm oil, sesame, canola oil, coconut oil, soybean oil, avocado oil and virgin olive oil [74, 82]. Literature has shown that infrared spectroscopy has been recognised in various analytical applications for evaluating quality and detecting of fraud in a variety of oil products. For instance, instance infrared spectroscopy have been applied to evaluate quality attributes such as peroxide value, refractive index, phenolic content, carotenoid content, fatty acids in olive oil [24, 188], maize oil [189], vegetable oil [190] and palm oil [75]. It has been successfully used for classification purposes [191, 192] and adulteration in a variety of oil products [79, 193].

Pomegranate seed oil (PSO) have been commercially available during the last 5–6 years. Pomegranate seeds constitute up to 6.6–24% of the total fruit weight and contain 12–25% oil content [194, 195, 196]. The seed oil has been reported to contain high levels of unsaturated fatty acids such as punicic acid, oleic acid, linoleic acid and palmitic acid [3, 195, 196, 197, 198].To date, no comparative studies for evaluating the performance of NIR and MIR spectroscopic techniques

in predicting pomegranate seed oil quality attributes have been published. Comparative research that focuses on the effect of spectral pre-processing, wavelength selection on model performance are limited. More efforts are needed to investigate how the spectral pre-processing techniques and wavelength ranges impact on the performance of PLS models developed with different spectroscopic techniques for predicting qualitative and quantitative attributes of pomegranate seed oil. This study aims to explore the application of FT-NIR and ATR-FT-MIR spectroscopy, combined with chemometrics to construct calibration models for the quality evaluation of pomegranate seed oil.

4.2 Materials and Methods

4.2.1 Fruit supply and processing

Fruit from three different pomegranate cultivars ('Wonderful', 'Acco', 'Herskiwitz') were procured from Sonlia pack-house, the Western Cape region. Fruit were delivered to Stellenbosch University, Postharvest Technology and Research Laboratory. Upon arrival, arils from each fruit were manually extracted at ambient conditions (21 °C ± 65% RH) and the seeds were separated from the arils using a cheesecloth. The obtained seeds were thoroughly washed with distilled water to remove the residual aril sacs and dried at 60 °C for 24 hr in a hot air oven (PROLAB, South Africa). The final moisture content of the seeds was observed to be 1.7 wt. % (dry basis). Pomegranate seeds were sealed in polyethylene bags and kept in -20 °C until further use.

4.2.2 Oil extraction and yield

In this study, the solvent extraction method was performed as described by Ampem [3]. Dried pomegranate seeds were grounded into a fine powder with a particle size of 0.25 mm using an IKA miller (Model A11B, Germany) in preparation for oil extraction [199]. Pomegranate seed oil was extracted from seed powder using the superheated hexane extraction method. Pomegranate seed powder (30 g) was weighed into a glass flask and extracted twice respectively with a 300 mL of hexane solvent at a time, reaching a total volume of 600 mL solvent solution for each sample. The mixture (600 mL) was sonicated in an ultrasonic bath (Model DC 400H, Haifa, Israel) which was operated at 40 °C for 40 min. The oil filtrates from repeated extractions were pooled and recovered through distillation process using a rotary evaporator (Heidolph Instruments GmbH & Co. KG, Germany). Thereafter, samples were placed within a vacuum oven at 60 °C for 1.5 hr to remove any remaining hexane solution [200]. A total of 45 samples of PSO was transferred into a 9 mL glass tubes and stored in a dark environment at room temperature until further analysis.

4.2.3 Spectral acquisition

FT-IR spectra was acquired in diffuse reflectance from two different spectrophotometers. The first, spectral acquisition was acquired using the Alpha ATR-FT-MIR spectrophotometer (Bruker Optics, Ettlingen, Germany) over a spectral region of 4000–400 cm^{-1}. The Alpha was equipped with a single bounce diamond crystal sample plate (area^2 mm^2) with the temperature maintained at 50 °C. Prior to obtaining FT-MIR spectra, reference measurements were performed against air background and periodically at intervals of 30 min during sample spectra acquisition. After each measurement, the scanned material was discarded and the diamond crystal surface was cleaned with a soft paper and undiluted methanol and then cleaned with distilled water to avoid cross-contamination between samples [201]. Sample measurement time was 120s using the following operating parameters 4 cm^{-1} resolution scan and 10 kHz scanner velocity with a total of 128 averaged background and sample scans per spectrum.

The second spectral acquisition was acquired using the Multi-Purpose Analyzer (MPA, Bruker Optics, Ettlingen, Germany). FT-NIR spectrometer, which was equipped with InGaAs detector. The MPA incorporates a high energy air-cooled NIR source (20 W tungsten-halogen lamp) and a permanently aligned Rocksolid interferometer, which is equipped with gold-coated mirrors (high reflective surface and inert). The permanent interferometer provides constant high-quality results which have a wave number reproducibility superior to 0.04 cm^{-1} and a wavenumber accuracy superior to 0.1 cm^{-1}. NIR spectral data for pomegranate seed oil were collected in diffuse reflectance using a sample compartment for the measurement of liquids. Prior to spectral acquisition, samples were heated over a heating block at 50 °C and placed in glass vials with 8mm path length. The glass vials were placed into the sample compartment of the MPA. PSO samples were conditioned by way of heating block to keep sample temperature at ±50 °C before spectra recording. This was done for both spectrophotometers to ensure a constant measuring temperature thought-out the scanning process. The spectral data were collected over the range 12 500 to 4 000 cm^{-1} (scanning resolution 4 cm^{-1}; scanner velocity 10 kHz; background with air, 128 scans).

4.2.4 Reference measurement

4.2.4.1 Refractive index

Refractive index (RI) of PSO was measured using a calibrated Abbé refractometer, Model 302 (ATAGO Co. Ltd., Japan) at room temperature [3, 202]. Three drops of PSO were loaded onto the refractometer prism, and the RI readings were recorded and expressed as mean. After each sample measurement, 100% methanol solvent followed by distilled H_2O and tissue paper was used to clean the refractometer prism.

4.2.4.2 Yellowness index

Yellowness index indicates the degree of yellowness associated with scorching, soiling, and general product degradation by light, chemical exposure and processing. The yellowness index of PSO was evaluated based on the CIE $L^*a^*b^*$ coordinates from a calibrated Minolta Chroma Meter, Model CR-400 (Japan). The yellowness index, as described by Pathare et al. [171], was calculated as

$$\mathrm{YI} = \frac{142.86 \times b^*}{L^*}. \tag{4.2.1}$$

4.2.4.3 Total phenolic content

Total phenolic content was performed using Folin-Ciocalteau assay as described by Abbasi et al. [203] with modification. Briefly, PSO (0.5 mL) was dissolved in 5.0 mL of 50% aqueous methanol. An aliquot of 2.0 mL from the resulting solution was pipetted into a test tube, followed by the addition of 0.5 mL of Folin-Ciocalteau reagent followed by the addition of 1.0 mL of anhydrous 35% Na_2CO_3 solution. The mixture was vortexed and stored in a dark environment for 30 min before the absorbance was recorded at 760 nm against blank aqueous methanol. A standard curve consisting of 0.02 –0.10 mg/mL Gallic acid was prepared following the same procedure. Total phenolic content (TPC) of PSO was extrapolated and reported as milligram Gallic acid equivalent (mg GAE/100 mL of oil). The results were presented as mean ±S.E (n=3).

4.2.4.4 Total carotenoid content

Total carotenoid content was evaluated in accordance to Association of Official Analytical Chemists (AOAC) International 958.05 assay [202] with modifications reported by Biehler et al. [204] and Siano et al. [9]. In brief, PSO (0.1 mL) was dissolved in 10 mL dimethyl sulfoxide (DMSO). The total carotenoid content (TCC) of the resulting mixture was recorded at 440 nm and 460 nm, against blank DMSO solvent. TCC for each sample was expressed as mean ± S.E (n=3) β-carotene/mL oil.

4.2.4.5 Peroxide value

The peroxide value assay was performed as described by AOAC [202] with modification, Briefly, PSO (0.2 mL) was dissolved in 9 mL of chloroform: methanol mixture (7:3 ratio) in screw-capped vials. The resultant solution was mixed with 50 μL of 10 Mm xylenol orange methanol solution and 50 μL of 36 Mm iron (II) chloride solution and vortexed respectively. The peroxide value of the resulting mixture was measured at an absorbance reading of 560 nm. The peroxide value was expressed as meq O_2/mL oil. The equation for calculating PV is given by

$$\mathrm{PV} = \frac{(\mathrm{As\text{-}Ab}) \times \mathrm{mi}}{W \times 55.84 \times 2} \tag{4.2.2}$$

where PV is the peroxide value, Ab the absorbance of the blank, As the absorbance of the sample, mi the inverse of the slope (obtained from calibration), W the weight of the sample (g) and 55.84 the atomic weight of iron.

4.2.5 Chemometric data analysis

OPUS version 7.0 software (Bruker Optics) was used for chemometric analysis. The spectral parameters used for multivariate analysis were optimised by subjecting spectral data to the software's "Optimise" function. This function provides a combination of parameters such as different pre-processing methods and wavelength regions and ranks results based on the number of latent variables and RMSECV values.

Calibration models were constructed by subjecting infrared (NIR and MIR) spectra to principal component analysis (PCA) and partial least squares (PLS) regression analysis (including mean centering). Spectral outliers and variation were explored by OPUS software using PCA (Figure 4.1). Spectral data with high residual and located far away from the zero line of the residual variance was perceived as potential outliers. Concentration outliers present in the dataset were removed and successive rounds of PLS regression done with the reduced dataset. After the outliers were removed, the resultant calibration models were validated with the test dataset. 'Leave one out' cross validation method was used for PLS analysis. To construct calibration models with high robustness, the data for all three cultivars were combined and randomly split into 2:1 subset, i.e. calibration (70%) and prediction (30%) sets, each subset containing sufficient samples of each cultivar. Several statistical pre-processing methods (first derivative, second derivative, straight line subtraction, multiplicative scatter correction, among others) and in combination were tested to develop the PLS models.

The performance of PLS models was evaluated according to the coefficient of determination (R^2) (Eq. 4.2.3), root mean square error of estimation (RMSEE) (Eq. 4.2.4) and root mean square error of prediction (RMSEP) (Eq. 4.2.5), as defined by

$$R^2 = 1 - \frac{\Sigma(y_{cal} - y_{act})^2}{\Sigma(y_{cal} - y_{mean})^2} \tag{4.2.3}$$

$$\text{RMSEE} = \sqrt{\frac{1}{M - R - 1} \times \text{SSE}} \tag{4.2.4}$$

$$\text{RMSEP} = \sqrt{\Sigma \frac{(y_{pred} - y_{act})^2}{n}} \tag{4.2.5}$$

where n is the number of spectra, y_{act} is actual value, y_{mean} is mean value, y_{cal} is calculated value, y_{pred} is predicted value of the attribute, M is number of calibration samples, R is the rank, and SSE is the sum of squared error.

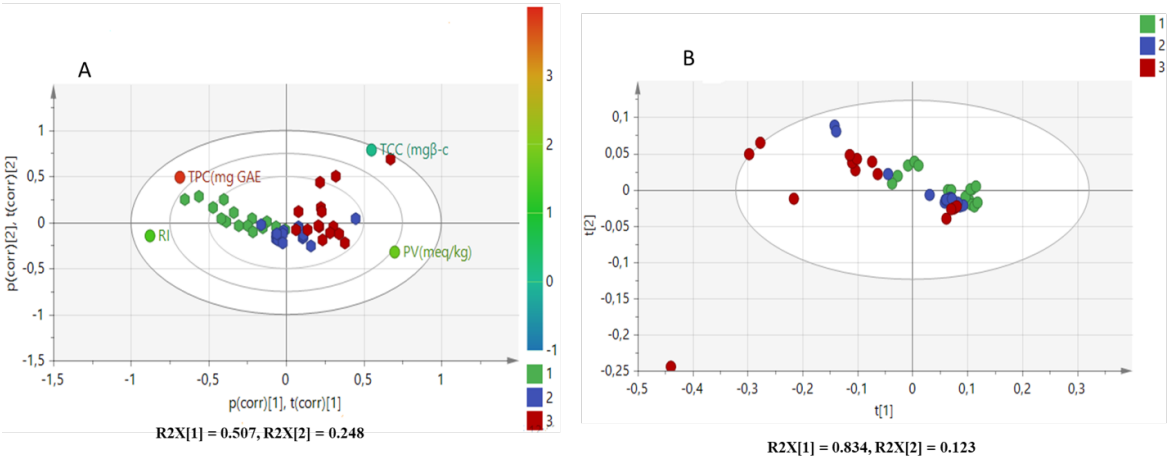

Figure 4.1: PCA plot representing MIR spectra and reference values (Fig. 4.1A). PCA scores plots based on spectra loadings for MIR spectra for pomegranate seed oil (Fig. 4.1B). The colours represent different cultivars; green 'Wonderful'; blue 'Herskawitz'; red 'Acco'.

Other statistical indicators for this study include models bias (Eq. 4.2.6), which gives an indication of the systematic error in the predicted values and is calculated values and the residual prediction deviation (RPD) (Eq. 4.2.7) value. This is defined as the ratio of the standard deviation of the reference data of the validation set, to the RMSEP value and provides an indication of the efficiency of a calibration model. These indicators are defined as

$$\text{Bias} = \frac{1}{n}\sqrt{\Sigma(y_{pred} - y_{act})^2} \tag{4.2.6}$$

$$\text{RPD} = \frac{\text{SD}}{\text{RMSEP}} \tag{4.2.7}$$

where SD is the standard deviation of reference values.

RPD is a statistic that is often used for the evaluation of calibration models in spectroscopy [180]. It was suggested that RPD values below 1.5 indicate that the developed model is unreliable, while RPD values ranging between 1.5 and 2.0 can be used for rough predictions, those between 2.0 and 2.5 are considered adequate for quantitative predictions, RPD values between 2.5 and 3.0 are considered good models, satisfactory models can be regarded when the RPD values are above 3.0 [180]. Best performing models were selected based on the best overall performance (low RMSEP, low RMSEE, high R^2 and higher RPD and low bias).

Pearson's correlation was performed on the reference data in order to demonstrate that the prediction of the different selected quality parameters is from the actual IR spectra and not due to possible correlations with the other measured parameters. Correlation analysis was performed using Statistica software (Statistica 13.0, StatSoft Inc., Tulsa, OK, USA) (Table 4.1).

Table 4.1: Pearson correlation coefficient matrix of chemical indices measured in pomegranate seed oil

Parameters	PV (meqO_2/mL)	TPC (mg GAE/mL)	RI	TCC (mg β-carotene/mL)	YI
PV	1.000000				
TPC	-0.09125	1.000000			
RI	0.080126	0.260478	1.000000		
TCC	0.334712	0.227483	0.176951	1.000000	
YI	0.021195	0.172994	0.258405	0.215358	1.000000

PV: Peroxide value, RI: Refractive index, TCC: Total carotenoid content, TPC: Total phenolic content, YI: Yellowness index

4.2.6 Chemicals and reagents

All chemical reagents were obtained from Sigma-Aldrich-Fluka Co. Ltd. (South Africa) unless otherwise stated.

4.3 Results and discussion

4.3.1 FT-NIR and ATR-FT-MIR spectral characteristics

Figure 4.2 show the NIR (Figure 4.2a) and MIR (Figure 4.2b) spectra of pomegranate seed oil, respectively. Peak assignment was done according to literature [24, 78, 201]. In the NIR region, bands around 8451 cm^{-1} arise from second overtones of C–H stretching vibrations while those at 7502.1 and 7498.3 cm^{-1} are due to the combination band of C–H. The peaks at 5774.1 and 5450 cm^{-1} arise from the first overtone of C–H stretching vibrations of methyl, methylene and ethylene groups [78, 205]. Small peaks at 4659 and 4597.7 cm^{-1} are associated with combination bands of C–H and C–O stretching vibration. The MIR spectra were dominated by peaks at 2918, 2556, 1837, 1463, 1377, 1238, 1163, 1114, 1099 and 721 cm^{-1}. Absorbance at 2924 and 2852 cm^{-1} could be ascribed to bands arising from CH2 stretching vibrations, asymmetric and symmetric, respectively [81, 206]. The major peak at 1743 cm^{-1} arises from C–O stretching vibrations; the bands at 1463 and 1377 cm^{-1} arise from CH_2 and CH_3 scissoring vibration, while those at 1238, 1163, 1114, 1099 cm^{-1} are associated with the C–O stretching vibration. The peak at 721 cm^{-1} corresponds to CH_2 rocking mode [80, 193]. The spectral profile for pomegranate seed oil are comparable to those reported for other oil samples like avocado oil [201], virgin olive oil [80, 81], rapeseed oil blend [76] and palm oil [75].

These peaks have been associated with the absorption profile of various compounds. For instance, in the FT-NIR region, Pereira et al. [190] reported that peaks in the range of 5888–5636 cm^{-1} for refractive index which is related to C–H stretching of aliphatic chain that characterizes carboxylic acids. Peaks in the

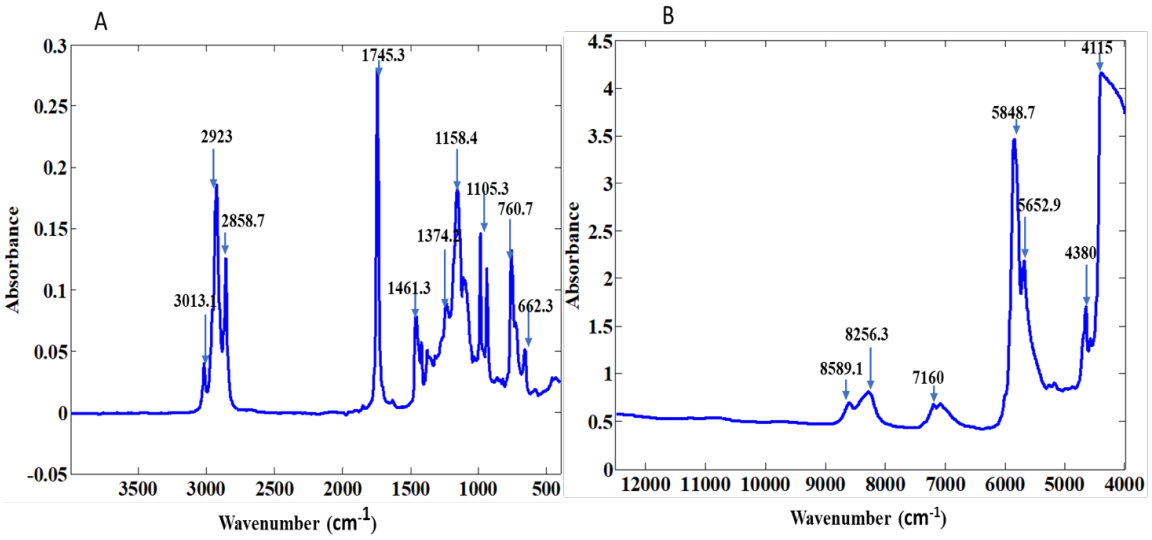

Figure 4.2: Representative absorbance spectra for ATR- FT-MIR (A) and FT-NIR (B) of pomegranate seed oil

frequency ranges of 7502.3–6800.2 cm^{-1} and 5450.2–4597.8 cm^{-1}, as in the case of hydroxytyrosol and tyrosol secoiridoids, corresponds to total phenolic content. Other chemical parameters reported for different wavelength ranges includes fatty acid (4761.9–4545.45 cm^{-1}), peroxide value (5313.5–4553 cm^{-1}), carotenoid content (1700–1750 nm), iodine value (8800–8200 cm^{-1}) [24, 75, 189, 190].

For ATR-FT-MIR region, the hydroperoxide bands have been reported peaks at 3450 cm^{-1}, due to –OO–H stretching vibration of the oxidized methyl octadecadieonate. Spectra between 1730–1690 cm^{-1} was used for quantitative determination of free fatty acids and for iodine value (1050–800 cm^{-1}) [73, 74, 77, 206, 207, 208].

4.3.2 Distribution of calibration and validation reference data

Table 4.2 shows the statistics (mean, standard deviation, coefficient of variation) for external and internal parameters of pomegranate seed oil. In this study, the reference data for all parameters were normally distributed around the mean. Lu et al. [184] stated that the validation and accuracy of calibration models would depend on enough variation present within the sample set in the physical and biochemical reference data. Furthermore, a large sample variation within the calibration and validation data sets have been shown to be predicted better by NIR spectroscopy [163, 185]. It was apparent from the standard deviation, minimum-to-maximum range and CV% statistics that most parameters had high CV% values of up to 40.52%, for both calibration and validation data sets covered a wide range of values, except for refractive index.

Table 4.2: Mean, standard deviation (SD), range and coefficient of variation (CV) for calibration and validation subsets for selected parameters of pomegranate seed oil

	Calibration set (n = 32)				Validation set (n = 13)				Overall CV%
Parameters	Mean	SD	Min	Max	Mean	SD	Min	Max	
PV	8.368	5.309	1.746	24.856	9.982	6.575	1.793	23.645	40.52
RI	1.521	0.0009	1.519	1.523	1.521	0.0009	1.519	1.522	0.06
TCC	0.094	0.038	0.05	0.27	0.098	0.0367	0.064	0.0192	38.66
TPC	4.296	1.209	2.563	9.003	4.507	1.319	2.893	7.417	28.70
YI	54.22	18.54	23.14	97.28	55.69	21.84	23.94	96.41	38.64

n: Number of sample, PV: Peroxide value, RI: Refractive index, TCC: Total carotenoid content, TPC: Total phenolic content, YI;:Yellowness index.

4.3.3 PLS regression models

The best model for each parameter was selected based on the evaluation of statistical parameters that have higher R^2, RPD values and lower RMSEE and RMSEP values. The models that performed the best for both NIR and MIR spectroscopy are presented in Table 4.3. Model development using the NIR and MIR spectral regions had a major influence on the regression statistics and the prediction accuracy. The overall performance of the developed models for all quality parameters is represented in Table 4.4. Scatter plots of FT-NIR and ATR- FT-MIR spectroscopy for predicted data plotted against measured reference data are presented in Figure 4.3. Calibration models developed using the ATR-Alpha instrument in the MIR spectral region gave relatively better prediction statistics for refractive index (R^2=80.92, RMSEP=0.0003 and RPD=2.32) compared to the MPA in NIR spectral region (R^2=72.29, RMSEP=0.0004 and RPD=2.00). The wavelength range used during the development of the calibration model for refractive index was between 3277 and 758 cm^{-1} which is within the range reported by Yang & Irudayaraj [209] for olive oil. The RPD value for RI suggested the models can you used for quantitative predictions, while the low bias (< 0.001) of the developed model suggest that the model is were stable and non-sensitive to factors such as cultivar, or growing location. Model development in the ATR-FT-MIR spectral region of 3996 to 1476 cm^{-1} for PV (R^2=62.00, RMSEP=3.88 and RPD=1.62) performed better than the MPA (R^2=55.24, RMSEP=4.34 and RPD=1.59) in the FT-NIR spectral region of 5450-4597.7 cm^{-1}. It can be attributed to the fact that model development using ATR-FT-MIR provided lower number of latent variables (7) and lower bias (-0.083) compared to the FT-NIR (LV=9, bias=1.49. Although, it is noteworthy that the RPD values for the developed models suggest that these models for PV can only be used for rough predictions.

Table 4.3: Model performance for oil parameter using different FT-NIR instruments

Parameter	Acquisition mode	Pre-processing	Wavelength range (cm^{-1})	Calibration (n = 32)			Validation (n = 13)				
				Rank	R^2	RMSEE	R^2	RMSEP	RPD	Bias	Slope	Corr.
PV	ATR-FT-MIR	1st	3996.1 – 3635.6, 1839.4 – 1476.9	7	95.17	1.33	62.00	3.88	1.62	-0.083	0.646	0.788
RI	ATR-FT-MIR	2nd	3277.2 – 2197.2, 1120.6 – 758	6	98.26	0.0001	80.92	0.0003	2.32	-0.00	0.909	0.907
TCC	FT-NIR	SLS	9403.7 – 7498.3, 6102 – 5774.1	5	89.25	0.015	80.45	0.0185	2.28	-0.0025	0.893	0.944
YI	FT-NIR	2nd	8451 – 7498.3, 6102 – 4597.7	5	55.66	13.6	53.19	14.30	1.49	2.64	0.543	0.740

Corr: Correlation coefficient, n: Number of sample, PV: Peroxide value, R^2: coefficient of determination, RI: Refractive index, RMSEE, Root mean square error of estimation, RMSEP: Root mean square error of prediction, RPD, residual predictive deviation, SLS: Straight line subtraction, TCC: Total carotenoid content, YI: Yellowness index, 1^{st}: First derivative, 2^{nd}: Second derivative.

Table 4.4: Best performing PLS regression models for pomegranate oil quality parameters

Parameter	Acquisition mode	Pre-processing	Wavelength range (cm^{-1})	Calibration (n = 32)			Validation (n = 13)				
				Rank	R^2	RMSEE	R^2	RMSEP	RPD	Bias	Slope	Corr.
PV	ATR-FT-MIR	1st	3996.1 – 3635.6, 1839.4 – 1476.9	7	95.17	1.330	62.00	3.88	1.62	-0.083	0.646	0.788
	FT-NIR	SLS	5450 – 4597.7	9	80.86	2.680	55.24	4.34	1.59	1.49	0.825	0.807
RI	ATR-FT-MIR	2nd	3277.2 – 2197.2 1120.6 – 758	6	98.26	0.000	80.92	0.000	2.32	0.000	0.909	0.907
	FT-NIR	2nd	6102 – 4597.7	8	92.31	0.000	72.29	0.000	2.00	0.000	0.761	0.865
TCC	ATR-FT-MIR	2nd	3637.7 – 3275.2, 2558.3 – 2197.9, 760.1 – 399.6	5	96.64	0.000	60.14	0.022	1.87	0.012	0.515	0.918
	FT-NIR	SLS	9403.7 – 7498.3, 6102 – 5774.1	5	89.25	0.015	80.45	0.019	2.28	-0.003	0.893	0.944
TPC	ATR-FT-MIR	1st +SLS	3277.2 – 2916.7, 2558.3 – 1837.4	1	44.86	0.913	6.773	1.22	1.04	0.007	0.234	0.369
	FT-NIR	SLS	7502.1 – 4597.7	2	33.22	0.855	18.5	1.39	1.26	0.657	0.226	0.774
YI	ATR-FT-MIR	2nd	2918.8 – 2556.3, 1120.6 – 758	1	30.77	11.900	20.52	15.0	1.15	-3.10	0.267	0.491
	FT-NIR	2nd	8451 –7498.3, 6102 – 4597.7	5	55.66	13.600	53.19	14.30	1.49	2.64	0.543	0.740

R^2: coefficient of determination: RMSEE, Root mean square error of estimation: RMSEP: Root mean square error of prediction, PV: Peroxide value, RI: Refractive index, TCC: Total carotenoid content, TPC: Total phenolic content, SLS: Straight line subtraction, 1^{st}: First derivative, 2^{nd}: Second derivative, RPD, residual predictive deviation, Corr: correlation coefficient, YI: Yellowness index

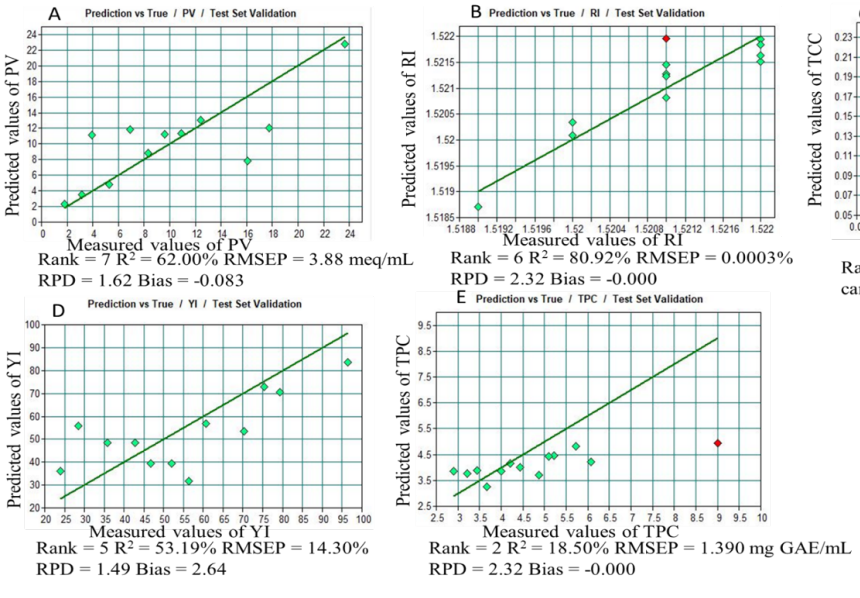

Figure 4.3: Scatter plots of FT-MIR predicted vs true test for PV (A), RI (B)

Model development using the FT-NIR in the spectral region of 9403 to 5774 cm^{-1} with pre-processing of straight-line subtraction showed good prediction statistics for total carotenoid content (R^2=80.45, RMSEP=0.0185 and RPD=2.28). The wavelength range used during the development of calibration model for TCC was 9403 to 5774 cm^{-1} which is within the range reported by [10, 189], for maize oil. Furthermore, the RMSEE and RMSEP values were very similar, indicating robust fitting and the low number of LVs (5) used for TCC suggest that overfitting noise to models were not evident. The RPD values for TCC suggest the models can you used for quantitative predictions. While, model development for yellowness index (R^2=53.19, RMSEP=14.30 and RPD=1.49) and total phenolic content (R^2=18.50, RMSEP=1.39 and RPD=1.26) gave relatively poor prediction statistics. This was characterised by low RPD values and high bias, suggesting that the developed models were unreliable, and overestimation may have occurred for these quality attributes.

4.4 Conclusion

The performance of FT-NIR and ATR-FT-MIR spectroscopic techniques combined with chemometrics for the determination of quality attributes for pomegranate seed oil was evaluated. Generally, the regression models developed within the MIR spectral region performed slightly better than that developed with FT-NIR spectroscopy. This can be due to the fact that the mid-infrared spectrum contains wavelengths for fundamental rotational molecular vibration, which is highly sensitive to specific chemical composition, whereas the near-infrared spectrum is associated mainly with overtone and combination bands of fundamental transition, making it less reproducible and accurate. This finding agrees with the study by Yang et al. [193]. In their study, FT-MIR spectroscopy was found to be more superior to FT-NIR for discrimination and classification of edible oil and fats, and for olive pomace oil adulteration in extra virgin olive oil [81, 209]. PLS prediction models were developed for three of the five quality parameters that were analysed. Considering the results, future research is required in order to improve the models performance for both NIR and MIR spectroscopy by either increasing the sample size, including growing location and seasonality or by application of different chemometric techniques.

Chapter 5

General discussion and conclusions

5.1 Introduction

Pomegranate (*Punica granatum* L) fruit has seen tremendous growth in commercial exports globally and within South Africa over the past decade with growth projected over 13%. Over 1000 has been commercially planted within South Africa and over 8000 tonnes per annum of pomegranate fruits is exported. On a global scale, 'Wonderful' is the most widely grown and consumed pomegranates cultivar, and accounts for of 64% of total production in South Africa. One of the major challenges the pomegranate industry faces is high incidence of postharvest losses and waste, which can reach up to 9% in some seasons [210]. One of the strategies to reduce wastage and increase grower returns is through value addition by processing of pomegranate fruit into different co-products such as pomegranate juice, fresh and dried arils. The by-products of the fresh aril and juice industries include fruit skin (peel), membranes, and kernels (also referred to as seed). Therefore, the utilization of pomegranate by-products from waste such as the dried arils, seed oil and powder can contribute to value addition.

However, the need for safety and quality control of processed products that meet the desire of local and international consumer has necessitated the advancement of research into non-invasive quality testing. Although conventional quality measurement methods on processed products exist, these analytical methods are destructive in nature, often requiring sample preparation that are time consuming and expensive often reflecting only the specific sample being analysed. An extensive review of literature show a recent trend in postharvest research and analytical chemistry are shifting towards the use of objective techniques that provide accurate, fast and cost-effective solutions for the evaluation of physical, chemical, microbial and sensory attributes of agricultural materials and its processed co-products [16, 167, 170, 186, 211]. Infrared spectroscopy (IRS), which includes visible to near infrared (Vis/NIR) and mid infrared (MIR) region used in conjunction with multivariate analysis, has arguably become the most used method for quality control due to its ability to predict compounds containing polar functional groups such as –OH, C–O, and N–H. The overall aim of this research study

evaluated infrared spectroscopy (IRS) as non-invasive method for the evaluation of quality attributes, of pomegranate co products.

5.2 General discussion

5.2.1 Application of Fourier-transformed near infrared spectroscopy (FT-NIRS) combined with chemometrics for evaluation of quality attributes of dried pomegranate arils.

Some of the main quality aspects consumers are confronted with when purchasing food or any horticultural product are purely based on external aspects related to size, appearance and colour characteristics [46]. While repeated, purchase of the same product are dependent upon consumers satisfaction based on sensory characteristics such as soluble solids content (SSC), titratable acidity (TA), soluble solids to acid (SSC/TA) ratio and texture [25, 33, 158]. The study conducted in Chapter 3 evaluated the application of Fourier transform near infrared (FT-NIR) spectroscopy using two different regression techniques namely PLS and SVM regression to evaluate the quality attributes of dried pomegranate arils. The developed models were optimized by selecting different wavelength ranges and different pre-processing techniques. This study has shown that both visual key visual (a^*, C^*) and sensory attributes (titratable acidity, TSS:TA ratio) of dried pomegranate arils were successfully predicted, with SVM regression performing slightly better than PLS regression. Future research on dried pomegranate arils should try to improve the robustness of the developed models by adding different cultivars or seasonality. Additionally, research needs to shift its focus on using a contactless infrared spectrophotometer to provide a realistic representation for commercial online analysis and extend the work to evaluate and predict the shelf life of dried pomegranate arils. This research study is considered novel as it?s the first application of infrared spectroscopy known to evaluate quality attributes of dried pomegranate arils.

5.2.2 Application of Fourier transform (FT) near-infrared (NIR) and attenuated total reflection (ATR) FT mid-infrared (MIR) spectroscopy for the evaluation of pomegranate seed oil quality

Global trends in postharvest research and the food industry has shifted its focus towards the use of vibrational spectroscopy for objective measurement which provide accurate, fast and cost-effective solutions [212, 213]. Infrared spectroscopy combined with multivariate analysis is a powerful tool capable of measuring quality attributes at a speed compatible with commercial pack-lines, which may be as high as 10 fruit per second [15]. Therefore, chapter 4 evaluates the usage of infrared spectroscopy using two instruments to assess the quality attributes of po-

megranate seed oil. The first being Multi-purpose Analyzer (MPA) based on near infrared spectroscopy in the spectral region of 12 500 to 4000 cm^{-1}. While, the second instrument uses Alpha ATR-FT-IR spectrophotometer in the mid infrared region of 4000–400 cm^{-1}. Partial least squares analysis was used to construct calibration models for 5 parameters these include peroxide value (PV), refractive index (RI), yellowness index (YI), total phenolic content (TPC) and total carotenoid content (TCC). The developed calibration models in the NIR spectral region provided best prediction statistics for TCC (R^2=80.45, RMSEP=0.0185, RPD=2.28). While, MIR spectral region provided good prediction statistics for PV (R^2=62.00, RMSEP=3.88, RPD=2.32) and RI (R^2=80.92, RMSEP=0.0003, RPD=2.32). For this study, MIR spectroscopy provided better prediction for the quality attributes of pomegranate oil. This may be due to fact that MIR spectra contain more spectral information due to the higher resolution of the fundamental vibrational absorption bands compared to the broad overtone and combination absorption bands in the NIR region. For successful commercial application either online or at-line, implementation of infrared spectroscopy is highly depended on model robustness and for this study three different cultivars were included. Future studies should look at evaluating various other parameters such as free fatty acids, acid value, iodine value and saponification value which is used for quality evaluation this will allow for the simultaneous measurement of multiple quality parameters. Therefore, this study provided a significant contribution towards potential development of an online or at-line application of infrared spectroscopy to evaluate quality attributes for pomegranate oil.

5.3 General conclusion and recommendations

In conclusion, this thesis has made a significant contribution to the non-invasive measurement and potential prediction of quality attributes for pomegranate co-products (dried seeds and oil). This study showed that infrared spectroscopy could be implemented as a rapid online tool for the assessment of various quality parameters in different co-products of pomegranate fruit. Another important aspect of this research work was to provide robust models for the developed parameters. This was taken into account by looking at two aspects; firstly, we looked at three different growing locations, afterwards we considered three different cultivars ('Acco', 'Wonderful' and 'Herskawitz'). Consequently, same techniques can be applicable to all cultivars and orchards. A limitation with the use of infrared spectroscopy within this study was that fruit from only one season was considered. Therefore, such factors as seasonality was not considered for the model development within this thesis. It is therefore, recommended that for successful commercial online application, future studies need to consider such factors as increased sample size, additional different cultivars, growing locations, and seasonality. Future recommendations should also focus its efforts on evaluating other processed pomegranate products such as powder, juices in order to reduce losses and waste by value addition. Additionally, research needs to shift its focus to noon-invasive evaluation and detection of fraud or adulteration within processed

pomegranate products which is a global concern, this will allow the pomegranate industry in South Africa to maintain its competitive edge in the global markets.

Bibliography

[1] E. P. Lansky and R. A. Newman, '*Punica granatum* (pomegranate) and its potential for prevention and treatment of inflammation and cancer', *Journal of Ethnopharmacology*, vol. 109, no. 2, pp. 177–206, 2007.

[2] A. Khoddami, Y. B. C. Man, and T. H. Roberts, 'Physico-chemical properties and fatty acid profile of seed oils from pomegranate (*Punica granatum* L.) extracted by cold pressing', *European Journal of Lipid Science Technology*, vol. 116, no. 5, pp. 553–562, 2014.

[3] G. Ampem, 'Quality attributes of pomegranate fruit and co-products relevant to processing and nutrition', Masters thesis, 2017.

[4] N. P. Seeram, Y. Zhang, J. D. Reed, C. G. Krueger, and J. Vaya, Pomegranates. In: Ancient Roots to Modern Medicine. CRC Press Taylor and Francis Group, pp. 3–29, 2006.

[5] L. U. Opara, M. R. Al-Ani, and Y. S. Al-Shuaibi, 'Physico-chemical properties, vitamin C content, and antimicrobial properties of pomegranate fruit (*Punica granatum* L.)', *Food Bioprocess Technology*, vol. 2, no. 3, pp. 315–321, 2009.

[6] M. Viuda-Martos, J. Fernández-López, and J. A. Pérez-Álvarez, 'Pomegranate and its many functional components as related to human health: A review', *Comprehensive Review Food Science*, vol. 9, pp. 635–654, 2010.

[7] V. Jaiswal, A. DerMarderosian, and J. R. Porter, 'Anthocyanins and polyphenol oxidase from dried arils of pomegranate (*Punica granatum* L.)', *Food Chemistry*, vol. 118, no. 1, pp. 11–16, 2010.

[8] M. Dak, V. R. Sagar, and S. K. Jha, 'Shelf-life and kinetics of quality change of dried pomegranate arils in flexible packaging', Food Packaging and Shelf Life, vol. 2, no. 1, pp. 1–6, 2014.

[9] F. Siano, M. C. Straccia, M. Paolucci, G. Fasulo, F. Boscaino, and M. G. Volpe, 'Physico-chemical properties and fatty acid composition of pomegranate, cherry and pumpkin seed oils', *Journal of Science Food Agriculture*, vol. 96, no. 5, pp. 1730–1735, 2016.

[10] Pomegranate Association of South Africa (POMASA), 2018. Pomegranate industry statistics. Paarl, South Africa http://www.hortgro.co.za/portfolio/pomegranates/ (last accessed on 19.09.19).

[11] Pomegranate Association of South Africa (POMASA), 2017. Pomegranate industry statistics. Paarl, South Africa http://www.hortgro.co.za/portfolio/pomegranates/ (last accessed on 19.09.19).

[12] Pomegranate Association of South Africa (POMASA), 2016. Pomegranate industry statistics. Paarl, South Africa http://www.hortgro.co.za/portfolio/pomegranates/ (last accessed on 19.09.19).

[13] I. Doymaz, 'Drying of pomegranate seeds using infrared radiation', *Food Science Biotechnology*, vol. 21, no. 5, pp. 1269–1275, 2012.

[14] A. Cayuela and J. F. García, 'LWT - Food Science and Technology Nondestructive measurement of squalene in olive oil by near infrared spectroscopy', *LWT - Food Science and Technology*, vol. 88, pp. 103–108, 2018.

[15] B. M. Nicolaï, K. Beullens, E. Bobelyn, A. Peirs, W. Saeys, K. I. Theron, and J. Lammertyn, 'Nondestructive measurement of fruit and vegetable quality by means of NIR spectroscopy: A review', *Postharvest Biology and Technology,* vol. 46, pp. 99–118, 2007.

[16] W. Su and D. Sun, Fourier transform infrared and Raman and hyperspectral imaging techniques for quality determinations of powdery foods: A review', *Comprehensive Reviews in Food Science and Food Safety*, vol. 17, pp. 104–122, 2018.

[17] D. M. Musingarabwi, H. H. Nieuwoudt, P. R. Young, H. A. Eyéghè-Bickong, and M. A. Vivier, 'A rapid qualitative and quantitative evaluation of grape berries at various stages of development using Fourier-transform infrared spectroscopy and multivariate data analysis', *Food Chemistry*, vol. 190, pp. 253–262, 2016.

[18] E. Arendse, O. A. Fawole, L. S. Magwaza, H. Nieuwoudt, and U. L. Opara, 'Fourier transform near infrared diffuse reflectance spectroscopy and two spectral acquisition modes for evaluation of external and internal quality of intact pomegranate fruit', *Postharvest Biology Technology*, vol. 138, pp. 91–98, 2018.

[19] E. Arendse, O. A. Fawole, L. S. Magwaza, H. H. Nieuwoudt, and U. L. Opara, 'Development of calibration models for the evaluation of pomegranate aril quality by Fourier-transform near infrared spectroscopy combined with chemometrics', *Biosystems Engineering*, vol. 159, pp. 22–32, 2017.

[20] E. Arendse, O. A. Fawole, L. S. Magwaza, H. Nieuwoudt, and U. L. Opara, 'Comparing the analytical performance of near and mid infrared spectrometers for evaluating pomegranate juice quality', *LWT - Food Science and Technology*, vol. 91, pp. 180–190, 2018.

[21] N. S. S. A. Barringer, Fruits and Vegetables – Food Processing: Principles and Applications, Processing Technologies and Applications, Second Edition, 2014.

[22] E. D. van Asselt, H. J. van der Fels-Klerx, H. J. P. Marvin, H. van Bokhorst-van de Veen, and M. N. Groot, 'Overview of Food Safety Hazards in the European Dairy Supply Chain', *Comprehensive Review in Food Science and Food Safety*, vol. 16, no. 1, pp. 59–75, 2017.

[23] S. Tripathi and H. N. Mishra, 'A rapid FT-NIR method for estimation of aflatoxin B1 in red chili powder', *Food Control*, vol. 20, no. 9, pp. 840–846, 2009.

[24] A. M. Inarejos-Garcıa, S. Gomez-Alonso, G. Fregapane, and M. D. Salvador, 'Evaluation of minor components, sensory characteristics and quality of virgin olive oil by near infrared (NIR) spectroscopy', *Food Research International*, vol. 50, no.1, pp.250–258, 2013.

[25] L. Chen and U. L. Opara, 'Texture measurement approaches in fresh and processed foods – A review', Food Research International, vol. 51, no. 2, pp. 823–835, 2013.

[26] C. Malegori, J. E. N. Marques, T. S. Freitas, M. F. Pimentel, C. Pasquini, and E. Casiraghi, 'Comparing the analytical performances of Micro-NIR and FT-NIR spectrometers in the evaluation of acerola fruit quality, using PLS and SVM regression algorithms', *Talanta*, vol. 165, no. 2016, pp. 112–116, 2017.

[27] A. A. Gowen, C. P. O'Donnell, P. J. Cullen, G. Downey, and J. M. Frias, 'Hyperspectral imaging - an emerging process analytical tool for food quality and safety control', *Trends in Food Science Technology,* vol. 18, no. 12, pp. 590–598, 2007.

[28] T. M. Moghaddam, S. M. A. Razavi, and M. Taghizadeh, 'Applications of hyperspectral imaging in grains and nuts quality and safety assessment: A review', *Journal of Food Measurement and Characterization*, vol. 7, pp. 129–140, 2013.

[29] T. Das and R. S. Agrawal, 'Raman spectroscopy: Recent advancements, techniques and applications', *Vibrational Spectroscopy*, vol. 57, pp. 163–176., 2011.

[30] M. F. Marcone, S. Wang, W. Albabish, S. Nie, D. Somnarain, and A. Hill, 'Diverse food-based applications of nuclear magnetic resonance (NMR) technology', *Food Research International*, vol. 51, no. 2, pp. 729–747, 2013.

[31] E. Arendse, O. A. Fawole, L. S. Magwaza, and U. L. Opara, 'Non-destructive estimation of pomegranate juice content of intact fruit using X-ray computed tomography', *Acta Horticulturae*, vol. 1201, pp. 297–302, 2018.

[32] K. Mollazade, M. Omid, F. A. Tab, and S. S. Mohtasebi, 'Principles and applications of light backscattering imaging in quality evaluation of agro-food products?: A review', *Food Bioprocess Technology*, vol. 5, pp. 1465–1485, 2012.

[33] L. S. Magwaza and U. L. Opara, 'Analytical methods for determination of sugars and sweetness of horticultural products-A review', *Scientia Horticulturae*, vol. 184. pp. 179–192, 2015.

[34] A. F. L. Camelo, 'The quality in fruits and vegetables.' In: Manual for the preparation and sale of fruits and vegetables., FAO, *Agricultural Service Bulletin*, vol. 151, no. 5, pp. 88–90, 2004.

[35] J. M. Juran, 'Quality Control Handbook, rev', McGraw-Hill, New York, NY, USA., 1988.

[36] P. B. Crosby, 'Quality Is Free', McGraw-Hill, New York, NY, USA., 1979.

[37] P. J. Ross, 'Taguchi techniques for quality engineering.', New York McGraw-Hill, 1989.

[38] A. A. Kader, 'Quality of horticultural products', *Acta Horticulturae*, vol. 517, pp. 17–18, 2000.

[39] D. Straker, 'What is Quality? Part 1'. Quality World, April Issue., *J. Chart. Qual. Institute*, UK., no. April, 2001.

[40] D. Straker, 'What is Quality? Part 1'. Quality World., *Chart. Qual. Institute*, UK., no. May, 2001.

[41] A. A. Kader, 'Quality in relation to marketability of fresh fruits and vegetables.', *Outlook. Third Quart.*, pp. 5–6, 1986.

[42] J. A. Abbott, 'Quality measurement of fruit and vegetables', *Postharvest Biology Technology*, vol. 15, pp. 207–225., 1999.

[43] A. E. Watada, 'Quality evaluation of horticultural crops the problems.', *Hortic. Sci.*, vol. 15, pp. 47–51, 1980.

[44] W. Florkowski, R. Shewfelt, B. Brueckner, and S. E. Prussia, 'Postharvest Handling', *Postharvest Handling*, 2009.

[45] A. A. Kader, 'Quality assurance of harvested horticultural perishables.', *Acta Horticulturae*, vol. 553, pp. 51–55, 2001.

[46] P. B. Pathare, U. L. Opara, and F. A. J. Al-Said, 'Colour measurement and analysis in fresh and processed foods: A review', *Food Bioprocess Technology,* vol. 6, no. 1, pp. 36–60, 2013.

[47] K. Flores and J. E. Guerrero, 'Prediction of total soluble solid content in intact and cut melons and watermelons using near infrared spectroscopy', *Journal of Infrared Spectroscopy*, vol. 16, pp. 91–98, 2008.

[48] L. S. Magwaza, U. L. Opara, H. Nieuwoudt, P. J. R. Cronje, and W. Saeys, 'NIR spectroscopy applications for internal and external quality analysis of citrus fruit – A review', *Food Bioprocess Technology*, vol. 5, pp. 425–444, 2012.

[49] D. Wu and D. W. Sun, 'Advanced applications of hyperspectral imaging technology for food quality and safety analysis and assessment: A review - Part I: Fundamentals', *Innovative Food Science and Emerging Technologies*, vol. 19, pp. 1–14, 2013.

[50] J. F. D. Kelly, G. Downey, and V. Fouratier, 'Initial Study of Honey Adulteration by Sugar Solutions Using Midinfrared (MIR) Spectroscopy and Chemometrics', *Journal of Agricultural and Food Chemistry*, vol. 52, no. 1, pp. 33–39, 2004.

[51] Q. Chen, J. Zhao, S. Chaitep, and Z. Guo, 'Simultaneous analysis of main catechins contents in green tea (Camellia sinensis (L.)) by Fourier transform near infrared reflectance (FT-NIR) spectroscopy', *Food Chemistry*, vol. 113, no. 4, pp. 1272–1277, 2009.

[52] Y. Li, X., Sun, C., Luo, L. & He, 'Determination of tea polyphenols content by infrared spectroscopy coupled with iPLS and random frog techniques.', *Computers and Electronics in Agriculture*, vol. 112, pp. 28–35., 2015.

[53] X. Li, Y. Zhang, and Y. He, 'Rapid detection of talcum powder in tea using FT-IR spectroscopy coupled with chemometrics.', *Scientific Reports*, vol. 6, p. 30313, 2016.

[54] S. & C. B. K. Lohumi, S., Lee, 'Optimal variable selection for Fourier transform infrared spectroscopic analysis of starch-adulterated garlic powder.', *Sensors and Actuators B: Chemical*, vol. 216, pp. 622–628., 2015.

[55] L. L. Chen, H. Z, Song, Q. Q. Tang, and G. Q. Xu, 'An optimization strategy for waveband selection in FT-NIR quantitative analysis of corn protein.', *Journal of Cereal Science*, vol. 60, pp. 595–601., 2014.

[56] S. Dhakal, K. Chao, W. Schmidt, J. Qin, M. Kim, and D. Chan, 'Evaluation of turmeric Powder adulterated with metanil yellow using FT-Raman and FT-IR spectroscopy', *Foods*, vol. 5, no. 2, pp. 36–50, 2016.

[57] G. Ren, S. Wang, J. Ning, R. Xu, Y. Wang, Z. Xing, X. Wan, and Z. Zhang, 'Quantitative analysis and geographical traceability of black tea using Fourier transform near-infrared spectroscopy (FT-NIRS)', *Food Research International*, vol. 53, no. 2, pp. 822–826, 2013.

[58] S. A. Haughey, P. Galvin-King, Y. C. Ho, S. E. J. Bell, and C. T. Elliott, 'The feasibility of using near infrared and Raman spectroscopic techniques to detect fraudulent adulteration of chili powders with Sudan dye', *Food Control*, vol. 48, pp. 75–83, 2015.

[59] Z. Hu, L., Yin, C., Ma, S. & Liu, 'Assessing the authenticity of black pepper using diffuse reflectance mid-infrared Fourier transform spectroscopy coupled with chemometrics', *Computer Electronics in Agriculture*, vol. 154, pp. 491–500, 2018.

[60] L. Xie, X. Ye, D. Liu, and Y. Ying, 'Quantification of glucose, fructose and sucrose in bayberry juice by NIR and PLS', *Food Chemistry*, vol. 114, no. 3, pp. 1135–1140, 2009.

[61] K. Włodarska, I. Khmelinskii, and E. Sikorska, 'Evaluation of quality parameters of apple juices using near-infrared spectroscopy and chemometrics', *Journal of Spectroscopy*, 2018. [Online]. Available; https://doi.org/10.1155/2018/5191283.

[62] R. E. Masithoh, R. Haff, and S. Kawano, 'Determination of soluble solids content and titratable acidity of intact fruit and juice of satsuma Mandarin using a hand-held near infrared instrument in transmittance mode', *Journal of Near Infrared Spectroscopy*, vol. 24, no. 1, pp. 83–88, 2016.

[63] L. Cassani, M. Santos, E. Gerbino, M. del Rosario Moreira, and A. Gómez-Zavaglia, 'A combined approach of infrared spectroscopy and multivariate analysis for the simultaneous determination of sugars and fructans in strawberry juices during storage', *Journal of Food Science*, vol. 83, no. 3, pp. 631–638, 2018.

[64] H. Ayvaz, A. Sierra-Cadavid, D. P. Aykas, B. Mulqueeney, S. Sullivan, and L. E. Rodriguez-Saona, 'Monitoring multicomponent quality traits in tomato juice using portable mid-infrared (MIR) spectroscopy and multivariate analysis', *Food Control*, vol. 66, pp. 79–86, 2016.

[65] D. Wu, Y. He, P. Nie, F. Cao, and Y. Bao, 'Hybrid variable selection in visible and near-infrared spectral analysis for non-invasive quality determination of grape juice', *Analytical Chim. Acta*, vol. 659, no. 1?2, pp. 229–237, 2010.

[66] L. Xie and Y. Ying, 'Use of near-infrared spectroscopy and least-squares support vector machine to determine quality change of tomato juice', *Journal of Zhejiang University. Science* vol. 10, no. 6, pp. 465–471, 2009.

[67] C. Camps, R. Robic, M. Bruneau, and F. Laurens, 'Rapid determination of soluble solids content and acidity of Black currant (Ribes nigrum L.) juice by mid-infrared spectroscopy performed in series', *LWT - Food Science and Technology*, vol. 43, no. 7, pp. 1164–1167, 2010.

[68] S. N. Jha and S. Gunasekaran, 'Authentication of sweetness of mango juice using Fourier transform infrared-attenuated total reflection spectroscopy', *ournal of Food Engineering*, vol. 101, no. 3, pp. 337–342, 2010.

[69] E. T. S. Caramês, P. D. Alamar, R. J. Poppi, and J. A. L. Pallone, 'Rapid assessment of total phenolic and anthocyanin contents in grape juice using

infrared spectroscopy and multivariate calibration', *Food Analytical Methods*, vol. 10, no. 5, pp. 1609–1615, 2017.

[70] L. J. Xie, X. Q. Ye, D. H. Liu, and Y. Bin Ying, 'Application of principal component-radial basis function neural networks (PC-RBFNN) for the detection of water-adulterated bayberry juice by near-infrared spectroscopy', *Journal of Zhejiang University Science B*, vol. 9, no. 12, pp. 982–989, 2008.

[71] P. Šnurkovic, 'Quality assessment of fruit juices by nir spectroscopy', *Acta Univ. Agric. Silvic. Mendelianae Brun.*, vol. 61, no. 3, pp. 803–812, 2013.

[72] M. M. Snyder, A. B., Sweeney, C. F., Rodriguez-Saona, L. E. & Giusti, 'Rapid authentication of concord juice concentration in a grape juice blend using Fourier-Transform infrared spectroscopy and chemometric analysis.', *Food Chemistry*, vol. 147, pp. 295–301., 2014.

[73] A. M. Marina, W. I. Wan-Rosli, and M. Noorhidayah, 'Quantitative analysis of peroxide value in virgin coconut oil by ATR- FTIR spectroscopy', *Open Conference Proceedings Journal*, vol. 4, no. 2, pp. 53–56, 2013.

[74] A. M. Marina, W. I. Wan Rosli, and M. Noorhidayah, 'Rapid quantification of free fatty acids in virgin coconut oil by FTIR spectroscopy', *Malaysian Applied Biology*, vol. 44, no. 2, pp. 45–49, 2015.

[75] O. Mba, P. Adewale, M. J. Dumont, and M. Ngadi, 'Application of near-infrared spectroscopy to characterize binary blends of palm and canola oils', *Industrial Crops and Products*, vol. 61, pp. 472–478, 2014.

[76] J. Ma, H. Zhang, T. Tuchiya, Y. Miao, and J. Y. Chen, 'Rapid determination of degradation of frying oil using near-infrared spectroscopy', *Food Science and Technology Research*, vol. 20, no. 2, pp. 217–223, 2014.

[77] R. M. Maggio et al., 'Monitoring of fatty acid composition in virgin olive oil by Fourier transformed infrared spectroscopy coupled with partial least squares', *Food Chemistry*, vol. 114, no. 4, pp. 1549–1554, 2009.

[78] İ. S. Özdemir, Ç. Dağ, G. Özinanç,Ö. Suçsoran, E. Ertaş, and S. Bekiroğlu, 'Quantification of sterols and fatty acids of extra virgin olive oils by FT-NIR spectroscopy and multivariate statistical analyses', *LWT - Food Science Technology*, vol. 91, no. September 2017, pp. 125–132, 2018.

[79] G. Gurdeniz and B. Ozen, 'Detection of adulteration of extra-virgin olive oil by chemometric analysis of mid-infrared spectral data', *Food Chemistry*, vol. 116, no. 2, pp. 519–525, 2009.

[80] N. Sinelli, L. Cerretani, V. D. Egidio, A. Bendini, and E. Casiraghi, 'Application of near (NIR) infrared and mid (MIR) infrared spectroscopy as a rapid tool to classify extra virgin olive oil on the basis of fruity attribute intensity', *Food Research International*, vol. 43, no. 1, pp. 369–375, 2010.

[81] N. Dupuy, O. Galtier, D. Ollivier, P. Vanloot, and J. Artaud, 'Comparison between NIR, MIR, concatenated NIR and MIR analysis and hierarchical PLS model. Application to virgin olive oil analysis', *Analytical Chimica Acta*, vol. 666, no. 1, pp. 23–31, 2010.

[82] K. N. Basri, M. N. Hussain, J. Bakar, Z. Sharif, M. F. A. Khir, and A. S. Zoolfakar, 'Classification and quantification of palm oil adulteration via portable NIR spectroscopy', *Spectrochim. Acta - Part A Mol. Biomolecular Spectroscopy*, vol. 173, pp. 335–342, 2017.

[83] W. Su and D. Sun, 'Multispectral imaging for plant food quality analysis and visualization', *Comprehensive Reviews in Food Science and Food Safety* vol. 17, pp. 220–239, 2018.

[84] E. Arendse, O. A. Fawole, L. S. Magwaza, and U. L. Opara, 'Non-destructive prediction of internal and external quality attributes of fruit with thick rind: A review', *Journal of Food Engineering*, vol. 217, pp. 11–23, 2018.

[85] X. G. Zhang, B.H, Li, J.B, Fan, S.X, Huang, W.Q, Zhang C, Wang Qing-Yan, 'Principles and applications of hyperspectral imaging technique in quality and safety inspection of fruits and vegetables', *Guang Pu Xue Yu Guang Pu Fen Xi*, vol. 34, no. 10, pp. 2743–51, 2014.

[86] A. Baiano, 'Applications of hyperspectral imaging for quality assessment of liquid based and semi-liquid food products: A review', *Journal of Food Engineering*, vol. 214, pp. 10–15, 2017.

[87] J. Qin, K. Chao, M. S. Kim, R. Lu, and T. F. Burks, 'Hyperspectral and multispectral imaging for evaluating food safety and quality', *Journal of Food Engineering*, vol. 118, no. 2, pp. 157–171, 2013.

[88] H. Wang, J. Peng, C. Xie, Y. Bao, and Y. He, 'Fruit quality evaluation using spectroscopy technology: A review', *Sensors* vol. 15, no. 5, pp. 11889–11927, 2015.

[89] S. Shrestha, L. C. Deleuran, and R. Gislum, 'Classification of different tomato seed cultivars by multispectral visible-near infrared spectroscopy and chemometrics', *Journal of Spectral Imaging*, vol. 5, pp. 1–9, 2016.

[90] Z. L. Xiong, C, Liu, C, Pan W, Ma F, Xiong C, Qi L, Chen F, Lu X, Yang J, 'Non-destructive determination of total polyphenols content and classification of storage periods of Iron Buddha tea using multispectral imaging system', *Food Chemistry*, vol. 176, pp. 130–136., 2015.

[91] N. Shetty, M. H. Olesen, R. Gislum, L. C. Deleuran, and B. Boelt, 'Use of partial least squares discriminant analysis on visible near-infrared multispectral image data to examine germination ability and germ length in spinach seeds', *Journal of Chemometrics*, vol. 26, pp. 462–476., 2012.

[92] H. Lee, M. S. Kim, H-S. Lim, E. Park, W-H. Lee, and B-K. Cho, 'Detection of cucumber green mottle mosaic virus-infected watermelon seeds using a near-infrared (NIR) hyperspectral imaging system: Application to seeds of the 'Sambok Honey' cultivar', *Biosystems Engineering*, vol. 148, pp. 138–147., 2016.

[93] Y. Guo, H. Ding, J. Xu, and H. Xu, 'Clustering analysis based on hyperspectral DN values of waste oil', *Remote Sensing for Land and Resources*, vol. 26, pp. 37–41, 2014.

[94] D. Martinez-Gila, P. Cano-Marchal, J. Gámez-Garcia, and O. J. Gómez, 'Hyperspectral imaging for determination of some quality parameters for olive oil.', Proceedings of the 18th International Conference on Automation and Computing (ICAC), Loughborough, UK, pp. 7–8, 2012.

[95] B. M. Nicolaï, I. Bulens, J. De Baerdemaker, B. De Ketelaere, M. L. A. T. M. Hertog, P. Verboven, and J. Lemmertyn 'Non-destructive evaluation: detection of external and internal attributes frequently associated with quality and damage. In: Postharvest Handling: A Systems Approach (edited by W.J. Florkowiski, R.L. Shewfelt, B. Brueckner & S.E. Prussia)', Academic Press, Elsevier, Amsterdam, pp. 421– 442, 2009.

[96] N. Kotwaliwale, K. Singh, A. Kalne, S. N. Jha, N. Seth, and A. Kar, 'X-ray imaging methods for internal quality evaluation of agricultural produce', *Journal of Food Science and Technology*, vol. 51, pp. 1–15, 2014.

[97] R. C. J. Curry, T.S., Dowdey, J.E. & Murry, 'Christensen?s physics of diagnostic radiology', Williams Wilkins, Balt., vol. 4^{th} edn., 1990.

[98] D. A. Casasent, M. A. Sipe, T. F. Schatzki, P. M. Keagy, and L. C. Lee, 'Neural net classification of X-ray pistachio nut data. Lebensm- Wiss u-Technology', *Food Science and Technology*, vol. 31, pp. 122–128., 1998.

[99] E. Arendse, O. A. Fawole, L. S. Magwaza, and U. L. Opara, 'Non-destructive characterization and volume estimation of pomegranate fruit external and internal morphological fractions using X-ray computed tomography', *Journal of Food Engineering*, vol. 186, pp. 42–49, 2016.

[100] L. S. Magwaza and U. L. Opara, 'Investigating non-destructive quantification and characterization of pomegranate fruit internal structure using X-ray computed tomography', *Postharvest Biology and Technology*, vol. 95, pp. 1–6, 2014.

[101] A. Léonard, S. Blacher, C. Nimmol, and S. Devahastin, 'Effect of far-infrared radiation assisted drying on microstructure of banana slices: An illustrative use of X-ray microtomography in microstructural evaluation of a food product', *Journal of Food Engineering*, vol. 85, no. 1, pp. 154–162, 2008.

[102] P. Pittia, G. Sacchetti, L. Mancini, M. Voltolini, N. Sodini, and G. Tromba, 'Evaluation of microstructural properties of coffee beans by synchrotron X-Ray microtomography: A methodological approach', *Journal of Food Science*, vol. 76, no. 2, 2011.

[103] P. Frisullo, M. Barnaba, L. Navarini, and M. D. Nobile, 'Coffea arabica beans microstructural changes induced by roasting: An X-ray microtomographic investigation', *Journal of Food Engineering*, vol. 108, no. 1, pp. 232–237, 2012.

[104] S. Lohumi, H. Lee, M. S. Kim, J. Qin, L. M. Kandpal, H. Bae, A. Rahman, and B-K. Cho, 'Calibration and testing of a Raman hyperspectral imaging system to reveal powdered food adulteration', *PLoS One*, vol. 13, no. 4, pp. e0195253, 2018. [Online]. Available: https://doi.org/10.1371/journal.pone.0195253

[105] D. Yang and Y. Ying, 'Applications of Raman spectroscopy in agricultural products and food analysis: A review', *Applied Spectroscopy Review*, vol. 46, no. 7, pp. 539–560, 2011.

[106] K. Ilaslan, I. H. Boyaci, and A. Topcu, 'Rapid analysis of glucose, fructose and sucrose contents of commercial soft drinks using Raman spectroscopy', *Food Control*, vol. 48, pp. 56–61, 2015.

[107] N. Reis, A. S. Franca, and L. S. Oliveira, 'Quantitative evaluation of multiple adulterants in roasted coffee by Diffuse reflectance infrared Fourier transform spectroscopy (DRIFTS) and chemometrics', *Talanta*, vol. 115, pp. 563–568, 2013.

[108] L. Pei, Y. Ou, W. Yu, Y. Fan, Y. Huang, and K. Lai, 'Au-Ag Core-Shell Nanospheres for Surface-Enhanced Raman Scattering Detection of Sudan i and Sudan II in Chili Powder', *Journal of Nanomaterials*, vol. 16, pp. 1–8, 2015.

[109] F. Gao, Y. Hu, D. Chen, E. C. Y. Li-chan, E. Grant, and X. Lu, 'Determination of Sudan I in paprika powder by molecularly imprinted polymers – thin layer chromatography – surface enhanced Raman spectroscopic biosensor', *Talanta*, vol. 143, pp. 344–352, 2015.

[110] X-L. Li, C-J. Sun, L-B. Luo, and Y. He, 'Nondestructive detection of lead chrome green in tea by Raman spectroscopy', *Scientific Reports*, vol. 5:15729, 2015.

[111] C. H. Ma, J. Zhang, Y. C. Hong, Y. R. Wang, and X. Chen, 'Determination of carbendazim in tea using surface enhanced Raman spectroscopy', *Chinese Chemical Letters*, vol. 26, no. 12, pp. 1455–1459, 2015.

[112] C. Shende, F. Inscore, A. Sengupta, J. Stuart, and S. Farquharson, 'Rapid extraction and detection of trace Chlorpyrifos-methyl in orange juice by surface-enhanced Raman spectroscopy', *Sensing Instrumentation for Food Quality and Safety*, vol. 4, no. 3, pp. 101–107, 2010. [

[113] R. Malekfar, A. M. Nikbakht, S. Abbasian, F. Sadech, and M. Mozaffari, 'Evaluation of tomato juice quality using surface enhanced Raman spectroscopy', *Acta Physica Polonica*, vol. 117, no. 6, pp. 971–973, 2010.

[114] F. Nekvapil, I. Brezestean, D. Barchewitz, B. Glamuzina, V. Chi?, and S. Cint?-Pinzaru, 'Citrus fruits freshness assessment using Raman spectroscopy', *Food Chemistry*, vol. 242, no. 2017, pp. 560–567, 2018.

[115] R. M. El-Abassy, P. Donfack, and A. Materny, 'Assessment of conventional and microwave heating induced degradation of carotenoids in olive oil by VIS Raman spectroscopy and classical methods', *Food Research International*, vol. 43, no. 3, pp. 694–700, 2010.

[116] R. M. El-Abassy, P. Donfack, and A. Materny, 'Visible Raman spectroscopy for the discrimination of olive oils from different vegetable oils and the detection of adulteration', *Journal of Raman Spectroscopy*, vol. 40, no. 9, pp. 1284–1289, 2009.

[117] N. Ahmad, M. Saleem, H. Ali, M. Bilal, S. Khan, R. Ullah, M. Ahmed, and S. Mahmood, 'Defining the temperature range for cooking with extra virgin olive oil using Raman spectroscopy', *Laser Physics Letters*, vol. 14, no. 095603, 2017.

[118] P. V. Jentzsch and V. Ciobota, 'Raman spectroscopy as an analytical tool for analysis of vegetable and essential oils', *Flavour and Fragrance Journal*, vol. 29, pp. 287–295, 2014.

[119] J. H. Cheng, Q. Dai, D. W. Sun, X. A. Zeng, D. Liu, and H. Bin Pu, 'Applications of non-destructive spectroscopic techniques for fish quality and safety evaluation and inspection', *Trends in Food Science and Technology*, vol. 34, no. 1, pp. 18–31, 2013.

[120] J. F. I. Nturambirwe, 'Non-destructive measurement of internal fruit quality using SQUID-NMR techniques', Masters thesis, Stellenbosch University, 2012

[121] U. Erikson, I. B. Standal, I. G. Aursand, E. Veliyulin, and M. Aursand, 'Use of NMR in fish processing optimization: A review of recent progress', *Magnetic Resonance in Chemistry*, vol. 50, 471–480, 2012.

[122] P. Butz, C. Hofmann, and B. Tauscher, 'Recent developments in noninvasive techniques for fresh fruit and vegetable internal quality analysis', *Journal of Food Science*, vol. 70, no. 9, pp. 131–141, 2005

[123] D. W. M. Flores, L. A. Colnago, M. D. Ferreira, and M. H. F. Spoto, 'Prediction of Orange juice sensorial attributes from intact fruits by TD-NMR', *Microchemical Journal*, vol. 128, pp. 113–117, 2016.

[124] C. W. P. S. Grandizoli, F. R. Campos, F. Simonelli, and A. Barison, 'Grape juice quality control by means of ^{1}H NMR spectroscopy and chemometric analyses', *Quim. Nova*, vol. 37, no. 7, pp. 1227–1232, 2014.

[125] E. Vigneau and F. Thomas, 'Model calibration and feature selection for orange juice authentication by ^{1}H NMR spectroscopy', *Chemometrics and Intelligent Laboratory Systems*, vol. 117, pp. 22–30, 2012.

[126] M. Koda, K. Furihata, F. Wei, T. Miyakawa, and M. Tanokura, 'Metabolic discrimination of mango juice from various cultivars by band-selective NMR spectroscopy', *Journal of Agricultural and Food Chemistry*, vol. 60, no. 5, pp. 1158–1166, 2012.

[127] C. Skiera, P. Steliopoulos, T. Kuballa, U. Holzgrabe, and B. Diehl, 'Determination of free fatty acids in edible oils by 1H NMR spectroscopy', *Lipid Technology*, vol. 24, no. 12, pp. 279–281, 2012.

[128] D. F. Andrade, J. L. Mazzei, C. R. Kaiser, and L. A. D'Avila, 'Assessment of different measurement methods using ^{1}H-NMR data for the analysis of the transesterification of vegetable oils', *Journal of the American Oil Chemists' Society*, vol. 89, no. 4, pp. 619–630, 2012.

[129] A. Sega, I. Zanardi, L. Chiasserini, A. Gabbrielli, V. Bocci, and V. Travagli, 'Properties of sesame oil by detailed ^{1}H and 13C NMR assignments before and after ozonation and their correlation with iodine value, peroxide value, and viscosity measurements', *Chemistry and Physics of Lipids*, vol. 163, no. 2, pp. 148–156, 2010.

[130] H. Lizhi, K. Toyoda, and I. Ihara, 'Discrimination of olive oil adulterated with vegetable oils using dielectric spectroscopy', *Journal of Food Engineering*, vol. 96, no. 2, pp. 167–171, 2010. [

[131] K. Toyoda, 'The utilization of electric properties'. In: Sumio K (ed) The handbook of non-destructive detection, Science Forum, Tokyo., vol. 8, pp. 108–126., 2003.

[132] S. N. Jha, K. Narsaiah, A. L. Basediya, R. Sharma, P. Jaiswal, R. Kumar, and R. Bhardwaj, 'Measurement techniques and application of electrical properties for nondestructive quality evaluation of foods-A review', *Journal of Food Science and Technology*, vol. 48, no. 4, pp. 387–411, 2011.

[133] M. E. Sosa-Morales, G. Tiwari, S. Wang, J. Tang, H. S. Garcia, and A. Lopez-Malo, 'Dielectric heating as a potential post-harvest treatment of disinfesting mangoes, Part I: Relation between dielectric properties and ripening', *Biosystems Engineering*, vol. 103, no. 3, pp. 297–303, 2009.

[134] J. C. Valeur, B., & Bochon, 'New trends in fluorescence spectroscopy?Applications to chemical and life sciences.', Berlin Edn. Springer., 2001.

[135] R. Karoui and C. Blecker, 'Fluorescence spectroscopy measurement for quality assessment of food systems?A review', *Food Bioprocess Technology*, vol. 4, no. 3, pp. 364–386, 2011.

[136] T. Boubellouta and E. Dufour, 'Cheese-matrix characteristics during heating and cheese melting temperature prediction by synchronous fluorescence and mid-infrared spectroscopies', *Food and Bioprocess Technology*, vol. 5, no. 1, pp. 273–284, 2010. [Online], Available : doi:10.1007/s11947-010-0337-1.

[137] Y. Saito, Monitoring raw material by laser-induced fluorescence spectroscopy in the production. New York: CRC, 2009.

[138] J. Tan, R. Li, Z-T. Jiang, S-H. Tang, Y. Wang, M. Shi, Y-Q. Xiao, B. Jia, T-X. Lu, and H. Wang, 'Synchronous front-face fluorescence spectroscopy for authentication of the adulteration of edible vegetable oil with refined used frying oil', *Food Chemistry*, vol. 217, pp. 274–280, 2017.

[139] E. Guzmán, V. Baeten, J. A. F. Pierna, and J. A. García-Mesa, 'Evaluation of the overall quality of olive oil using fluorescence spectroscopy', *Food Chemistry*, vol. 173, pp. 927–934, 2015.

[140] F. Ammari, L. Redjdal, and D. N. Rutledge, 'Detection of orange juice frauds using front-face fluorescence spectroscopy and independent components analysis', *Food Chemistry*, vol. 168, pp. 211–217, 2015.

[141] P. Valderrama, P. H. Março, N. Locquet, F. Ammari, and D. N. Rutledge, 'A procedure to facilitate the choice of the number of factors in multi-way data analysis applied to the natural samples: Application to monitoring the thermal degradation of oils using front-face fluorescence spectroscopy', *Chemometric Intelligent Laboratory Systems*, vol. 106, no. 2, pp. 166–172, 2011.

[142] Y. Liu, H. Pu, and D. Sun, 'Trends in Food Science & Technology Hyperspectral imaging technique for evaluating food quality and safety during various processes?: A review of recent applications', *Trends in Food Science and Technology*, vol. 69, pp. 25–35, 2017.

[143] J. F. I. Nturambirwe, 'Advances in spectral techniques for fruit quality evaluation?: case of ULF-NMR and NIRS', PhD dissertation, Stellenbosch University, 2017.

[144] H. Z. Chen, Q. Q. Song, G. Q. Tang, and L. L. Xu, 'An optimization strategy for waveband selection in FT-NIR quantitative analysis of corn protein', *Journal of Cereal Science*, vol. 60, no. 3, pp. 595–601, 2014.

[145] J. Liu, Y. Wena, N. Dong, C. Lai, and G. Zhao, 'Authentication of lotus root powder adulterated with potato starch and/or sweet potato starch using

Fourier transform mid-infrared spectroscopy', *Food Chemistry*, vol. 141, no. 3, pp. 3103–3109, 2013.

[146] L. Wang, D. W. Sun, H. Pu, and J. H. Cheng, 'Quality analysis, classification, and authentication of liquid foods by near-infrared spectroscopy: A review of recent research developments', *Critical Reviews in Food Science and Nutrition*, vol. 57, no. 7, pp. 1524–1538, 2017.

[147] E. Arendse, O. A. Fawole, L. S. Magwaza, and U. L. Opara, 'Estimation of the density of pomegranate fruit and their fractions using X-ray computed tomography calibrated with polymeric materials', *Biosystems Engineering*, vol. 148, pp. 148–156, 2016.

[148] Y. Fan, K. Lai, B. A. Rasco, and Y. Huang, 'Analyses of phosmet residues in apples with surface-enhanced Raman spectroscopy', *Food Control*, vol. 37, no. 1. pp. 153–157, 2014.

[149] T. Pan, D. W. Sun, H. Pu, Q. Wei, W. Xiao, and Q. J. Wang, 'Detection of A. alternata from pear juice using surface-enhanced Raman spectroscopy-based silver nanodots array', *Journal of Food Engineering*, vol. 215, pp. 147–155, 2017.

[150] D. P. Killeen, C. E. Sansom, R. E. Lill, J. R. Eason, , K. C. Gordon, and N. B. Perry, 'Quantitative Raman spectroscopy for the analysis of carrot bioactives', *Journal of Agricultural and Food Chemistry*, vol. 61, no. 11, pp. 2701–2708, 2013.

[151] L. Zhang and M. J. McCarthy, 'Assessment of pomegranate postharvest quality using nuclear magnetic resonance', *Postharvest Biology and Technology*, vol. 77, pp. 59–66, 2013.

[152] R. I. M. Almoselhy, M. H. Allam, M. H. El-Kalyoubi, and A. A. El-Sharkawy, '1H NMR spectral analysis as a new aspect to evaluate the stability of some edible oils', *Annals of Agricultural Science*, vol. 59, no. 2, pp. 201–206, 2014.

[153] D. Holland, K. Hatib, and I. Bar-ya, 'Pomegranate: Botany, horticulture, breeding', In: Horticultural Reviews Edited by J. Janick, John Wiley and Sons, Inc, vol. 35, pp. 127–192, 2009.

[154] O. A. Fawole and U. L. Opara, 'Changes in physical properties, chemical and elemental composition and antioxidant capacity of pomegranate (cv. Ruby) fruit at five maturity stages', *Scientia Horticulturae*, vol. 150, pp. 37–46, 2013.

[155] O. J. Caleb, U. L. Opara, P. V. Mahajan, M. Manley, L. Mokwena, and A. G. J. Tredoux, 'Effect of modified atmosphere packaging and storage temperature on volatile composition and postharvest life of minimally-processed pomegranate arils (cvs. 'Acco' and 'Herskawitz')', *Postharvest Biology Technology*, vol. 79, pp. 54–61, 2013.

[156] B. Gaspardo, S. D. Zotto, E. Torelli, S. R. Cividino, G. Firrao, G. D. Riccia, and B. Stefanon 'A rapid method for detection of fumonisins B1 and B2 in corn meal using Fourier transform near infrared (FT-NIR) spectroscopy implemented with integrating sphere', *Food Chemistry*, vol. 135, no. 3, pp. 1608–1612, 2012.

[157] M. Alfouzan, B. Al-Otaibi, K. Issa, and S. A. Alshebeili, 'Near infrared (NIR)-based classification of orange juice', 2017 International Conference on Electrical and Computing Technologies and Applications ICECTA 2017, vol. 2018, no. 2017, pp. 1–5, 2018.

[158] L. Chen and U. L. Opara, 'Approaches to analysis and modeling texture in fresh and processed foods – A review', *Journal of Food Engineering*, vol. 119, no. 3, pp. 497–507, 2013.

[159] M. W. Davey, W. Saeys, E. Hof, H. Ramon, R. L. Swennen, and J. Keulemans, 'Application of visible and near-infrared reflectance spectroscopy (vis/NIRS) to determine carotenoid contents in banana (musa spp.) fruit pulp', *Journal of Agriculture and Food Chemistry* vol. 57, no. 5, pp. 1742–1751, 2009.

[160] H. Huang, H. Yu, H. Xu, and Y. Ying, 'Near infrared spectroscopy for on/in-line monitoring of quality in foods and beverages: A review', *Journal of Food Engineering*, vol. 87, pp. 303–313, 2008.

[161] M. Manley and V. Baeten, 'Spectroscopic technique: Near infrared (NIR) spectroscopy in modern techniques for food authentication', (Second Edition), vol. Chapter 3, Academic press, pp. 51–102. 2018

[162] C. A. T. dos Santos, M. Lopo, R. N. M. J. Pascao, and J. A. Lopes, 'A review on the applications of portable near-infrared spectrometers in the agro-food industry', *Applied Spectroscopy*, vol. 67, pp. 1215–1233, 2013. [

[163] L. S. Magwaza, U. L. Opara, L. A. Terry, S. Landahl, P. J. R. Cronje, H. H. Nieuwoudt, A. Hanssens, W. Saeys, and B. M. Nicolaï, 'Evaluation of Fourier transform-NIR spectroscopy for integrated external and internal quality assessment of Valencia oranges', *Journal of Food Composition and Analysis*, vol. 31, no. 1, pp. 144–154, 2013.

[164] P. Maniwara, K. Nakano, D. Boonyakiat, and S. Ohashi, 'The use of visible and near infrared spectroscopy for evaluating passion fruit postharvest quality', *Journal of Food Engineering*, vol. 143, pp. 33–43, 2014.

[165] O. O. Olarewaju, I. Bertling, and L. S. Magwaza, 'Non-destructive evaluation of avocado fruit maturity using near infrared spectroscopy and PLS regression models', *Scientia Horticulturae*, vol. 199, no. February, pp. 229–236, 2016.

[166] S. Wold, M. Sjöström, and L. Eriksson, 'PLS-regression: A basic tool of chemometrics', *Chemometric and Intelligent Laboratory Systems*, vol. 58, no. 2, pp. 109–130, 2001.

[167] L. S. Magwaza, U. L. Opara, H. Nieuwoudt, P. J. R. Cronje, and W. Saeys, 'NIR spectroscopy applications for internal and external quality analysis of citrus fruit ? A review', *Food and Bioprocess Technology*, vol. 5, pp. 425–444, 2012.

[168] S. N. Raghavendra and P. C. Deka, 'Support vector machine applications in the field of hydrology: A review', *Applied Soft Computing Journal*, vol. 19, pp. 372–386, 2014.

[169] E. Arendse, O. A. Fawole, L. S. Magwaza, H. Nieuwoudt, and U. L. Opara, 'Evaluation of biochemical markers associated with the development of husk scald and the use of diffuse reflectance NIR spectroscopy to predict husk scald in pomegranate fruit', *Scientia Horticulturae*, vol. 232, pp. 240–249, 2018.

[170] E. Arendse, O. A. Fawole, L. S. Magwaza, H. H. Nieuwoudt, and U. L. Opara, 'Development of calibration models for the evaluation of pomegranate aril quality by Fourier-transform near infrared spectroscopy combined with chemometrics', *Biosystems Engineering*, vol. 159, pp. 22–32, 2017.

[171] P. B. Pathare, U. L. Opara, and F. A.-J. Al-Said, 'Colour measurement and analysis in fresh and processed foods: A review', *Food Bioprocess Technology*, vol. 6, no. 1, pp. 36–60, 2013.

[172] K. Makkar, H.P.S., Siddhuraju, and P. Becker, 'Plant secondary metabolites', *Totowa Humana Press.*, pp. 74–75, 2007.

[173] O. A. Fawole, U. L. Opara, and K. I. Theron, 'Chemical and phytochemical properties and antioxidant activities of three pomegranate cultivars grown in South Africa', *Food Bioprocess Technology*, vol. 5, no. 7, pp. 2934–2940, 2012.

[174] M. M. Giust and R. E. Wrolstad, 'Characterization and measurement of anthocyanins by UV–visible spectroscopy. In: Current Protocols in Food Analytical Chemistry (edited by R.E. Wrolstad, T.E. Acree & H. An)',. John Wiley Sons, Inc., New York, NY., 2001.

[175] E. Arendse, O. A. Fawole, and U. L. Opara, 'Effects of postharvest storage conditions on phytochemical and radical-scavenging activity of pomegranate fruit (cv. Wonderful)', *Scientia Horticultuare*, vol. 169, pp. 125–129, 2014.

[176] P. C. Williams and D. C. Sobering, 'Comparison of commercial near Infrared transmittance and reflectance instruments for analysis of whole grains and seeds', *Journal of Near Infrared Spectroscopy*, vol. 1, no. 1, pp. 25–32 1993.

[177] B. G. Osborne, T. Fearn, and P. H. Hindle, 'Spectroscopy with application in food and beverage analysis. *Longman Scientific and Technical*, Singapore, pp. 1–77, 1993.

[178] P. C. Williams, 'Implementation of near-infrared technology. In: Williams, P.C. and Norris, K., Eds., Near-Infrared Technology in the Agricultural and Food Industries', 2^{nd} Ed. American Association of Cereal Chemist, pp. 145–169, 2001.

[179] P. Williams, P. Dardenne, and P. Flinn, 'Tutorial: Items to be included in a report on a near infrared spectroscopy project', *Journal of Near Infrared Spectroscopy*, vol. 25, no. 2, pp. 85–90, 2017.

[180] P. Williams, ' The RPD Statistic: A Tutorial Note ', NIR news, vol. 25, no. 1, pp. 22–26, 2014.

[181] M. Manley, 'Near-infrared spectroscopy and hyperspectral imaging: non-destructive analysis of biological materials', *Chemical Society Reviews*, vol. 43, pp. 8200–8214, 2014.

[182] A.H. Gomez, Y. He, and A. G. Pereira, 'Non-destructive measurement of acidity , soluble solids and firmness of Satsuma mandarin using Vis / NIR-spectroscopy techniques', *Journal of Food Engineering*, vol. 77, pp. 313–319, 2006.

[183] E. D. Louw and K. I. Theron, 'Robust prediction models for quality parameters in Japanese plums (Prunus salicina L.) using NIR spectroscopy', *Postharvest Biology and Technology*, vol. 58, pp. 176–184, 2010.

[184] H. Lu, H. Xu, Y. Ying, X. Fu, H. Yu, and H. Tian, 'Application Fourier transform near infrared spectrometer in rapid estimation of soluble solids content of intact citrus fruits.', *Journal of Zhejiang University Science B*, vol. 7, no. 10, pp. 794–799, 2006.

[185] L. S. Magwaza, U. L. Opara, P. J. R. Cronje, S. Landahl, H. H. Nieuwoudt, A. M. Mouazen, B. M. Nicolaï, and L. A. Terry, 'Assessment of rind quality of 'Nules Clementine' mandarin fruit during postharvest storage: 2. Robust Vis/NIRS PLS models for prediction of physico-chemical attributes', *Scientia Horticulturae*, vol. 165, pp. 421–432, 2014.

[186] H. Shi and P. Yu, 'Comparison of grating-based near-infrared (NIR) and Fourier transform mid-infrared (ATR-FT/MIR) spectroscopy based on spectral preprocessing and wavelength selection for the determination of crude protein and moisture content in wheat', *Food Control*, vol. 82, pp. 57–65, 2017.

[187] C. Socaciu, F. Fetea, and F. Ranga, 'IR and Raman Spectroscopy – Advanced and versatile techniques for agrifood quality and authenticity assessment', *Bulletin of the University of Agricultural Sciences and Veterinary Medicine, Cluj-Napoca Agriculture*, vol. 66, no. 2, pp. 459–464, 2009.

[188] J. A. Cayuela and J. F. García, 'Sorting olive oil based on alpha-tocopherol and total tocopherol content using near-infra-red spectroscopy (NIRS) analysis', *Journal of Food Engineering*, vol. 202, pp. 79–88, 2017.

[189] F. Kahriman, İ. Onaç, F. Mert Türk, F. Öner, and C. Ö. Egesel, 'Determination of carotenoid and tocopherol content in maize flour and oil samples using near-infrared spectroscopy', *Spectroscopy Letters*, vol. 7010, pp. 1–9, 2019.

[190] A. F. C. Pereira, M. J. C. Pontes, F. F. G. Neto, S. R. B. Santos, R. K. H. Galvão, and M. C. U. Araújo, 'NIR spectrometric determination of quality parameters in vegetable oils using iPLS and variable selection', *Food Research International*, vol. 41, no. 4, pp. 341–348, 2008.

[191] P. Lin, Y. Chen, and Y. He, 'Identification of geographical origin of olive oil Using visible and near-infrared spectroscopy technique combined with chemometrics', *Food Bioprocess Technology*, vol. 5, no. 1, pp. 235–242, 2012.

[192] G. B. da Costa, D. D. S. Fernandes, A. A. Gomes, V. E. de Almeida, and G. Veras, 'Using near infrared spectroscopy to classify soybean oil according to expiration date', *Food Chemistry*, vol. 196, pp. 539–543, 2016.

[193] H. Yang, J. Irudayaraj, and M. M. Paradkar, 'Discriminant analysis of edible oils and fats by FTIR, FT-NIR and FT-Raman spectroscopy', *Food Chemistry*, vol. 93, no. 1, pp. 25–32, 2005.

[194] A. Khoddami and T. H. Roberts, 'Pomegranate oil as a valuable pharmaceutical and nutraceutical', *Lipid Technology*, vol. 27, no. 2, pp. 40–42, 2015.

[195] M. Akbari, A. Vaziri, and A. H. Nasab, 'Comparison of quantitative and qualitative seed oil of pomegranate extracted by cold-press and hexane solvent', *Indian Journal of Fundamental and Applied Life Sciences*, vol. 5, pp. 3704–3709, 2015.

[196] M. T. Boroushaki, H. Mollazadeh, and A. R. Afshari, 'Pomegranate seed oil: A comprehensive review on its therapeutic effects', *International Journal of Pharmaceutical Sciences and Research*, vol. 7, no. 2, pp. 430–442, 2016.

[197] A. Fadavi, M. Barzegar, and M. Hossein Azizi, 'Determination of fatty acids and total lipid content in oilseed of 25 pomegranates varieties grown in Iran', *Journal of Food Composition and Analysis*, vol. 19, no. 6–7, pp. 676–680, 2006.

[198] P. Jing et al., 'Antioxidant properties and phytochemical composition of China-grown pomegranate seeds', *Food Chemistry*, vol. 132, no. 3, pp. 1457–1464, 2012.

[199] M. H. Eikani, F. Golmohammad, and S. S. Homami, 'Extraction of pomegranate (*Punica granatum* L.) seed oil using superheated hexane', *Food and Bioproducts Processing*, vol. 90, no. 1, pp. 32–36, 2012.

[200] A. Parashar, S. K. Gupta, and A. Kumar, 'Studies on separation techniques of pomegranate seeds and their effect on quality of Anardana', *African Journal of Biochemistry Research*, vol. 3, no. 10, pp. 340–343, 2009.

[201] B. U. S. Foudjo, G. Kansci, I. M. Lazar, G. Lazar, E. Fokou, F-X. Etoa, 'ATR-FTIR characterization and classification of avocado oils from five Cameroon cultivars extracted with a friendly environmental process', *Environmental Engineering and Management Journal*, vol.12, no. 1, pp. 97–103, 2013.

[202] A. of O.A. Chemists, Official methods of analysis of AOAC International, Association of Official Analytical Chemists International (2012)

[203] H. Abbasi, K. Rezaei, Z. Emamdjomeh, and S. M. Ebrahimzadeh Mousavi, 'Effect of various extraction conditions on the phenolic contents of pomegranate seed oil', *European Journal of Lipid Science Technology*, vol. 110, no. 5, pp. 435–440, 2008.

[204] E. Biehler, F. Mayer, L. Hoffmann, E. Krause, and T. Bohn, 'Comparison of 3 spectrophotometric methods for carotenoid determination in frequently consumed fruits and vegetables', *Journal of Food Science*, vol. 75, no. 1, 2010.

[205] V. Di Egidio, N. Sinelli, S. Limbo, L. Torri, L. Franzetti, and E. Casiraghi, 'Evaluation of shelf-life of fresh-cut pineapple using FT-NIR and FT-IR spectroscopy', *Postharvest Biology and Technology*, vol. 54, no. 2, pp. 87–92, 2009.

[206] K. Wójcicki, I. Khmelinskii, M. Sikorski, and E. Sikorska, 'Near and mid infrared spectroscopy and multivariate data analysis in studies of oxidation of edible oils', *Food Chemistry*, vol. 187, pp. 416–423, 2015.

[207] R. M. Maggio, L. Cerretani, E. Chiavaro, T. S. Kaufman, and A. Bendini, 'A novel chemometric strategy for the estimation of extra virgin olive oil adulteration with edible oils', *Food Control*, vol. 21, no. 6, pp. 890–895, 2010.

[208] N. Quiñones-Islas, O. G. Meza-Márquez, G. Osorio-Revilla, and T. Gallardo-Velazquez, 'Detection of adulterants in avocado oil by Mid-FTIR spectroscopy and multivariate analysis', *Food Research International*, vol. 51, no. 1, pp. 148–154, 2013.

[209] H. Yang and J. Irudayaraj, 'Comparison of near-infrared, Fourier transform-infrared, and Fourier transform-Raman methods for determining olive pomace oil adulteration in extra virgin olive oil', *Journal of the American Oil Chemists' Society*, vol. 78, no. 9, pp. 889–895, 2001.

[210] 'Pomegranate Association of South Africa (POMASA)', Pomegranate Ind. Stat. Paarl, South Africa http//www.hortgro.co.za/portfolio/ pomegranates/ (last accessed 19.09.19)., 2012.

[211] G. Alves, D. Oliveira, S. Bureau, C. M. Claire, A. B. Pereira-netto, and F. De Castilhos, 'Comparison of NIRS approach for prediction of internal quality traits in three fruit species', *Food Chemistry*, vol. 143, pp. 223–230, 2014.

[212] D. W. Sun, 'Progress on bioproducts processing and food safety', *Journal of Food Engineering*, vol. 77, no. 2, pp. 201–202, 2006.

[213] M. R. Ahmed, J. Yasmin, W. Lee, C. Mo, and B. Cho, 'Imaging Technologies for Nondestructive Measurement of Internal Properties of Agricultural Products: A review', *Journal of Biosystems Engineering*, vol. 42, no. 3, pp. 199–216, 2017.

Appendices

Appendix A: Supplementary information

Table 1: Summary of model performance for PLS regression analysis using different pre-processing methods for textural and colour parameters of dried arils

Quality parameter	Pre-processing	Wavelength range (nm)	Calibration model			Validation model			
			R^2	RMSEC	Bias	R^2	RMSEP	RPD	Bias
L*	None	1445–1640, 1881–2319	0.52	1.92	-0.03	0.48	1.71	1.29	0.67
	1st derivative		0.70	1.62	-0.01	0.30	2.18	1.01	0.88
	Smoothing		0.08	3.03	-0.09	0.01	2.34	0.94	1.14
	MSC		0.70	1.60	0.00	0.31	2.16	1.02	0.97
	MSC+SNV		0.64	1.75	-0.00	0.30	2.14	1.03	0.90
a*	None	1445–1640, 1881–2319	0.84	1.50	-0.01	0.21	2.96	1.05	0.95
	1st derivative		0.87	1.32	0.00	0.14	3.26	0.95	0.94
	Smoothing		0.84	1.50	-0.01	0.21	2.96	1.05	0.95
	MSC		0.86	1.41	0.00	0.26	2.83	1.10	0.95
	MSC+SNV		0.86	1.41	-0.00	0.26	2.84	1.10	0.96
C*	None	1445–1640, 1881–2319	0.75	2.19	-0.02	0.32	2.65	1.33	0.27
	1st derivative		0.81	1.87	-0.01	0.14	3.30	1.07	0.03
	Smooth		0.75	2.19	-0.02	0.32	2.65	1.33	0.27
	MSC		0.79	2.00	0.00	0.36	2.53	1.40	0.12
	MSC+SNV		0.79	2.00	0.00	0.36	2.53	1.40	0.12
h*	None	1045–1295, 1431–1668,	0.33	2.91	-0.02	0.00	2.54	1.13	0.25
	1st derivative	1718–1807, 1874–2319	0.58	2.31	-0.01	0.05	2.68	1.07	0.43
	Smoothing		0.33	2.92	-0.19	0.00	2.55	1.13	0.26
	MSC		0.30	2.27	-0.00	0.19	2.23	1.29	0.14
	MSC+SNV		0.59	2.27	0.00	0.19	2.23	1.29	0.15
TSS	None	1445–2319	0.05	0.77	-0.01	0.22	0.78	0.83	-0.31
	1st derivative		0.12	0.75	-0.03	0.06	0.82	0.79	-0.33
	Smoothing		0.14	0.72	-0.01	0.08	0.78	0.83	-0.23
	MSC		0.06	0.77	0.00	0.03	0.78	0.83	-0.12
	MSC+SNV		0.00	0.77	0.00	0.00	0.78	0.83	-0.12
TA	None	1052–1204, 1208–2319	0.58	0.06	0.00	0.57	0.07	1.43	0.02
	1st derivative		0.69	0.05	0.00	0.58	0.07	1.43	0.03
	Smoothing		0.19	0.08	0.00	0.33	0.08	1.25	0.00
	MSC		0.50	0.05	0.00	0.66	0.03	2.00	0.02
	MSC+SNV		0.25	0.08	0.00	0.13	0.10	1.00	0.02

R^2: Coefficient of determination, PLS: Partial least squares, SVM: Support vector machine, MSC: multiplicative scatter correction, SNV: Standard normal variate, RMSEC: Root mean square error of calibration, RMSEP: Root mean square error of prediction, RPD: Residual prediction deviation

Table 2: Summary of model performance for PLS regression analysis using different pre-processing methods for chemical and phytochemical parameters of dried arils

Quality parameter	Pre-processing	Wavelength range (nm)	Calibration model			Validation model			
			R^2	RMSEC	Bias	R^2	RMSEP	RPD	Bias
pH	None	2280–2319	0.47	0.22	-0.01	0.68	0.17	1.82	-0.01
	1st derivative		0.78	0.13	0.00	0.81	0.14	2.21	-0.01
	Smoothing		0.42	0.24	-0.01	0.69	0.17	1.82	-0.00
	MSC		0.81	0.12	-0.00	0.86	0.13	2.38	-0.03
	MSC+SNV		0.81	0.12	0.00	0.86	0.13	2.38	-0.03
TSS/TA	None	834–1042, 1437–1826, 1967–2003, 2049–2092	0.55	1.44	-0.02	0.76	1.95	1.45	-0.66
	1st derivative		0.68	1.22	-0.00	0.73	1.74	1.63	-0.43
	Smoothing		0.55	1.44	-0.02	0.76	1.95	1.45	-0.66
	MSC		0.53	1.47	-0.00	0.74	1.69	1.67	-0.35
	MSC+SNV		0.53	1.47	-0.00	0.74	1.68	1.68	-0.35
Brim A	None	952–1083, 1123–1232, 1498–1701, 2139–2278, 2280–2319	0.04	0.75	-0.00	0.04	0.66	0.83	0.03
	1st derivative		0.74	0.39	-0.00	0.17	0.77	0.71	0.27
	Smoothing		0.04	0.75	-0.00	0.04	0.66	0.83	0.03
	MSC		0.04	0.77	0.00	0.06	0.67	0.82	0.06
	MSC+SNV		0.00	0.77	0.00	0.05	0.67	0.82	0.06
Firmness	None	1037–1248, 1277–2319	0.64	10.05	-0.13	0.04	10.35	1.02	-0.11
	1st derivative		0.60	10.52	-0.05	0.30	8.69	1.22	0.99
	Smoothing		0.64	10.05	-0.14	0.03	10.42	1.01	-0.16
	MSC		0.59	10.63	0.00	0.26	8.64	1.21	0.63
	MSC+SNV		0.59	10.63	-0.00	0.26	8.63	1.21	0.65
TPC	None	1037–1248, 1277–2319	0.00	14.81	-0.03	0.00	10.41	0.82	3.26
	1st derivative		0.04	14.99	-0.19	0.05	10.28	0.83	3.41
	Smoothing		0.00	14.81	-0.03	0.00	10.41	0.82	3.26
	MSC		0.02	14.80	0.00	0.06	10.44	0.82	3.33
	MSC+SNV		0.00	14.80	0.00	0.03	10.44	0.82	3.33
TAC	None	1037–1248, 1277–2319	0.00	6.05	-0.04	0.03	3.64	1.00	-0.16
	1st derivative		0.69	3.36	0.00	0.05	5.84	0.62	-0.66
	Smoothing		0.00	6.05	-0.04	0.03	3.64	1.00	-0.16
	MSC		0.04	6.00	0.00	0.13	3.57	1.02	-0.10
	MSC+SNV		0.04	6.00	0.00	0.00	3.57	1.02	-0.10

R^2: PLS: Partial least square, SVM: Support vector machine, MSC: multiplicative scatter correction, SNV: Standard normal variate, RMSEC: Root mean square error of calibration, RMSEP: Root mean square error of prediction, RPD: Residual prediction deviation

Table 3: Summary of model performance for SVM regression analysis using different pre-processing methods for textural and colour parameters of dried pomegranate arils

Quality parameter	Pre-processing	Calibration model			Validation model			
		R^2	RMSEC	Bias	R^2	RMSEP	RPD	Bias
L*	None	0.54	1.92	-0.08	0.26	2.28	1.08	0.92
	1st derivative	0.38	2.33	-0.15	0.18	2.46	1.00	1.06
	Smoothing	0.53	1.92	-0.08	0.25	2.28	1.08	0.92
	MSC	0.70	1.57	2.32	0.26	2.32	1.06	0.03
	MSC+SNV	0.75	1.41	0.01	0.27	2.33	1.06	1.04
a*	None	0.77	1.84	0.17	0.72	1.81	1.72	-0.56
	1st derivative	0.47	2.90	0.53	0.50	2.16	1.45	0.21
	Smoothing	0.77	1.84	0.17	0.72	1.82	1.71	-0.56
	MSC	0.77	1.84	0.24	0.68	1.84	1.69	-0.21
	MSC+SNV	0.77	1.87	0.27	0.69	1.82	1.71	-0.20
C*	None	0.75	2.15	0.25	0.70	1.99	1.77	-0.49
	1st derivative	0.47	3.32	0.60	0.53	2.44	1.45	0.30
	Smooth	0.75	2.16	0.25	0.70	1.99	1.77	-0.49
	MSC	0.78	2.01	-0.06	0.68	2.19	1.61	-0.66
	MSC+SNV	0.77	2.04	-0.04	0.66	2.19	1.61	-0.57
h*	None	0.39	2.70	-0.07	0.04	2.86	1.01	-0.36
	1st derivative	0.12	3.18	-0.18	0.11	2.74	1.05	-0.38
	Smoothing	0.39	2.70	-0.07	0.04	2.87	1.00	-0.39
	MSC	0.39	2.62	-0.07	0.06	2.87	1.00	-0.33
	MSC+SNV	0.40	2.58	-0.09	0.07	2.86	1.01	-0.35
TSS	None	0.36	0.70	0.01	0.03	0.73	0.86	0.02
	1st derivative	0.24	0.77	-0.07	0.01	0.65	0.97	0.01
	Smoothing	0.36	0.70	0.01	0.03	0.73	0.86	0.02
	MSC	0.33	0.71	-0.03	0.01	0.70	0.90	0.04
	MSC+SNV	0.33	0.72	0.01	0.01	0.69	0.91	0.04
TA	None	0.79	0.04	-0.00	0.85	0.04	2.50	-0.01
	1st derivative	0.78	0.05	-0.01	0.56	0.07	1.43	-0.03
	Smoothing	0.96	0.02	0.00	0.42	0.07	1.43	-0.02
	MSC	0.80	0.04	-0.00	0.54	0.07	1.43	-0.02
	MSC+SNV	0.85	0.02	-0.00	0.83	0.03	2.00	-0.00

R^2: PLS: Partial least square, SVM: Support vector machine, MSC: multiplicative scatter correction, SNV: Standard normal variate, RMSEC: Root mean square error of calibration, RMSEP: Root mean square error of prediction, RPD: Residual prediction deviation

Table 4: Summary of model performance for SVM regression analysis using different pre-processing methods for chemical and phytochemical parameters of dried pomegranate arils

Quality parameter	Pre-processing	Calibration model			Validation model			
		R^2	RMSEC	Bias	R^2	RMSEP	RPD	Bias
pH	None	0.89	0.10	0.02	0.78	0.14	1.79	0.08
	1st derivative	0.82	0.13	-0.01	0.83	0.13	1.92	0.09
	Smoothing	0.88	0.11	0.02	0.79	0.14	1.79	0.08
	MSC	0.98	0.04	0.00	0.75	0.13	1.92	0.05
	MSC+SNV	0.99	0.02	-0.00	0.63	0.16	1.56	0.06
TSS/TA	None	0.86	1.09	-0.21	0.58	1.31	1.52	0.34
	1st derivative	0.32	2.23	-0.27	0.10	1.99	1.00	0.78
	Smoothing	0.86	1.10	0.34	0.57	1.32	1.51	0.34
	MSC	0.82	1.10	0.11	0.48	1.67	1.19	0.80
	MSC+SNV	0.86	1.01	-0.25	0.58	1.39	1.43	0.53
Brim A	None	0.42	0.61	-0.01	0.03	0.64	0.86	0.02
	1st derivative	0.31	0.69	-0.11	0.00	0.59	0.93	-0.03
	Smoothing	0.42	0.62	-0.01	0.03	0.64	0.86	0.02
	MSC	0.37	0.64	-0.04	0.02	0.61	0.90	0.03
	MSC+SNV	0.27	0.70	0.10	0.27	0.65	0.85	0.22
Firmness	None	0.59	11.44	-1.03	0.46	8.79	1.12	-3.44
	1st derivative	0.51	14.35	-0.73	0.39	7.91	1.25	-2.15
	Smoothing	0.59	11.46	-1.04	0.46	8.80	1.12	-3.43
	MSC	0.65	10.78	-1.09	0.49	7.81	1.27	-2.20
	MSC+SNV	0.68	10.31	-0.79	0.47	8.33	1.19	-2.20
TPC	None	0.94	3.92	-0.62	0.03	10.33	0.82	6.23
	1st derivative	0.01	15.29	-3.69	0.00	8.93	0.95	3.26
	Smoothing	0.95	4.35	-0.58	0.03	10.34	0.82	6.28
	MSC	0.77	7.30	-1.32	0.02	14.66	0.58	4.42
	MSC+SNV	0.63	9.26	-1.15	0.02	13.82	0.62	4.59
TAC	None	0.62	4.44	-0.34	0.00	3.59	1.01	0.48
	1st derivative	0.17	15.92	0.50	0.22	3.82	0.95	1.42
	Smoothing	0.62	4.44	-0.34	0.00	3.59	1.01	0.48
	MSC	0.72	3.36	-0.51	0.02	3.72	0.98	-0.52
	MSC+SNV	0.76	3.13	-0.47	0.03	3.60	1.01	0.61

R^2: PLS: Partial least square, SVM: Support vector machine, MSC: Multiplicative scatter correction, SNV: Standard normal variate, RMSEC: Root mean square error of calibration, RMSEP: Root mean square error of prediction, RPD: Residual prediction deviation, 1^{st} derivative: First-order derivative, smooth: Smoothing

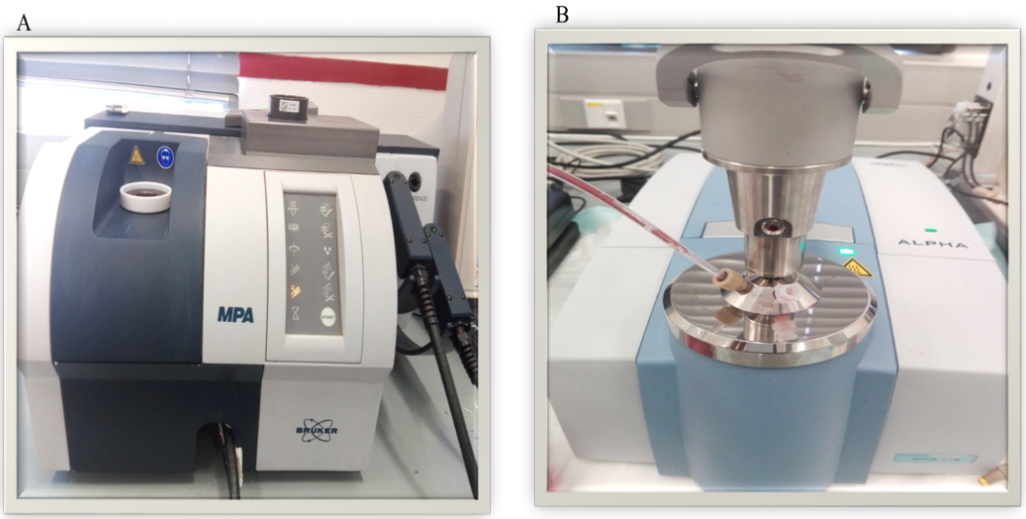

Figure 1: Two instrument for spectral acquisition: FT-NIR Multipurpose analyser (A) and (ATR) FT-MIR spectrometer (B)

Figure 2: Samples of the different pomegranate co-products for non-invasive analysis. Dried pomegranate aril (A) and pomegranate seed oil (B)

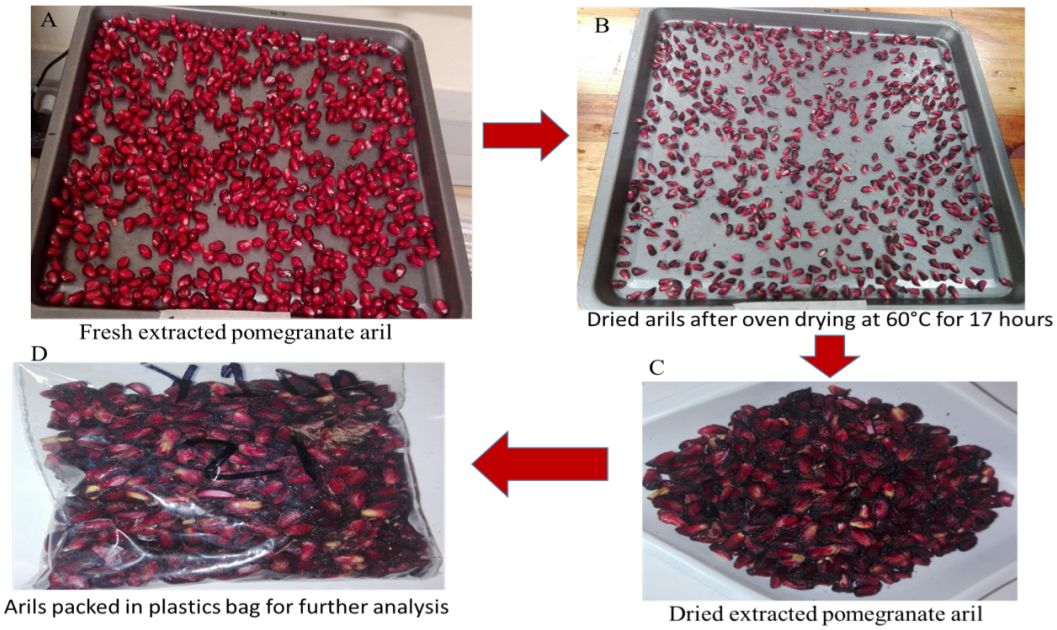

Figure 3: Steps in processing dried pomegranate arils